5-2016

Accumulation and Release of Trace Inorganic Contaminants from Biofilm Matrices Produced and Challenged Under Drinking Water Distribution System Conditions

William W. Kent
Utah State University

ACCUMULATION AND RELEASE OF TRACE INORGANIC CONTAMINANTS FROM BIOFILM MATRICES PRODUCED AND CHALLENGED UNDER DRINKING WATER DISTRIBUTION SYSTEM CONDITIONS

by

William W. Kent

A thesis submitted in partial fulfillment
of the requirements for the degree

of

MASTER OF SCIENCE

in

Civil and Environmental Engineering
(Environmental Engineering)

Approved:

_____	_____
Professor Joan E. McLean Major Professor	Professor Laurie S. McNeill Committee Member
_____	_____
Professor David K. Stevens Committee Member	Mark R. McLellan Vice President for Research and Dean of the School of Graduate Studies

UTAH STATE UNIVERSITY
Logan, Utah

2016

ABSTRACT

Accumulation and Release of Trace Inorganic Contaminants from Biofilm Matrices Developed and Challenged under Drinking Water Distribution System Conditions

by

William W. Kent, Master of Science

Utah State University, 2016

Major Professor: Joan McLean
Department: Civil and Environmental Engineering

Over the legacy time frames experienced by drinking water distribution systems (DWDS), trace inorganic contaminants (TICs) such as arsenic, lead, antimony, thallium, and chromium can accumulate in high concentrations within a biofilm matrix containing iron (Fe) and manganese (Mn) oxyhydroxides. Release of TICs can occur when these matrices are disturbed by a physical or chemical change. A bench scale factorial design using recirculating glass columns (25 mm x 300 mm) with abraded 3 mm glass beads, was used to establish biofilm matrices under a standard conditions at 16°C, 0.2 mg/l chlorine (Cl_2,) and 1 mg/L dissolved organic carbon (DOC) for 6 months. The developed matrix was then challenged by altering the temperature (7 and 25°C) and concentrations of Cl_2 (0 and 2 mg/L) and DOC (0 and 2 mg/L). During this 4 week challenge phase, effluent TIC concentrations were monitored, after which each column was sacrificed and analyzed for ATP and DNA, and TIC distribution within the solids using sequential extractions and total digestions. Solid phase Mn and Fe were associated with the organic fraction of the biofilm matrix. With increased Cl_2, more accumulation of Mn occurred due to the oxidation of

Mn(II) to Mn(IV). This resulted in increased surfaces for sorption of Fe and the TICs, Pb, Tl, Cu, and Cr. Increased Cl_2 also resulted in a less active biofilm as indicated by lower ATP concentrations within the biofilm matrix. Less As accumulated with increased DOC as a result of surface site competition. Lead was impacted by Cl_2 and DOC, where the addition of Cl_2 increased the retention of lead while the addition of DOC caused a decrease. The outcome of this investigation was the identification of conditions that cause accumulation of TICs to biofilm matrices under DWDS conditions, demonstrating a high potential for accumulation when the DWDS is sourced with Fe/Mn and TICs at secondary and primary MCLs. Though not the focus of this study, these highly concentrated solids are susceptible to physical disturbance and release showing the importance of both minimizing accumulation and conducting regular pipe cleaning activities.

(125 pages)

PUBLIC ABSTRACT

Accumulation and Release of Trace Inorganic Contaminants from Biofilm Matrices Developed and Challenged under Drinking Water Distribution System Conditions

Willie Kent

Drinking water distribution systems (DWDS) are used to transport drinking water from the place of treatment to your home. DWDS are made of many types of pipe materials and have the potential to accumulate materials such as iron and manganese oxides and biofilms that serve as reservoirs for toxic trace inorganic contaminants (TICs) such as thallium, arsenic, and lead. These materials can be stable, but changes in water quality or a physical disturbance such as road construction or water use changes may result in a TIC release, causing water quality degradation. This study used glass columns filled with glass beads with the purpose to accumulate biofilm material and TICs on the bead surface. Water quality parameters such as temperature, chlorine (Cl_2), and dissolved organic carbon (DOC) were then changed in order to challenge the biofilm material. Analysis of the effluent and accumulated material in the columns showed the effects of temperature, Cl_2, and DOC on the accumulation/release of TICs. It was observed that with increased Cl_2 an increase in the retention of some TICs occurred. This was the result of the chemical reaction of Mn and Cl_2, causing increased surfaces in the columns for TICs to accumulate onto. Increasing the concentration of DOC also affected the amount of accumulation in the columns, causing less accumulation of arsenic and lead in the biofilm material. No chemical parameter was shown to cause any major release into the water, but the columns

did accumulate high concentrations of the contaminants. Though not the focus of this study, these highly concentrated solids are susceptible to physical disturbance and release, such as changes in consumer demand causing higher flow rates in the pipe. This study demonstrated the ease by which TICs accumulate and the importance of both minimizing accumulation and conducting regular pipe cleaning activities.

ACKNOWLEDGMENTS

This project was funded in part by the Water Research Foundation and the Utah Water Research Laboratory. I would like to thank the support and participation of Park City Municipal Corporation as well as the entire research team. Particularly, thanks to Michelle DeHann, Paul Jerominski, Melinda Friedman, Andrew Hill, Tiana Hammer, Tessa Guy, Jared Richens, Wayne Breon, Darianne Willey, Paul McManus, Nate Rogers, Jason Blankenagel, and Christel Olsen. I would like to acknowledge my family, in particular my sister Sammie Macfarlane, for inspiring me to take chances and strive to accomplish goals I did not think possible. Thanks to each of you for the examples you set and encouragement you offered. Also, a special thanks to Matt Miller for his friendship and his assistance in building and maintaining the Arduino leak detector used in this study.

I am forever grateful and proud to have worked with and associated with my friends, colleagues, and professors at Utah State University. This is especially true of my major advisor Joan McLean, who relentlessly put in the hard work and dedication in teaching me the endeavor of science. Her open door policy and willingness to teach was the cornerstone to my success and I am sincerely grateful to her. I am equally grateful to the rest of my research committee and team: Laurie McNeill, David Stevens, and Darwin Sorensen. Thank you for sharing your knowledge and experiences with me. I especially admire the example you all set in working together to provide warm and skillful leadership, as well as the freedom and support you afforded me to undertake such a project as this. I strive to lead a professional and personal life like the ones each of you have demonstrated to me.

TABLE OF CONTENTS

Page

LIST OF TABLES

LIST OF FIGURES

CHAPTER I

INTRODUCTION

Drinking water distribution systems (DWDS) are not sterile environments because microorganisms may regularly and inadvertently enter the system. To ensure the safety of drinking water, water utilities employ a variety of methods to mitigate the risks these organisms may pose to consumers. Strategies such as maintaining a chlorine (Cl_2) residual and/or limiting the amount of nutrients throughout the system are frequently used. As a stress response to these environments, microorganisms coalesce, secrete extracellular polymeric substances (EPS), and form biofilms. These biofilms in drinking water distribution systems may pose a health risk to consumers in a variety of ways; one of which is their potential to accumulate, release, or aid in the leaching of trace inorganic contaminants (TICs) into finished water. TICs are regulated inorganic ions in drinking water, such as thallium (Tl), antimony (Sb), arsenic (As), lead (Pb), chromium (Cr), or copper (Cu). TICs enter the DWDS at concentrations regulated by the National Primary Drinking Water Standards (NPDWS). These regulations set maximum contaminant levels (MCLs) at the entry point of the DWDS to assure that TICs entering the system occur at concentrations within an acceptable risk as regulated by the USEPA. It is only when TICs accumulate within scale and biofilm matrices in the DWDS that they can potentially cause significant concentrations in drinking water if the matrices are destabilized and release accumulated TICs. Because biofilms have been shown to be prevalent and widespread in DWDS (Lechevallier et al. 1987) and because of their high potential to accumulate TICs

(Flemming 2011; Tuovinen et al. 1980), it is important to investigate the major factors influencing the accumulation and release of TICs from DWDS biofilms.

In 2007 and 2010, Park City, a mountain resort town located in northern Utah, experienced high levels of TICs during two discolored water events. Monthly monitoring of the system from 2013-2014 demonstrated evidence of TIC release from pipe scale/biofilm matrices, with the majority of release events co-occurring in particulate form with iron (Fe) and manganese (Mn). The monitoring study also observed soluble release of Tl when Cl_2 residual levels dropped below 0.2 mg/L. The goal of the laboratory study discussed here was to determine the impacts of water quality challenges on the accumulation and release of TICs from biofilm matrices. The water quality parameters chosen to challenge the biofilm matrices were those known to affect biofilms at levels observed during the monitoring study at Park City.

Problem Statement

DWDS have significant impacts on finished water quality during conveyance from distribution entry point to customer tap. Biofilms are known to exist in all DWDS and are also known to act as contaminant reservoirs with the ability to accumulate TICs. The drinking water community is in need of information on the significance of these reservoirs within the DWDS and also the potential triggers of release that may cause water quality degradation to occur.

Project Objective

The objective of this study was to determine to what extent combinations of changes in temperature (7 and 25°C), Cl_2 residual concentration (0 and 2 mg/L), and DOC concentration (0 and 2 mg/L) impact the accumulation and release of TICs in the presence of the developed pipe matrix consisting of biofilms with Fe and Mn oxides. Biofilms matrices were grown on 3 mm glass beads in 25 mm by 300 mm glass columns fed with tap water spiked with TICs and developed under drinking water conditions of 16°C, 0.2 mg/L Cl_2, and 1 mg/L DOC. The biofilm matrix developed under these conditions is defined as the "standard condition" within the "pipe".

CHAPTER II

PARK CITY CASE STUDY

Background

Park City was founded in the mid 1800's beginning when large deposits of silver ore were discovered in the surrounding mountains. The resulting mining industry produced over 253 million ounces of silver (John 1998). In the 1970's the mining economy began to falter, due to increasingly scarce high-grade ore. As a result, the ski industry became the dominant economic driver (Giddings 2001). Now, Park City is a major recreational urban area and according to the U.S. Bureau of Census (2013) has a population of about 7,962 residents.

The Park City Municipal Corporation (PCMC) currently services 5,098 connections and is one of the most complex water systems in the western US due to its wide elevation range, variety of sources, and seasonal water use trends (McAffee 2012). The city receives its water from several sources including one surface water source, two drainage tunnels, three wells, a spring, and water purchased from the Jordanelle Special Service District (JSSD) (Friedman 2010). Table 1 summarizes the sources, their classification, and contaminant levels.

Table 1. Park City sources.

Source	Classification	Contaminant Levels
Weber River	Surface Water	Low
Spiro Tunnel	Ground Water	Approaching or Exceeding MCL
Judge Tunnel	Ground Water	Approaching or Exceeding MCL
Thiriot Springs	Ground Water	Low
Divide Well	Ground Water	Low
Middle School Well	Ground Water	Low
Park Meadows Well	Ground Water (GWUDI)	Low
JSSD (Ontario Tunnel)	Ground Water	Approaching or Exceeding MCL

The wells, with the exception of Park Meadows, are classified as ground water and require no disinfection. Park Meadows however is considered Ground Water Under Direct Influence of Surface Water (GWUDI) and therefore a UV system has been implemented there (McAffee 2012). Judge, Spiro, and Ontario Tunnels were built for the purpose of relieving the enormous underground flow of water throughout the mines. The water from these tunnels is now reclaimed by the city for use as drinking water. The other sources, such as Thiriot Springs and the three wells, are free of contaminants; however, the two drainage tunnels are not.

Judge Tunnel, located about 3 km south east of Spiro Tunnel, has been reported to have measurable levels of TICs such as As, Sb, selenium (Se), and Tl (Friedman et al. 2010). In 2009, the Judge Tunnel source was found to exceed the MCL of 6 μg/L for Sb by 1 μg/L, forcing PCMC to publish a public notice to its consumers, as well as to acquire an Sb variance from the Utah DEQ (Freidman, 2010; McAffee, 2012b; PC Municipality, 2009).

Spiro Tunnel has also been reported to have significant concentrations of TICs including As, Sb, and Tl (Friedman, 2010; McAffee, 2021a; McAffee, 2012b). The water

is treated with Cl_2, ferric chloride coagulation, and a filtration system designed for Fe and As removal. The water is then blended with Thiriot Springs in order to reduce the Sb levels to below the MCL of 6 µg/L (Friedman et al. 2010).

JSSD sources its water from Ontario Tunnel and is treated by lime softening. The treated water is used for both potable water and snow making at Park City. Significant concentrations of Tl have been reported in the JSSD source as well as detectable levels of As (Friedman et al. 2015).

In Fall 2007 and in November 2010 water quality events occurred in the Thaynes area. This area is located in the same vicinity as the Spiro Tunnel bulkhead. These events were detected by colored water complaints from a large number of consumers. PCMC responded immediately by providing clean bottled water, taking samples, and implementing a flushing program.

The analysis of the samples, performed after the Thaynes event, detected above MCL level TICs such as As, Tl, Mn, and mercury (Hg) at the point of use. The consumer complaints began about a month after a major source change, in which the water utility shut off the Spiro Tunnel source and switched to a Judge Tunnel and Thiriot Spring blend (McAffee, 2012a). The event suggests an acute release of chronic accumulation within the distribution system of the Thaynes area as a result of changes in water quality.

Monthly Monitoring

In order to more fully understand the fate and transport of TICs within the DWDS of Park City and also to inform this laboratory investigation, monthly monitoring of 14 locations within the DWDS was conducted from November 2012 to October 2013. Of the

14 sites monitored there were six pump stations, two pressure reducing valves, one storage reservoir, one system tap, and four premise taps. The eight sources (Table 1) were sampled on two occasions in July and September 2013.

Field measurements such as pH, temperature, dissolved oxygen (DO), electric conductivity (EC), oxidation-reduction potential (ORP), and Cl_2 residual were taken. Along with the field measurements, laboratory analyses were conducted on samples brought back to the Utah Water Research Laboratory at Utah State University. These included total and dissolved TICs, dissolved organic carbon (DOC) and total organic carbon (TOC), major anions and cations, and alkalinity. Solids analysis was also conducted for total suspended solids (TSS), total dissolved solids (TDS), and volatile suspended solids (VSS).

Cleaning Trials

In September 2013, cleaning trials were conducted on Park City's distribution system. Three different cleaning techniques, including unidirectional flushing, swabbing, and ice pigging were employed at two locations: Upper Park Avenue (UPA) and Aspen Springs Drive (AST). To understand the effectiveness of each technique, analysis of both the bulk water and scrapings from the pipe were conducted during each trial. During the swabbing trial, a foam plug was propelled through the pipe to dislodge accumulated material. The suspended solids associated with the swab were centrifuged and collected. The solids were then stored at 4° C to be used in the laboratory investigation described herein.

CHAPTER III

LITERATURE REVIEW

Microbial Growth in DWDS

Microbial numbers are able to increase in DWDS in one of three defined ways: regrowth, after-growth, and breakthrough (Batté et al. 2003; Momba et al. 2000). Regrowth occurs when bacteria that survive the treatment process recover and establish themselves in the system. This is possible even if 99.9%-99.99% of all bacteria are inactivated or eliminated during treatment (Flemming 2002). After-growth refers to microbial growth that occurs as a result of regrowth, when native microbes reproduce and populate new areas of the DWDS. When unwanted events such as cross connections, treatment failures, or backflows occur the resulting growth is referred to as breakthrough. All types of growth occur in a variety of phases: by attachment to the pipe wall, to suspended particles, loose deposits, settled material, or within the bulk water.

Biological Stability

The ability of a drinking water to maintain a consistently low biological concentration as well as an unvarying composition throughout the DWDS is referred to as its biological stability (Lautenschlager et al. 2013). Most utilities with the exception of a few in some European countries such as Denmark, Luxembourg, and the Netherlands (Smeets et al. 2009), use a chorine residual in order to promote biological stability. There are situations however where a Cl_2 residual is ineffective, such as near the surface of the pipe wall where Cl_2 diffusion is limited due to boundary layers inherent in pipe flow.

Microbes are able to utilize these boundary layers when attaching to the pipe wall, particles, or other surfaces, and in combination with a protective layer secreted by the biofilm, are able to shield themselves from disinfection (LeChevallier et al. 1987). This protective environment also has the ability to harbor a variety of other microorganisms that may include human pathogens (LeChevallier et al. 1987) such as *Legionella pneumophila* (Payment and Robertson 2004).

The few utilities in Europe that do not use a Cl_2 residual go to great lengths to create biologically stable source water, limiting and carefully controlling the amount of nutrients entering the DWDS. In this way they are not required to enforce stability using a disinfectant residual, and are able to avoid many of the disadvantages related to disinfection residuals such as harmful disinfection byproducts (DBP). The United States on the other hand relies heavily on a Cl_2 residual to maintain DWDS biological stability, mandating a detectable residual in all the DWDS that are served by surface water influenced sources (USEPA 2011a).

Van der Kooij (1992) concluded that assimilable organic carbon (AOC) concentrations are a measure of biological stability and that AOC < 10 μg acetate equivalent-C/L was the major factor in limiting the growth potential of the DWDS. In a survey of 64 surface water treatment plants across the United States conducted by Camper et al. (2000), the average value of effluent AOC measured was 100 μg acetate equivalent-C/L with only 6% of treatment plants having AOC levels less than 50 μg acetate equivalent-C/L. In the same survey it was observed that AOC levels tend to change seasonally, with an increase of about 20 μg acetate equivalent-C/L during the fall and winter months. This

survey not only demonstrates the relative difficultly in maintaining AOC levels below 10 μg acetate equivalent-C/L in order to limit growth in the DWDS as well as the need for residual disinfection but also demonstrates the difficulty in maintaining consistent biological stability in the system. The main contributor to organic carbon found in DWDS is derived from humic substances, where AOC typically constitutes less than 10% of the total organic carbon (TOC) (Camper et al. 2000).

Biofilm Formation

Though microbial growth in the DWDS may occur in planktonic form, up to 95% of the entire DWDS biomass is composed of sessile organisms attached as biofilms (Flemming 2002). Biofilms are complex communities of sessile microorganisms that are conglomerated in an extracellular polysaccharide (EPS) matrix. Eukaryotic microorganisms such as protozoa are also able to colonize the biofilm and feed off the biofilm constituents. The process by which biofilms attach to the pipe surface is illustrated in Fig. 1, where planktonic cells undergo initial attachment, growth, and finally detachment, renewing the cycle to begin again (Mann and Wozniak 2012). During the attachment phase, planktonic cells use their flagella to attach to the surface, after which they spread out by excreting bio-surfactants and eventually become sessile, losing their flagella in the process. After initial adhesion, the conglomeration of cells begins to excrete substances that compose the EPS. As cell densities become greater, cell-signaling molecules such as acyl-homoserine lactone activate pathways in the cells that promote cellular dispersal and the cycle continues (Shrout and Nerenberg 2012).

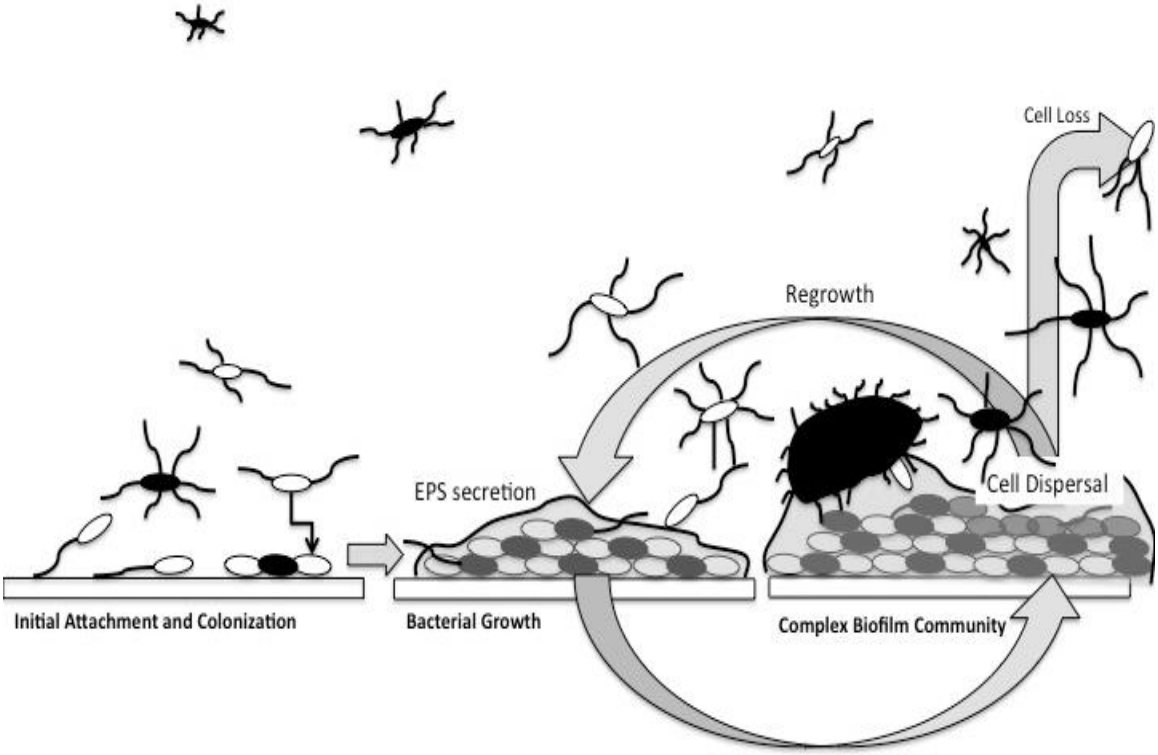

Fig. 1. Biofilm growth cycle.

Contaminant Reservoir

Accumulation and release of regulated TICs in a DWDS is a complex assortment of chemical, physical, and biological processes. Until recently, TICs were considered to be conservative from source to tap. It has now become more apparent that this is not the case and that non-conservative contaminant reservoirs can form within a DWDS. Contaminant reservoirs, as described by Friedman et al. (2010), are the result of regulated inorganic or radiological elements that accumulate on the surface of or within materials commonly found in DWDS such as corrosion products and biofilms.

Corrosion Products

In a study by Schock et al. (2008) the authors conclude that corrosion products and accumulated material composing pipe scale, being primarily comprised of Fe and Mn oxyhydroxides, have a high affinity for As and other TICs. Therefore, the scale is able to act as a reservoir for otherwise safe (below the MCL) concentrations of contaminants, and if released by some event or change in water quality may pose a risk to consumers.

It is evident that Fe and Mn play a significant role in the cycling and transport of elements within a distribution system. Fe exists in most distribution systems as a result of Fe corrosion byproducts such as Fe oxyhydroxides. These adsorb TICs. Where Mn exists as a measurable residual, hydrous Mn oxides may form. Comparatively, Mn oxides are generally more effective sinks than Fe oxides due to their larger surface area and higher adsorption capacity (Peng et al. 2012). For example, in a case study conducted by Friedman et al. (2010), Tl was measured in high concentrations associated with the pipe scale. A strong correlation was found to exist between deposited Mn and Tl, suggesting an association or sorptive capacity for Tl to Mn oxyhydroxides.

In the case of Fe corrosion products, stagnant and flowing water have been shown to have a strong effect on the structure and resilience of scale attached to the surfaces of DWDS (Sarin et al. 2004). As water flows through the pipes, the passing water provides the scale with fresh oxidants such as dissolved oxygen and residual Cl_2. These oxidants are consumed at a higher rate during flowing conditions than during stagnation and act to maintain the Fe within the scale as ferric [Fe(III)] precipitate. During stagnation, when oxidants are not continually supplied to the scale, the ferric iron more readily reduces to

ferrous [Fe(II)] iron, weakening the scale, and resulting in the release of iron and presumably associated TICs into the finished water.

Biofilms

Biofilms in aquatic systems are known to concentrate and bind metals from passing water. In a study conducted by Toner et al. (2006) the investigators found that the mechanism by which Zn is concentrated in a biofilm works primarily by binding to biogenically formed Mn oxides. The biofilm first oxidized soluble Mn(II) to the less soluble Mn oxide which became embedded into the biofilm (Toner et al. 2005). Zn ions then preferentially bound to the Mn oxides. It was not until the Mn oxide binding sites were fully saturated did the Zn begin to bind to organic structures that exist within the biofilm such as carboxyl and phosphoryl functional groups.

Ginige et al. (2011) studied the deposition of Fe and Mn onto biofilms and found that with increased biofilm activity came an increase in Fe and Mn accumulation. The study also found that lower temperature and increased Cl_2, which resulted in a decrease in biofilm activity, resulted in the release of accumulated Fe and Mn. Since Fe and Mn both have a high affinity for TICs, the dissolution of these solid phases may also cause elevated levels of TICs in the bulk water as water quality changes occur. This is contrary to Camper et al. (2003) findings where Cl_2 acted to increase the bioavailability of nutrients which resulted in an increase in biofilm activity. This is likely due to the difference in target Cl_2 concentrations in the two studies where Camper et al. (2003) used a target Cl_2 concentration of only 0.2 mg/L whereas Ginige et al. studied concentrations up to 3 mg/L.

Dong et al. (2002) studied biofilms grown on glass sides (5.0 x 7.5 x 0.1 cm) submerged in fresh water aquatic environments located in Jilin Province, China. The investigators used a sequential extraction technique they developed in a 2001 investigation (Dong et al.), in order to evaluate contributions of the biofilm components to the accumulation of Pb. The three fractions distinguished were 1) Mn oxides, 2) Fe oxides, and 3) organic material (the cells and EPS composing the biofilm). The study concluded that the Mn and Fe oxides played the most significant role in the direct accumulation of Pb from the surrounding lake water. The direct contribution of the organic fraction to the accumulation of Pb was negligible; however, it is assumed from the study that organic matter contributed indirectly through interaction with the Mn and Fe oxides.

Interrelation of Corrosion Products, Biofilms, and Water Quality

Corrosion products, biofilms, and water quality interact with each other in many ways. Corrosion products that accumulate inside pipes may react with the Cl_2 in the bulk water and ultimately reduce the residual Cl_2 thereby benefiting the biofilm. Corrosion products may also offer sorption sites not only for TICs but also the accumulation of nutrients, offering advantages to biofilm growth. Biofilms are known to impact the rate of corrosion in processes known as biocorrosion, where microbe activity within the biofilm can enhance the cathodic and anodic reactions involved in corrosion of metal pipes (Beech and Sunner 2004), resulting in release of TICs leaching from the piping material itself.

Chemical Properties of Matrix Elements and TICs

Matrix Elements: Iron (Fe) and Manganese (Mn)

The USEPA regulates Fe and Mn under the Secondary Drinking Water Regulations, which limit Fe and Mn concentrations to 0.3 and 0.05 mg/L respectively. These non-enforceable guidelines are recommended limits to avoid aesthetic defects of the finished water (USEPA 2012). Fe and Mn exist in the DWDS in a variety of forms and may be released into the water from many sources. They can originate directly from the materials making up the DWDS when the oxidation of metallic pipes results in Fe and Mn corrosion products. Or they can originate from the source water itself and accumulate within the DWDS. Once accumulated they can then dissolve back into the water or be scoured off the pipe surface due to hydraulic disturbance. Fe corrosion products are composed of both Fe(II) and Fe(III) solids of which Fe(II) is more soluble. Fe(II) is expected in layers closer to the pipe wall where reducing conditions are more prominent (Sarin et al. 2001).

Oxidation and deposition of Mn does not occur at neutral pH ranges unless aided by chemical or biological oxidation, so Mn(II) that enters the DWDS remains mobile unless oxidized by a Cl_2 residual or microbial process to form Mn oxide solids (Sly et al. 1990). In aqueous environments at pH values of most natural waters Mn(II) is the most common form of Mn (Crittenden et al. 2012). In a study performed by Cerrato et al. (2010) it was found that chemical and microbial oxidation, as well as microbial reduction of Mn occurs simultaneously despite the inhibitory effects of disinfection on microbial growth. The authors concluded that these reactions were occurring simultaneously due to chemical

gradients as a function of biofilm thickness. These gradients resulted in a range of microenvironments within the biofilm, allowing for the simultaneous chemical and biological oxidation/reduction of Mn.

Both Fe and Mn oxides can form abiotically or as a result of biological processes known as biogenic oxidation. Hua et al. (2012) noted that biogenically formed oxides exhibit different sorption characteristics than abiotic Fe and Mn oxides mainly due to the presence of other ions and organic matter that simultaneously form or are incorporated into the newly formed oxides such as EPS components. Hua et al. (2012) also noted that although TICs are known to more readily adsorb to Mn oxides, Fe oxides normally play a more significant role due to their relative abundance compared to Mn oxides in natural aquatic environments. However, when Mn oxides are present they tend to dominate TIC behavior due to their high reactivity and greater adsorption capacity.

Thallium (Tl)

The MCL for Tl is 0.002 mg/L (USEPA 2012). Thallium exists as a cation Tl(I) and only under extreme oxidizing conditions does it oxidize to Tl(III) and precipitate as Tl_2O_3. Tl(III) is relatively unstable and has strong oxidizing properties; therefore, Tl(III) is likely to transform back to its more common mono-valent state. Tl is highly toxic to humans; behaving like potassium it gains easy access to mammalian cells after which it greatly influences and disturbs protein folding processes causing inhibition of enzymatic reactions. Exposure causes nerve damage, hair loss, kidney failure, and death (Peter and Viraraghavan 2005). Tl(I) competes strongly for sorption sites with Na(I), K(I), and Ca(II) which may indicate water quality factors affecting accumulation and release of Tl in the

DWDS (Wan et al. 2014). In a study by Jacobson et al. (2005), the investigators found that Tl(I) very poorly sorbed to Fe oxides. The investigators also confirmed the high affinity of Tl(I) to Mn oxides suggesting the mechanism of adsorption being the oxidation of Tl(I) to Tl(III) catalyzed by the Mn oxide resulting in the precipitation of insoluble Tl_2O_3 directly onto the Mn oxide surfaces.

Arsenic (As)

The MCL for As is 0.01 mg/L. In aqueous environments As exists predominatly in two oxidation states: As(III) and As(V). As(III) exists mainly as H_3AsO_3 in reducing environments and maintains a neutral charge under environmental values of pH. In oxidizing conditions As(V) exists mainly as $H_2AsO_4^-$ or $HAsO_4^{2-}$ forming a negativly charged oxyanion. In a study conducted by Lytle and Ligget (2011) they summarized from the literature that As has been found to accumulate in DWDS in amounts from 10 to 13,650 μg/g. In the same study, the authors observed that the predominant form of As in the raw water of a southwest Ohio DWDS was As(III). When they observed elevated levels of As at consumer taps they identified that the As was associated with suspended Fe solids. This was the case even though the entire DWDS they were studying was composed solely of plastic material which was accumulating and releasing As-bound Fe solids. Sorption competition of As to Fe oxides can occur under certain conditions. In a study by Holm (2002) it was conclued that at $7 < pH < 9$ As sorption to Fe oxides in the presence of inorganic carbonate or alkalinity at ~100 mg/L HCO_3 was inhibited. The results are consistant with the authors mechanistic theory that CO_3^{-2} competetes with As(V) for

sorption sites on the Fe oxides. Other substances such as phosphate, silicate, and organic matter can also compete with As for adsorption sites (Smedley and Kinniburgh 2002).

Arsenic also has a high affinity for Mn, especially biogenically oxidized Mn. In a study by Watanabe (2012), the investigators demonstrated the concurrent sorption of As(V) and Mn(II) onto newly formed biogenic Mn oxides, calling it the predominant mode for As sequestration in aquatic environments being constantly supplied by Mn(II).

Antimony (Sb)

The MCL for Sb is 0.006 mg/L (USEPA 2012). Sb is a metalloid with similar properties to As. The most common oxidation states of Sb are -3, +3, and +5, of which Sb(III) and Sb(V) are most commonly found in the environment (Filella et al. 2002). In a DWDS Sb typically occurs as $Sb(OH)^-_6$ and is likely to sorb to metal oxides due to its negative charge (Friedman et al. 2010). The lack of literature on Sb in DWDS shows the need for more research on Sb interaction with DWDS biofilms and pipe scale matrices.

Lead (Pb) and Copper (Cu)

Pb and Cu are regulated by the USEPA under the Pb and Cu rule. These are the only TICs that are regulated out in the DWDS rather than solely at the entry point to the DWDS. This rule requires utilities to monitor drinking water at consumer taps. If the Pb or Cu level exceeds their respective action levels of 15 µg/L or 1.3 mg/L in more than 10% of taps sampled, the utility is required to inform the public about the problem and take steps to manage the Pb and Cu levels in the system (USEPA 2012).

Cu exists in the environment generally in two oxidation states: Cu(II) and Cu(I). These species can occur in their ionic form but may also precipitate as a solid (Friedman et al. 2010). Cu is a common material used in premise plumbing systems which may leach Cu into the drinking water in a process known as cuprosolvencey. There is some evidence that biofilms have a signicant influence on cuprosolvencey, acting to either increase or decrease aqueous Cu concentrations depending on complex interactions between the DWDS and the biofilm (Critchley et al. 2001). Li et al. (2009) found that Mn oxides have a high affinity for Cu at approximatly one order of mangantiude greater than Fe oxides. This higher affinity for Cu to Mn oxides was confirmed by Hua et al. (2012) in a study of the adsorption of Cu to soil matrices consisting of Mn oxides, Fe oxides, and organic mater. The study found that Cu preferentially bound to these components in the following order: Mn oxides > Fe oxides > organics.

Lead exists as either Pb(II) or Pb(IV) under DWDS conditions and is likely to form corrosion products and accumulate as scale in a variety of mineral phases (Kim and Herrera 2010). The stability of these scales is highly dependent on the water quality passing by. In a study by Kim and Herrera (2010) the researchers observed that the presence of a Cl_2 residual of 0.5-1.0 mg/L was enough to provide favorable conditions for the formation of PbO_2 scale. In a study by Lin and Valentine (2009) the researchers found that changes in water quality such as an increase in reducing chemicals like natural organic matter (NOM), could reduce PbO_2 to Pb(II) resulting in elevated levels of aqueous Pb species in the water. In a study conducted by Nelson et al. (2002) it was determined that biologically oxidized Mn have a high adsorption capacity for Pb, an order of mangnitude greater than Fe oxides

and several times more than abiotically oxidized Mn. The study is quick to point out that the large increase in Pb adsorption to biologicaly oxidized Mn could be due to greater binding energies per unit surface area as a result of the influence of the cell surfaces on which the biogenic Mn oxides formed. Hua et al. (2012) also observed the high afinity of Pb for Mn and Fe oxides and found that these oxide matrix elements have much higher adsorption of Pb than organic materials, though the affinity for Pb to organic materials was equal to that of Cu.

Chromium (Cr)

The MCL for total Cr is 0.1 mg/L (USEPA 2012). Cr most commonly exists in aquatic environments as hexavalent chromium (Cr(VI)) or trivalent chromium (Cr(III)) which usually remains immobile as the precipitate $Cr(OH)_3$. Cr(III) is considered an essential nutrient for human health, whereas Cr(VI) is a potential carcinogen by ingestion (Costa and Klein 2006). A major source of Cr in the DWDS may come directly from infrastructure materials. Materials such as cement, cast iron, and stainless steel contain Cr (Friedman et al. 2010) and so the possibility of leaching exists. Cr(VI) is toxic to bacteria as well, with evidence suggesting stress response pathways giving biofilms the ability to accumulate and enzymatically reduce Cr(VI) to Cr(III) outside the individual cell within the EPS matrix (Priester et al. 2006). Cr has been observed to sorb to Fe hydroxides under DWDS conditions, though the sorption characteristics were shown to be highly affected by pH and competing ions in solution (Richard and Bourg 1991).

Factors Affecting Biofilm & TIC Stability

The development and stability of biofilms in DWDS are influenced by the microbial community structure in the system, the availability of a carbon and energy source and nutrients, the pH of the system, Cl_2 residual, and temperature. The Fe and Mn in the system precipitates within the biofilm as Fe and Mn oxides (Ginige et al. 2011), adding sites for interaction with TICs. In this study three factors were evaluated: temperature, Cl_2 residual, and DOC. These were chosen because they have been shown to have significant effects on the biological stability of DWDS (Lautenschlager et al. 2013).

Camper et al. (2000) studied the growth rates of biofilms in chlorinated and non-chlorinated systems with humic-derived carbon as the main substrate. The study found that growth rates significantly increased in chlorinated systems, where the Cl_2 acted to make the organic carbon more bioavailable, resulting in different growth kinetics between chlorinated and non-chlorinated systems. The study also found interesting results where adding more humic-derived carbon did not increase biofilm growth. The investigators concluded this was because nutrient diffusion through the biofilm was the limiting factor in the utilization of the carbon. In another study by Camper et al. (2003), similar results were obtained when higher concentrations of Cl_2 residuals did not lead to lower biofilm growth rates on Fe coupons. These studies demonstrate the possible interactions between Cl_2 concentrations and carbon loading on the growth kinetics of biofilms in DWDS. In another study (Ginige et al. 2011), a Cl_2 residual of 3 mg/L resulted in decreased biofilm activity with release of accumulated Fe and Mn. In the same study, lower temperature resulted in decreased biofilm activity. Additionally, organic molecules such as those found

in humic-derived carbon can compete with oxyanions such as As for sorption to matrix sites (Grafe et al. 2001), can complex cationic TICs increasing solubility, or can serve as a reducing agent for elements such as hexavalent Cr and Pb.

CHAPTER IV

MATERIALS AND METHODS

Experimental Design

The experiment was a full factorial design with three factors (temperature, Cl_2, and DOC) at two levels (high and low relative to the standard condition). The biofilms were developed within the test columns, as described below, under the standard conditions of 16°C, 0.2 mg/L Cl_2, and 1 mg/L DOC. Once biofilms were established within the columns, the challenges were applied. One set of triplicate columns was kept under the initial conditions and served to represent the unchallenged biofilm. Table 2 details the levels set for each challenge. The experiment was performed in triplicate, totaling 27 columns.

Table 2. Factor levels.

	Temp (°C)	Cl_2 (mg/L)	DOC (mg/L)
Standard Condition	16.0	0.2	1.0
Challenge 1	7.0	2.0	0.0
Challenge 2	7.0	0.0	0.0
Challenge 3	25.0	2.0	0.0
Challenge 4	25.0	0.0	0.0
Challenge 5	7.0	2.0	2.0
Challenge 6	7.0	0.0	2.0
Challenge 7	25.0	2.0	2.0
Challenge 8	25.0	0.0	2.0

During Phases 1 and 2, factor levels were held constant under the standard conditions (Temp=16°C, Cl_2=0.2 mg/L, and DOC=1 mg/L). During Phase 3, challenges were randomly assigned to each of the 27 columns so that each challenge was conducted in triplicate. The levels of each factor were increased or decreased from those of the

standard conditions (Table 2). These ranges were informed by data collected during monthly monitoring at Park City's DWDS (Table 3).

Table 3. Characteristics of Park City tap water.

Constituent	**Median (Range)**
Temperature	11.8 (2.2 - 21.7) °C
Cl_2 Residual	0.91 (0.02 - 1.32) mg/L
DOC	1.32 (0.8 - 4.17) mg/L

Column Apparatus

The columns were set up in a similar way to the design used by Ginige et al. (2011) and Vanderkooij et al. (1995). The dimensions of the columns are given in Table 4.

Table 4. Column dimensions.

Inside Diameter (mm)	25.4
Length (mm)	300
Column Volume (cm^3)	152
Bead Diameter (mm)	3
Void Fraction (bed porosity)	0.45
Number of Beads per Column	~5500

The glass columns were Bio-Rad chromatography columns (Model #737-2532, Hercules, CA) with a Bio-Rad flow adapter (Fig. 2) (Model #738-0017, Hercules, CA), which allowed the volume of the column to be adjustable in order to maintain a hydraulic retention time of 0.5 days. Because the column and flow adapters were designed for lower flow rates, a modification was required to accommodate the attachment of a larger tubing

size to allow for the higher flow rate. This modification consisted of enlarging the channel though the flow adapter bed support housing (Fig. 2) using a 3.18 mm drill bit and then press fitting a tube through the top of the flow adapter. A polyethylene mesh was placed into the bed support housing to eliminate flow interference from the column media. To block the light from entering the interior of the column a reflective insulation was wrapped around each column and secured with Velcro.

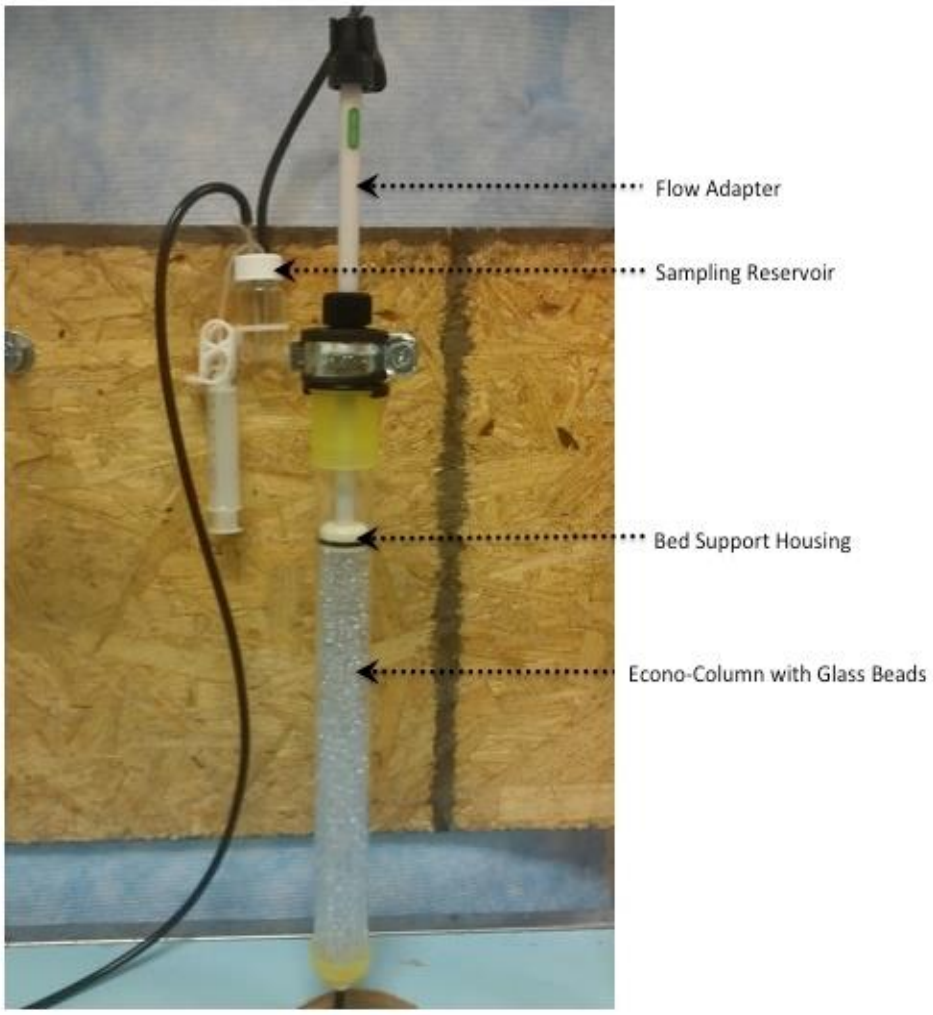

Fig. 2. Complete column apparatus including sampling reservoir.

The columns were filled with abraded, 3 mm Walter Stern solid glass beads (Model # 100C, Port Washington, NY). Abrasion was accomplished by tumbling the beads with ceramic grinding media for 24 hours, followed by acid washing. Fig. 3 illustrates the operating columns during Phase 1. A schematic of the column system is provided in Fig. 4.

Fig. 3. Front and back of column system in operation during Phase 1.

An Ismatec drive (Model # 78002-10, Glattbrugg, CH) with a 12 channel peristaltic head (Model# 78002-36, Glattbrugg, CH) manufactured by IDEX Health and Science was used to recycle the bulk water through the column (Fig. 4, item A) at a rate of 150 mL/min, to maintain a shear force equal to 0.183 N/m^2. This shear is representative of fluid flowing through a 100 mm pipe at a velocity of 0.247 m/s, similar to those found in other studies such as Camper et al. (2003) where shear forces were introduced at levels representative of a flow of 0.3 m/s in a 100 mm pipe. The flow was directed up through the bottom of the column and then out the top, after which the water entered the sampling reservoir (Fig. 4, item B). A feed tube intersected the recycle line to continually pump the feed solution from the feed reservoir (Fig. 4, item C) into the column at a rate of 0.150 mL/min or 1000 times less than the recycle rate. Under these conditions the column approached the characteristics of a complete mixed reactor. The feed pump (Fig. 4, item D) was a 12 channel peristaltic pump manufactured by Thermo Fisher (Model# 72-320-126, Waltham, MA). To maintain constant residual Cl_2 at the required concentrations, a commercial hypochlorite solution (Clorox®) was injected into the feed line using kdScientific syringe pumps (Fig. 4, item E) (Model# KDS230, Holliston, MA).

From the sampling reservoir a portion of the water was either recycled back to the recycle pump, was sampled via a syringe, or removed from the system through the effluent line to the effluent reservoir (Fig. 4, item F) at a rate equal to the combined flow rates of influent Cl_2 and feed water. The sampling reservoir also acted to eliminate bubbles in the column; as long as the recycle out line was submerged, bubbles were forced out through the effluent.

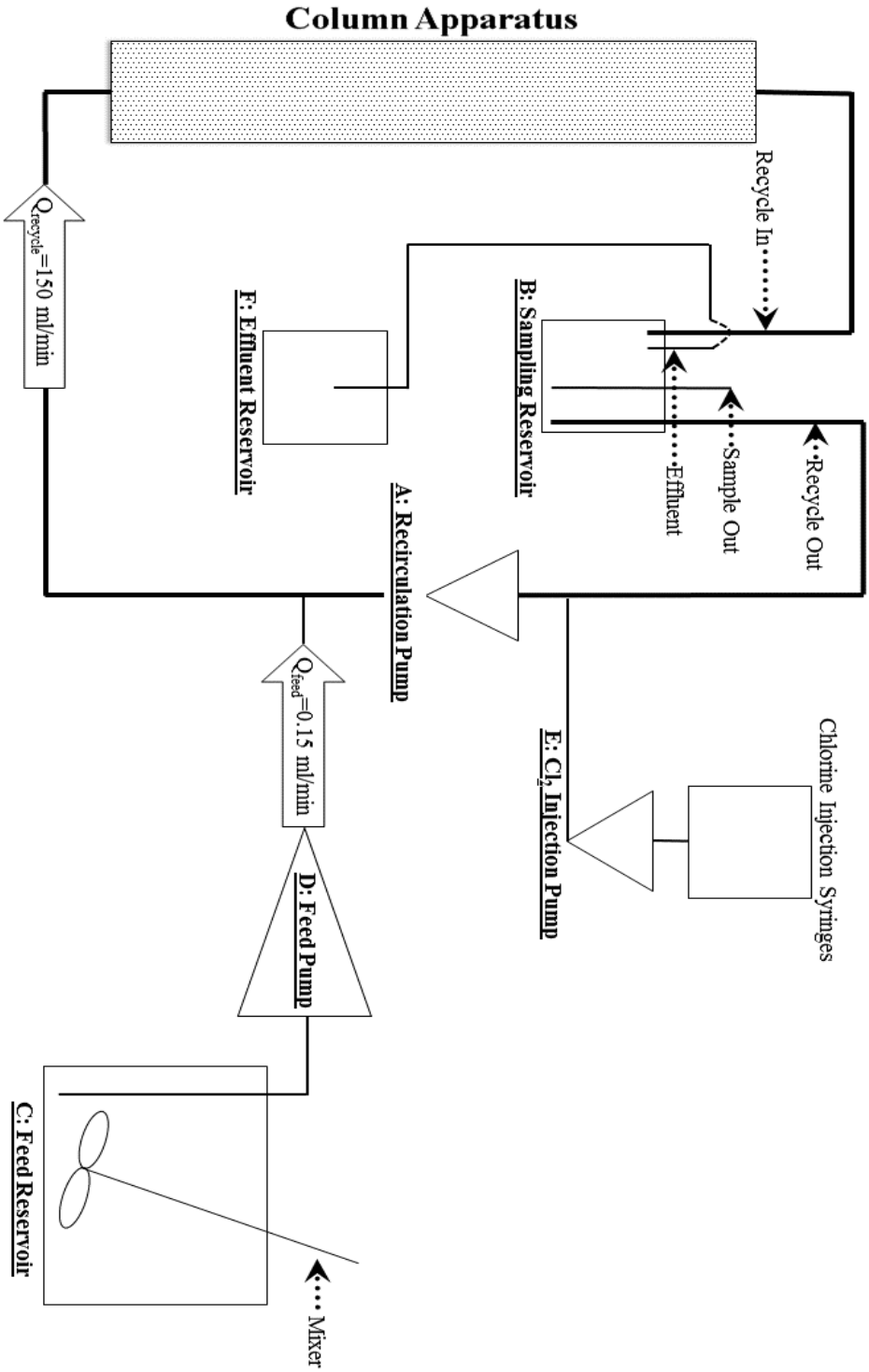

Fig. 4. System schematic.

Feed Solution

A feed solution containing TICs and DOC fed each reactor during all three phases (Table 5). The feed water was made up from City of Logan (UT) tap water spiked with Fe, Mn, Cr, As, Cu, Pb, Sb, and Tl. Arsenic, Pb, Sb, and Tl were added at their MCL concentrations. Copper, since its action level is orders of magnitude higher than observed in the distribution system, was added at concentrations observed during monitoring (Table 5). Chromium, as Cr(VI), was added at the potential new MCL of 10 µg/L. Before supplying the columns, the feed water was allowed to off gas overnight to rid the water of any residual Cl_2 resulting from Logan City's secondary disinfection treatment.

Table 5. Characteristics of Logan Tap, modified Logan tap, and Park City tap water.

Constituents	Logan Tap	Modified Logan Tap	Park City
TICs			
As (V) (µg/L)	< 0.2	10	< 0.2-10
Cr (VI) (µg/L)	< 0.3	10	< 0.3-3
Cu (II) (µg/L)	5.42	30	< 0.75-100
Pb (II) (µg/L)	1.09	15	< 0.4-8
Sb (V) (µg/L)	< 1.2	6	< 1.2-8
Tl (I) (µg/L)	< 0.1	2.25	< 0.1-1
Matrix elements			
Al (III) (µg/L)	<10	233	<10-120
Ca (II) (mg/L)	43.5	71.3	50-130
Fe (III) (µg/L)	26.6	450	< 10-500
K (I) (mg/L)	< 0.5	1.5	1.0-2.0
Mg (II) (mg/L)	19.4	20	18-30
Mn (II) (µg/L)	1.53	35	< 0.75-10
Na (I) (mg/L)	1.07	46.7	5.0-50
Other ions			
Cl (mg/L)	1.32	75	5.0-125
HCO_3 (mg/L)	203	203	30-255
NO_3-N (mg/L)	0.207	0.207	< 0.04-2.0
SO_4 (mg/L)	7.58	75	15-260

In addition, humic-derived carbon was added to the feed solution as a carbon source and measured as DOC. The humic solution was prepared using the protocol described by Camper et al. (2003) where 100 g of Elliot Silt Loam, obtained from the International Humic Substances Society, was added to 1 L of 0.1M NaOH. The suspension was then mixed continuously for two days before centrifugation at 4,000 × *g* for 20 minutes using a Beckman centrifuge (Model# J2-21, Indianapolis, IN) and a swinging bucket rotor (Model# JS-7.5, Indianapolis, IN). After filtering the suspension through a 0.45 µm nylon filter (Life Science Products, Model #8054-NS, Frederick, CO) it was added to the feed solution to obtain the desired DOC concentration. The pH of the feed solution was adjusted with hydrochloric acid (HCl) to 7.5.

Because the DOC stock solution contained Al, Cr, Mn, Fe, and As (Table 6), adjustments were made to the feed solution accordingly before the addition of DOC to allow for consistent TIC levels throughout all phases of the experiment.

Table 6. Matrix and TIC addition from DOC spikes.

	Fe (µg/L)	Mn (µg/L)	Cr (µg/L)	As (µg/L)	Al (µg/L)
DOC Stock Solution (800 PPM DOC)	97600	1050	148	174	150000
TIC Spike (1 ppm DOC)	122	1.31	0.185	0.218	187
TIC Spike (2 ppm DOC)	244	2.62	0.37	0.436	374

Tl, As, Mn, Cu, Pb, Cr, Sb, and Al were added to the feed solution by spiking from three separate stock solutions into 18 L of Logan tap water. Additionally, $FeCl_3$, KCl, $MgCl_2$, $CaSO_4$ and NaCl were added directly to the tap water. The type and mass of salts

used are further detailed in Table 7. Masses were weighed using a Mettler Toledo balance (Model # AJ100, Columbus, OH) with accuracy to 0.1 mg.

Table 7. Salt added to stock solution to modify Logan tap water.

Chemical Name	Product Number, Company, Location	Formula	0 mg/L DOC	1 mg/L DOC	2 mg/L DOC
Stock A (2 mL Spike into 18 L)			Salt Added to Stock A (g/L)		
Thallium(I) chloride	AC20888, Acros Organics, Geel, BE	$TlCl$	0.0211	0.0211	0.0211
Sodium Hydrogen Arsenate Heptahydrate	50-702-1930, Alfa Aesar, Ward Hill, MA	$NaH_2AsO_4 \cdot 7H_2O$	0.3748	0.3697	0.3646
Manganese(II) Chloride Tetrahydrate	AC20589, Acros Organics, Geel, BE	$MnCl_2 \cdot 4H_2O$	1.0852	1.0586	1.032
Copper(II) Chloride Dihydrate	AC31528, Acros Organics, Geel, BE	$CuCl_2 \cdot 2H_2O$	0.7142	0.6989	0.6836
Lead(II) Chloride	AC19331, Acros Organics, Geel, BE	$PbCl_2$	0.168	0.168	0.168
Stock B (2 mL Spike into 18 L)			Salt Added to Stock B (g/L)		
Potassium Chromate	P220, Fisher Scientific, Waltham, MA	CrK_2O_4	0.3178	0.3141	0.3104
Stock C (10 mL Spike into 18 L)			Salt Added to Stock C (g/L)		
Antimony(V) Chloride	255998, Sigma-Aldrich, St. Louis, MO	$SbCl_5$	0.0143	0.0143	0.0143
Stock D (2 mL Spike into 18 L)			Salt Added to Stock D (g/L)		
Al(III) Chloride	104F-0480, Sigma-Aldrich, St. Louis, MO	$AlCl_3$	10.401	5.2006	0
Straight to Feed Reservoir			Salt Added Straight to 18 L (g/18L)		
Iron(III) Chloride Hexahydrate	AC21709, Acros Organics, Geel, BE	$FeCl_3 \cdot 6H_2O$	0.0412	0.0346	0.028
Potassium Chloride	AC424090, Acros Organics, Geel, BE	KCl	0.0515	0.0515	0.0515
Magnesium Chloride Hexahydrate	AC41341, Acros Organics, Geel, BE	$MgCl_2 \cdot 6H_2O$	0.097	0.097	0.097
Calcium Sulfate	AC21752, Acros Organics, Geel, BE	$CaSO_4$	1.72	1.72	1.72
Sodium Chloride	S271, Fisher Scientific, Waltham, MA	$NaCl$	2.0609	2.0652	2.0696

Inoculum

The inoculation suspension was made using the solids collected in September 2013 during the swabbing cleaning trial (Friedman et al. 2015). The solids were stored at 4°C prior to use this study. Table 8 details both the carbon content and the ATP concentration of the solids. ATP was measured (see analytical method section) after blending a 1:50

suspension of the swab solids for 1 minute. The suspension was then allowed to settle for 16 hours before the ATP concentration was measured in the supernatant. Because of the greater organic carbon concentration and ATP content in the AST pipe solids, these were chosen for use as the inoculum for the biofilm.

Table 8. Some properties of collected pipe solids.

Swab Site	Organic Carbon	ATP in 1:50 Suspension (pg or 10^{-12} g/L)*
Aspen Springs Drive (AST)	38%	292 ± 11.3
Upper Park Avenue (UPA)	7.8%	63.9 ± 10.2

* ± is one standard deviation

Column Operation during Each Phase

Phase 1 – Inoculation

Before inoculation, a 1:50 solution by volume of AST swab solids and feed solution was mixed using a high-speed commercial blender for 3 minutes. After settling overnight, the supernatant was pumped into the columns until the total volume of the columns was filled with inoculum, after which the recirculation pumps were turned on. The effluent lines were directed back into the inoculation feed tank so that the inoculum was continually circulated through all of the columns. This process continued until ATP concentrations significantly increased on the beads. Phase 1 took place with test parameters set to 16°C, 0.2 mg/L Cl_2, 1 mg/L DOC (Table 2).

A 1:1000 dilution of 5.25% hypochlorite solution (Clorox®) was injected into the column system at a rate that achieved a Cl_2 residual of 0.2 mg/L. A 10 mL sample taken from the sampling reservoir was used to measure the Cl_2 residual in the system.

Phase 2 – Growth

The growth phase was similar to Phase 1 except the inoculation suspension was removed and replaced with the feed solution only. Effluent samples were collected from the effluent line by allowing 100 mL of effluent to be collected over 12 hours the night before sampling. From this, 40 mL were analyzed for dissolved and total metals. The remaining sample was used for DOC analysis.

Phase 2 lasted about 20 weeks and was conducted in a constant temperature room at 16 ± 2°C (average ± standard deviation). This growth time was based on visual evidence of biofilm growth as well as previous studies in which biofilms stabilized within 20-30 weeks (Boe-Hansen et al. 2002; Camper et al. 2003; Ginige et al. 2011).

Phase 3 – Challenge

Four reactor sets (12 columns) were removed from the 16°C constant temperature room and placed into refrigeration at 7 ± 0.4°C (Fig. 5). Of the four sets in the refrigerator, two triplicate sets of columns were given a higher dose of Cl_2 at 2 mg/L. The other two sets had no Cl_2 added. DOC concentrations were increased to 2 mg/L or decreased to 0 mg/L accordingly so that every combination of challenge factors was used. The same set of test conditions was applied to reactors placed into a 25 ± 0.5°C constant temperature room (Fig. 5). The three unchallenged columns remained under the standard conditions applied during Phase 1 and 2. During Phase 3 effluent from all 27 columns was sampled

for total and dissolved metals, as well as DOC. The columns were harvested after 4 weeks of challenges when it was evident that effluent TIC levels had equilibrated.

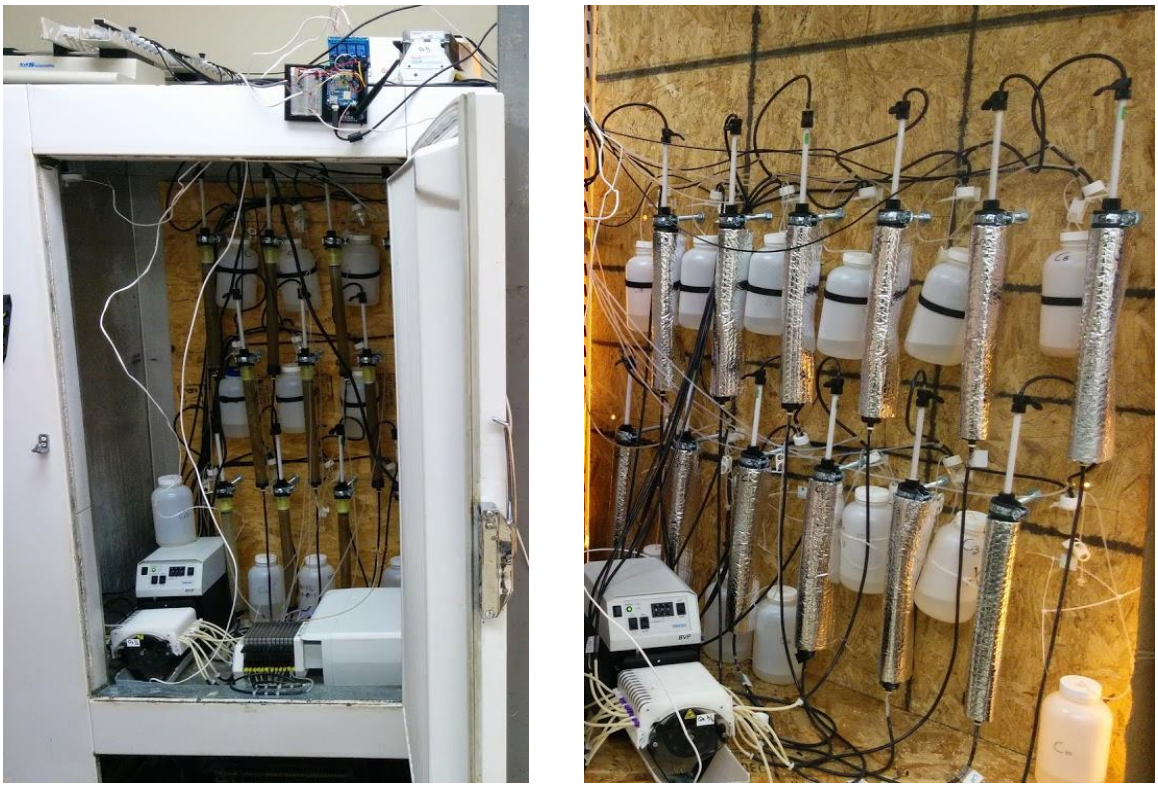

Fig. 5. Columns in operations during phase 3. Left 7°C refrigerator, right 25° constant temperature room.

Column Harvesting and Analysis

At harvesting, 25 beads were removed from the top of each column and extracted for ATP analysis. The remaining approximately 5500 beads along with about 64 ml of pore water were poured into a 250 mL plastic bottle and tumbled at 180 rpm for 10 minutes (Fig. 6), which proved to be adequate time and speed to remove the biofilm from the beads

by visual inspection. A Buchner funnel, with no filter paper, was then used to separate the beads from the suspension. The suspension was then weighed to determine the volume collected. Beads remaining in the Buchner funnel were washed with approximately 64 mL of DI water (depending on the volume of the collected pore water) resulting in a 1:1 diluted suspension.

The 128 mL suspension was then divided into thirds for analysis, taking care to homogenize the suspension by shaking prior to separating the three aliquots (Fig. 6). Thirty-five mL were filtered using a syringe though a Sterivex 0.22 μm Filter Unit (Part # SVGP01050) for DNA analysis (Fig. 6, Filter A). Another 35 mL was vacuum filtered through a Whatman 0.2 μm, 47 mm diameter nylon filter (Part # 7402) (Fig. 6, Filter B). The final 35 mL aliquot from the remaining suspension was filtered through a separate Whatman 0.2 μm filter, after which the entire filter was extracted using the sequential extraction sequence (Fig. 6, Filter C). Additionally, Filter B underwent a gravimetric analysis to determine total mass of oven dried solids collected on the filters before the entire filter was digested for total metals.

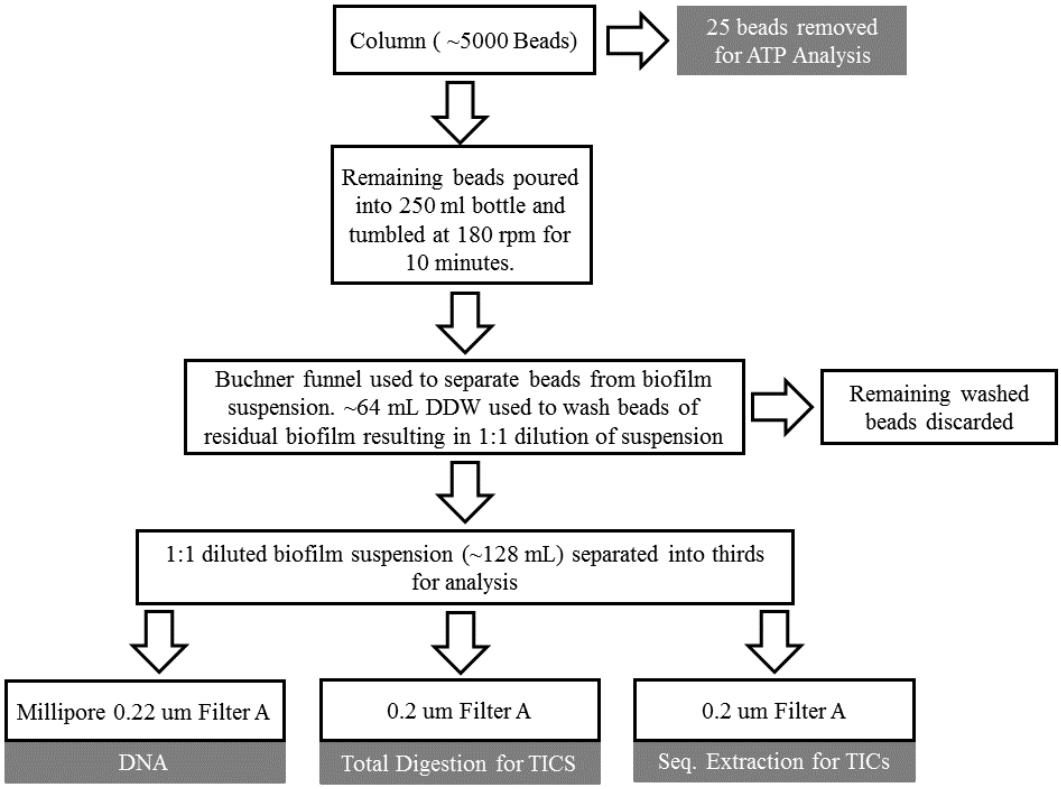

Fig. 6. Biofilm harvest process flow diagram.

Analytical Techniques

Initial Inoculum Analysis

A semi-quantitative analysis of ATP was performed on the centrifuge solids collected during the Swab trials from UPA and AST to determine which of these solids were best suited for use as the inoculum. A 1:50 suspension (by volume) of centrifuge solids was blended in a high-speed blender then settled overnight. The supernatant was filtered through a 0.2 μm LuminUltra filter (Model # DIS-SFQG, New Brunswick, CANADA). ATP was then extracted off the filter using 1 mL of LuminUltra's UltraLyse

7 lysing solution and then analyzed using a LuminUltra PhotonMaster (Product # QGA-100, New Brunswick, CANADA).

Organic carbon content of the centrifuge solids was determined using a Skalar Primacs-SLC TOC Analyzer (Skalar, NL) after drying the material in the oven at 105°C for 24 hours and grinding to 100 mesh.

Biofilm Analysis

For ATP extraction, 25 column beads were submerged into 3 mL of LuminUltra's UltraLyse 7 lysing solution and sonicated using a MISONIX Sonicator (Model #XL2020, Farmingdale, NY). The suspension was filtered and analyzed for ATP, as described above.

Biofilm matrix TIC analysis was performed by extracting metals from the entire harvest filter (Fig. 6, Filter B) by hot nitric acid-hydrogen peroxide extraction (USEPA 3050B) using an Environmental Life Science Hotblock (Model # SC154, Charleston, SC) and then analyzed by Method 6020 using an Agilent inductively coupled plasma mass spectrometer (ICPMS) (Model# 7700x, Santa Clara, CA). Blank filters were also digested to ensure that the filter media did not contribute metals.

A sequential extraction method was used to fractionate the collected biofilm from a separate harvest filter (Fig. 6, Filter C) into operationally defined phases using the method of Amacher (1996) with modifications. The filter was serially extracted in 50 mL centrifuge tubes as described in Table 9.

Table 9. Sequential extraction to characterize the association of TICs with surface and mineral phases.

Operationally defined phases	Analytical Method	Method description
Cation and Oxyanion Exchangeable	Modified Amacher (1996), Huang and Kretzschmar (2010), and USEPA (2011b).	1 M NH_4Cl and 5mM $(NH_4)_3PO_4$, pH 7 (20 ml). 2 hrs at uncontrolled room temperature. Analysis: ICPMS via Method 6020.
Carbonate	Amacher (1996), and USEPA 2011b,	1 M NH_4OAc pH 5 (25 mL). 24 hrs at uncontrolled room temperature. Analysis: ICPMS via Method 6020.
Organic Matter	Amacher (1996) and USEPA 2011b,	0.1 M sodium pyrophosphate (35 mL). 12 hrs at uncontrolled room temperature (in the dark). Analysis: ICPMS via Method 6020.
Mn oxides	Amacher (1996) and USEPA 2011b	0.01 M $NH_2OH.HCl$ pH 2 (25 mL). 30 min at uncontrolled room temperature. Analysis: ICPMS via Method 6020.
Amorphous iron oxide	Amacher (1996) and USEPA 2011b	0.25 $NH_2OH.HCL$+0.25 M HCl (25 mL) 2 hrs at 50°C. Analysis: ICPMS via Method 6020.
Crystalline iron oxides	Amacher (1996), USEPA 2011b	0.3M ammonium oxalate, 0.3M oxalic acid, 0.3M ascorbic acid 15 min boiling bath, repeat once. Analysis: ICPMS via Method 6020.
Residual	Peng and Korshin (2011) and USEPA 2011b	Hot nitric acid digestion Method 3050B[4]. Analysis: ICPMS via Method 6020

DNA collected on the Sterivex 0.22 μm filter was extracted using MoBio PowerLyzer PowerSoil DNA Isolation Kit (Model # 12855, Carlsbad, CA). The DNA was quantified using a Promega GloMax® Microplate Luminometer (Model# E6501, Madison, WI) by Pico Green analysis using Quant-iT PicoGreen dsDNA Reagents and Kit by Invitrogen method MP 07581.

Water Analysis

Dissolved and total metals as well as DOC water samples were collected from the effluent as composite samples over twelve hour periods intermittently over Phases 1 and 2, then 4-5 times per week during Phase 3. Twenty mL for each of the filtered and unfiltered samples were digested using a hotblock (Environmental Express Hotblock, Model # SC154, Charleston, SC) according to EPA Method 200.8 and then analyzed by ICPMS. Dissolved metals were operationally defined as those that pass through a 0.2 μm membrane filter (Life Science Products, Model # 8055-NS, Frederick, CO). Another 40 mL was filtered through a 0.2 μm filter for DOC analysis using a Teledyne TOC analyzer (Model # Apollo 9000, Mason, OH) by Standard Method 5310.

Cl_2 analysis was accomplished by sampling from the 25 mL sampling reservoir; 10 mL of sample was removed via a syringe and then analyzed using a Hach spectrophotometer (Model# DR-2800, Loveland, CO) by HACH Method 8167 (0.2 to 2.00 mg/L Cl_2).

CHAPTER VI

DATA ANALYSIS

To meet the objectives of the experiment, an analysis of variance (ANOVA) was carried out using the statistical program R (R Core Team 2013). The ANOVA was used to determine significant differences among challenge responses at the 95% confidence level. A Tukey's honestly significant difference multiple comparison analysis was performed to further explore the differences in challenges with a significant ANOVA. Correlation analysis was performed on each TIC to explore their relationship with Fe or Mn. Significance of the correlation was evaluated through correlation coefficients (r) and p values. p value < 0.05 indicates 95% confidence to reject the hypothesis that the correlation is due to random sampling. Residuals for ANOVA were evaluated to ensure the errors were independent, normally distributed, and had constant variance. Data were log transformed as appropriate and indicated as such in the plot caption. Box and whisker plots of effluent and solids data are presented in Appendix A to show distribution of data where significant ANOVA was demonstrated.

CHAPTER VII

RESULTS AND DISCUSSION

Column Conditions

A biofilm matrix was visually observed on the columns (Fig. 7). Accumulated material was uniform throughout and appeared reddish brown in color. The material was observed to be loosely attached to the surfaces of the glass beads and vulnerable to physical disturbance. Total dry mass of this material in all columns averaged 170 µg ± 54 µg. No significant difference in total mass was observed among treatments.

Fig. 7. Column before harvest showing developed biofilm matrix.

The pH of the feed solution was 7.6 ± 0.2 over the course of the study. The pH of a system controls biological and chemical processes. Cl_2 dosing may affect the pH of the system. To determine the effects of the addition of Cl_2 on the pH, a separate laboratory investigation was conducted (Appendix B). Cl_2 was added to samples of feed water to maintain a Cl_2 residual of 2 mg/L for 12 hours and the pH was measured intermittingly (Fig B-1). From these results it was determined that the addition of Cl_2 did not impact the pH of the system. The pH variability within this study was maintained within a range not to have significant additional effects on the test factors.

Dosing of Cl_2 into the feed solution was adjusted daily to maintain the designated concentrations (0, 0.2, and 2 mg/L) throughout the column as monitored in the sample reservoir. Sufficient Cl_2 was added to compensate for the Cl_2 demand within the columns.

The solution feeding the columns contained both dissolved and suspended matrix elements (Fe and Mn) and TICs (Table 10). The Fe was associated with suspended solids as were the majority of the Pb and Cu. The addition or absence of DOC did not significantly impact these values (data not shown).

Table 10. Percent suspended of feed elements.

Feed Element	% Suspended
Mn	9%
Fe	99%
As	34%
Pb	96%
Sb	13%
Tl	8%
Cu	71%
Cr	7%

A preliminary study was conducted to determine if the glass beads had a significant sorptive capacity for the TICs. This was done by placing 1200 beads into 80 mL amber glass vials along with 30 mL of the feed solution (Table 5). Another set of glass vials was tested without beads. The vials were then shaken for 2 days at a speed of 200 rpm, using a reciprocal shaker (Eberbach Corporation, Ann Arbor MI), after which the liquid was separated from the beads and tested for total TICs in addition to Mn and Fe by ICPMS. Though a sorptive capacity of the beads for matrix elements and TICs was demonstrated in this preliminary study (Fig. B-2), it accounted for less than 3% of the total accumulation that was observed in the columns when a biofilm matrix had formed (Fig. B-3). It was also determined from the test that the beads were contaminated with Sb. In the sorption test more Sb was measured in solution in contact with the class beads than was added at a surface concentration of 1.2 E -02 $\mu g/cm^2$ (Fig. B-3). This contamination was possibly made worse during the abrasion process. The solubility of Sb from the beads was likely from the glass as a result of fining agents used during manufacturing processes (Shelby 2005). Fining agents such as Sb oxides are used to reduce the size of bubbles that form at the surface of the newly formed glass, achieving a more transparent glass bead.

Relocation Disturbance

The original intent of the experiment was to look for release of TICs during the initial exposure of the biofilm matrix to the challenges. However, because the biofilm matrix was fragile and easily disturbed when moving the columns to their respective constant temperature rooms, it was difficult to determine immediate responses resulting from challenges. Disturbance of the biofilm matrix with moving the columns was evident

visually. Collection of effluent over the first 14 hours immediately after relocation confirmed release of matrix elements in some columns (Fig 8). For example; replicate 1 of treatment 3 demonstrated a disturbance due to handling, because a large increase in both Mn and Fe concentration was observed compared to the other replicates. For this reason, effects of challenges on the effluent were only determined when the columns reached steady-state conditions (Appendix C).

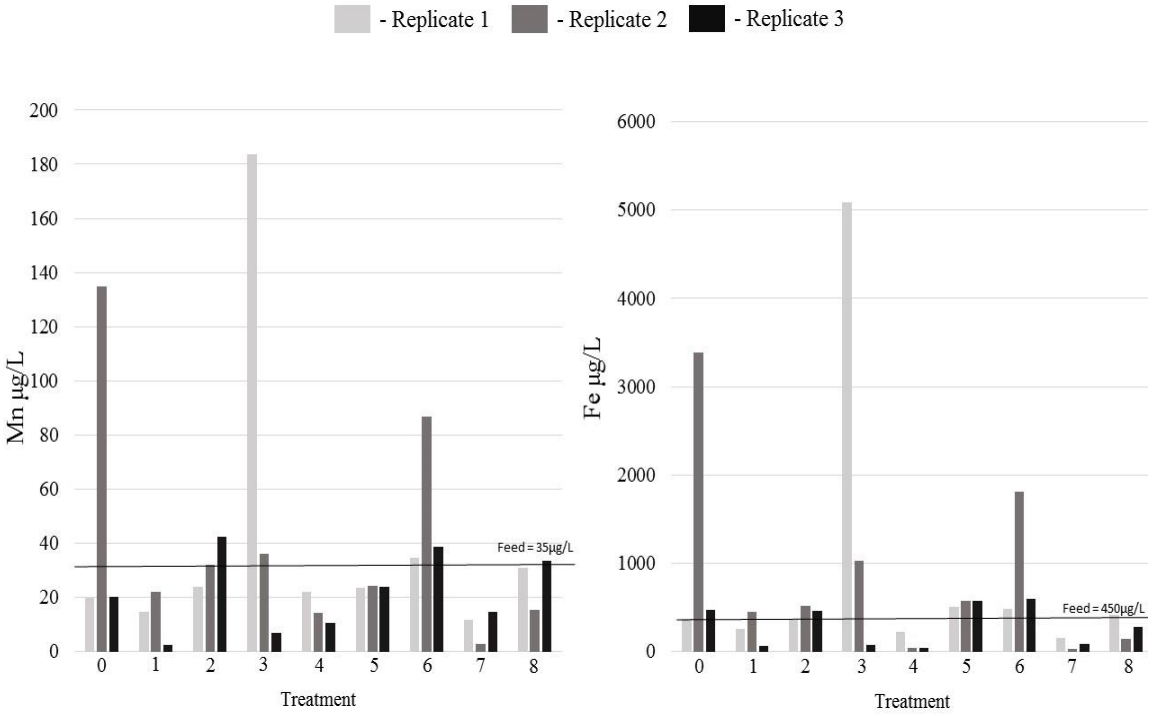

Fig. 8. Composite effluent samples of matrix elements collected over 14 hour period immediately after relocation.

Mass Balance

Mass balance calculations were performed to ensure total mass recoveries (Table 11). The calculations were performed on all 27 columns by summing the difference in

influent and effluent concentrations of each measured element and then dividing the summation by the mass on the beads to get µg/g. Percent recovery was then determined as the calculated influent/effluent mass summation divided by the element mass measured directly in the column solids. In some columns, poor recovery for Mn was consistent with poor recovery of other TICs indicating random release of biofilm matrix that went unmeasured. But in the majority of the columns the % recovery for Mn was consistently low without poor recovery for other TICs which cannot be explained by unmeasured release. Antimony measured much higher concentration on the solids than what calculations predicted. This, along with the sorption test results, indicate Sb contamination from the glass beads.

Table 11. Average mass balance recovery for all 27 columns and ± standard deviation

Mn	Fe	Tl	As	Pb	Sb	Cr	Cu
53 ± 15%	119 ± 46%	88 ± 30%	89 ± 30%	79 ± 24%	-12 ± 3%*	94 ± 3%	85 ± 31%

* Negative value due to Sb contamination of glass beads.

Effect of Challenges on the Biofilm

The center point (16°C, 0.2 mg/L Cl_2 and 1 mg/L DOC) was defined as the standard condition within the "pipe". The system was then challenged with changes in temperature (7°C, 25°C), Cl_2 (0 mg/L, 2 mg/L Cl_2) and DOC (0 mg/L, 2 mg/L DOC) in combinations as described in Table 2.

The presence of ATP (Fig. 9a) on the glass beads in the columns under all conditions proved that biofilms were grown over the course of this study. Cl_2 was the only challenge that affected ATP on the glass beads. Increasing the dose from 0.2 mg/L to 2

mg/L Cl_2 decreased the activity of the biofilm. Decreasing the dose to 0 mg/L Cl_2 caused an increase in ATP. Similar results were observed for DNA (Fig 9b) as those observed for ATP. However, due to the variations in the extraction procedure and inefficient extraction of some columns the DNA results are more qualitative than quantitative.

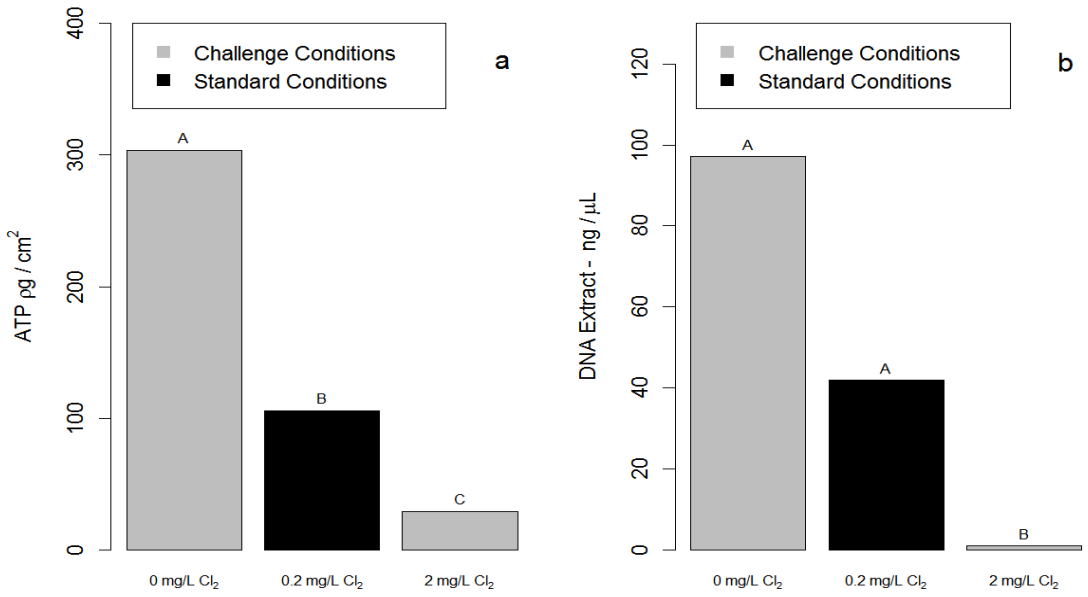

Fig. 9. a) ATP on surface of glass beads affected by Cl_2; b) DNA on surface of glass beads affected by Cl_2. ($n_{challenge}$=12; $n_{standard\ condition}$= 3). Bars connected by the same letter are not significantly different by Tukey HSD (α=0.05). Results of Tukey HSD based on log transformation of data (Fig A-1).

Ginige et al. (2011) also studied the effects of Cl_2 on laboratory grown biofilms. In their unchlorinated columns, they measured 43,500 pg/cm^2 ATP. When 3 mg/L Cl_2 was added, within 2 days the ATP concentration on the glass rings decreased to 371 pg/cm^2. In another study of biofilms grown on glass beads with no Cl_2 challenge, Van der Kooij et al. (1995) reported a maximum ATP concentration no greater than 1000 pg/cm^2. Unlike this

present study, Van der Kooij et al. (1995) reported an increase in ATP concentrations with the addition of a carbon source as acetate. The low concentration of ATP seen in this present study was the result of developing the biofilms with a Cl_2 residual during the entire study as well as the use of a less assimilable, though more relevant to DWDS, carbon source via humic-derived carbon.

The average DOC levels in the effluent during Phase 3 are illustrated in Fig. 10. Challenges of single test factors of temperature, Cl_2, and DOC, not interactions of the factors, led to an increased release of DOC compared with the standard condition. A decrease in temperature caused an increase in DOC at the effluent of the columns. Challenging the matrix with an increase in Cl_2 caused an increase in DOC in the effluent. As expected, the biofilm was destabilized with the addition of 2 mg/L Cl_2, as illustrated by the increase of DOC in the effluent and decreases in ATP and DNA on the beads. The Logan tap water contained 0.8 mg/L DOC. Influent concentrations of DOC were therefore 0.8 mg/L (0 added DOC), 1.8 mg/L (1 mg/L added DOC) and 2.8 (2 mg/L DOC). Average DOC without additional DOC (0 mg/L DOC added) was higher than the feed, indicating release of the biofilm. As expected, DOC in the effluent was influenced by the concentration in the feed solution.

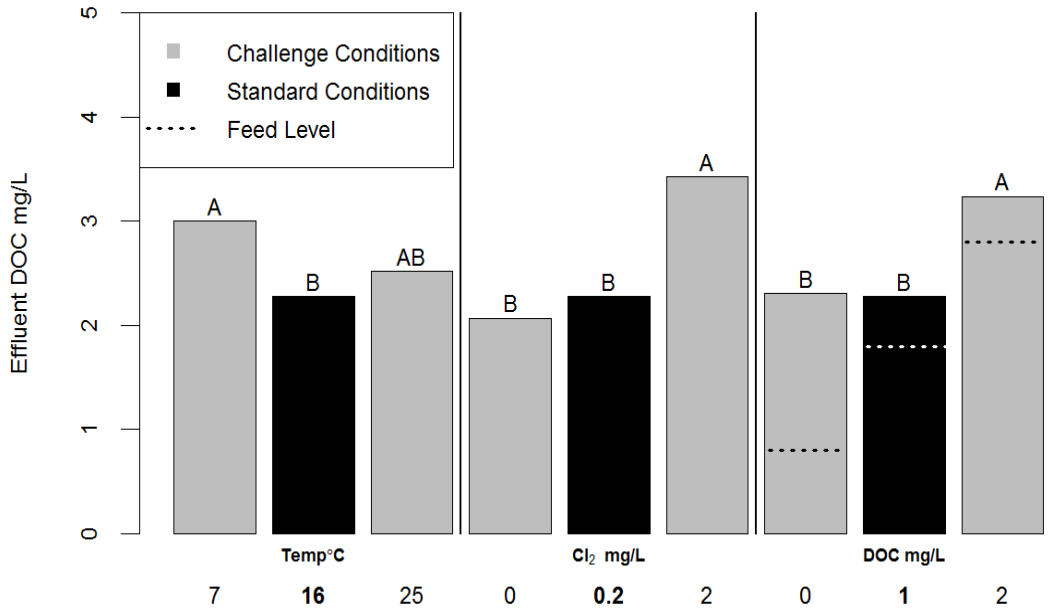

Fig. 10. Effluent DOC affected by temperature & Cl_2 & DOC ($n_{challenge}$=48; $n_{standard\ condition}$= 12) Bars connected by the same letter within factor group are not significantly different by Tukey HSD (α=0.05). Influent feed levels of DOC (Logan tap water (0.8 mg/L) plus humic derived carbon addition (0, 1, and 2 mg/L) indicated by dashed line). Box and Whisker Plot shown in Fig. A-2.

Matrix Elements

The solution concentration of the matrix elements, Mn and Fe, was determined in the effluent using the last four sampling intervals. Review of the effluent data indicated that the system was at steady-state over this time period (Fig C-1 and C-2). The following data are presented for this steady-state solution concentration and the corresponding total and sequential extraction concentration of each matrix element associated with the glass beads at the time of harvesting. Box and whisker plots of effluent and solids data are presented in Appendix A to show distribution of data where significant ANOVA was demonstrated.

Manganese (Mn)

Mn was added with the feed solution at a concentration of 35 µg/L. All effluent concentrations were less than the feed solution; therefore Mn sorbed or precipitated within the column, regardless of challenge (Fig. 11). Under standard conditions (16°C, 0.2 mg/L Cl_2 and 1 mg/L DOC) the average Mn concentration in the effluent was 10.8 µg/L. The interaction between Cl_2 and temperature affected Mn concentration in the effluent. With challenging the system, the effluent concentration of Mn decreased with addition of Cl_2 at 2 mg/L regardless of temperature compared with the standard condition. All other challenges had no effect on Mn compared with the standard condition.

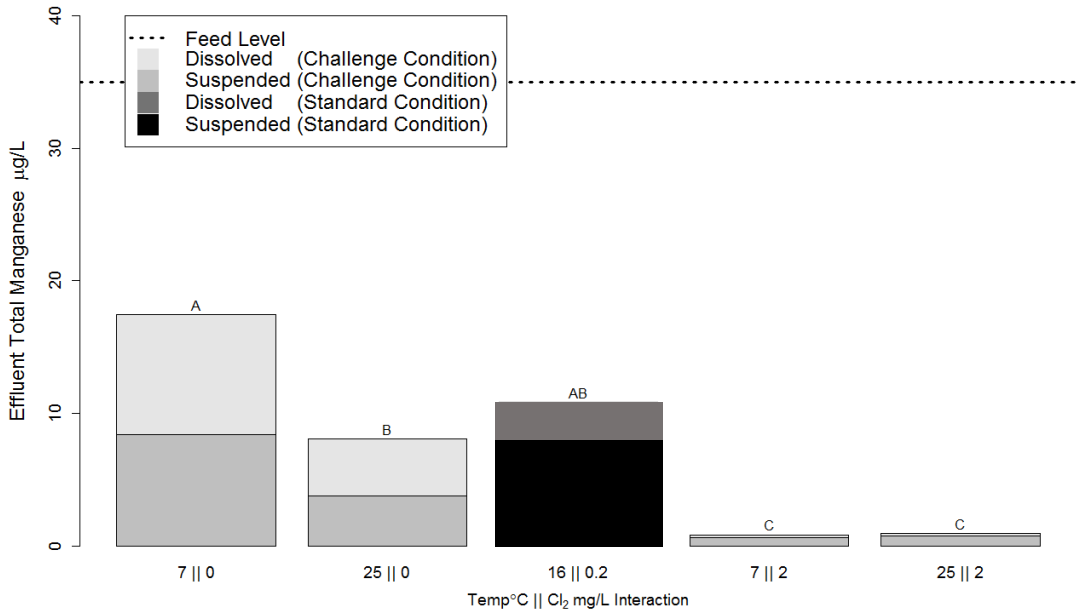

Fig. 11. Significant two way interaction of temperature||Cl_2 for effluent Mn ($n_{challenge}$= 24; $n_{standard\ condition}$= 12). The bars display the concentration of Mn associated with suspended solids and dissolved in solution. The ANOVA was performed on the total concentration of Mn in the effluent. Bars connected by the same letter are not significantly different by Tukey HSD (α=0.05) and was performed on log-transformed data (Fig A-3).

In the feed solution, 9% of the Mn was measured as suspended (Table 10). The amount of suspended solids in the effluent of the columns was impacted by the challenges as determined by significant ANOVA. Under standard conditions, 54% of Mn was associated with suspended solids (Fig. 11). The effect of redox conditions, as influenced by Cl_2 dosage, is evident with 78% of the Mn in the effluent being associated with the suspended solids at Cl_2 dosing of 2 mg/L, whereas 43% of Mn was suspended with 0 mg/l Cl_2.

Mn accumulated in the solid biofilm matrix across all columns at an average concentration of 1962 µg/g ± 431 µg/g. This equates to 30% of the total Mn added to the columns. No challenge was observed to have a significant impact on the total solid phase Mn within the biofilm matrix as analyzed by total digestion. The majority of Mn in the biofilm matrix under all challenge conditions was associated with the carbonate (~40%), organic (~35%), and Mn oxide (~20%) fractions averaging 762 µg/g, 717 µg/g, and 462 µg/g, respectively (Fig. 12).

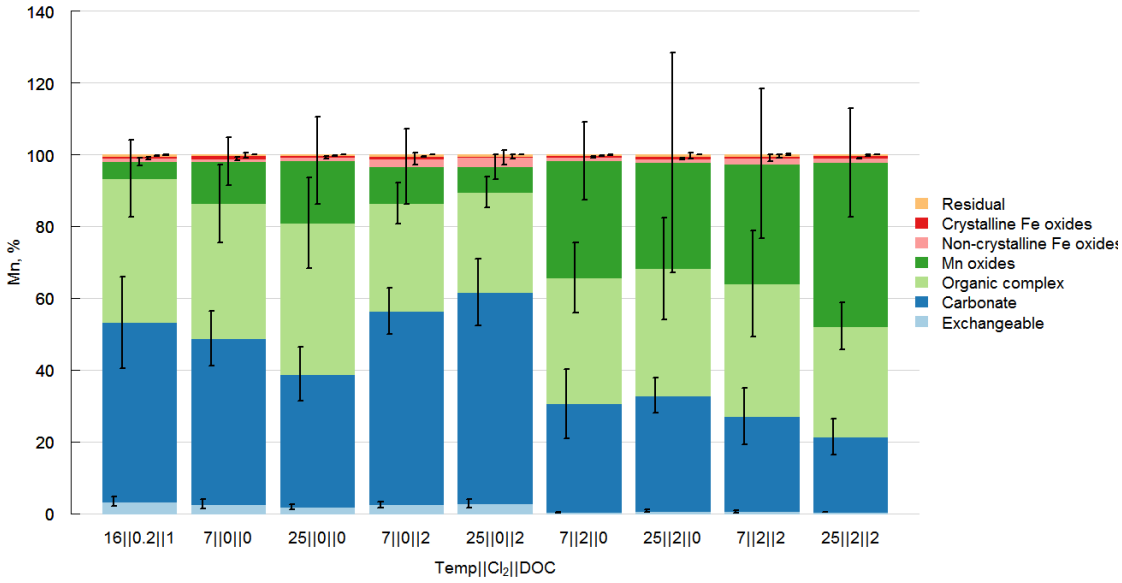

Fig. 12. Distribution of Mn as defined by sequential extractions. Units of x-axis for each challenge are °C ||mg/L Cl_2 ||mg/L DOC. Error bars equal one standard deviation (n=3).

In comparison to the swab solids, and in particular the AST swab solids due to its use as the inoculum, the column solids are dissimilar (Table 12). Within the swab solids, generated from cement lined ductile pipes, 90-100% of the Mn was associated with the more recalcitrant fractions; these include Mn oxides (24%) at 3170 µg/g and non-crystalline Fe oxides (65%) at 8560 µg/g. These differences between the column generated solids and the swab solids suggest relatively recent and short-lived growth in the column solids compared to the legacy time frames encountered in the DWDS due to mineral aging (Lock and Janssen 2003). The difference between the two swab sites is also noteworthy. The majority of Mn was in the Mn oxide fraction at UPA making up 70% of the solids rather than only 24% at AST, demonstrating the spatial variability of solid matrixes in DWDS.

Table 12: Mn sequential extraction comparison between swab and column solids.

	Mn Solid Fractions	Swab Solids		Column Solids
		AST (Fig. D-1)	UPA (Fig. D-2)	(Fig. 12)
Labile	Exchangeable	43.7 µg/g (0.32%)	0.418 µg/g (0.0%)	30.2 µg/g (1.5%)
	Carbonate	546 µg/g (4.2%)	175 µg/g (0.17%)	762 µg/g (38%)
	Organic	712 µg/g (5.4%)	540 µg/g (0.52%)	717 µg/g (36%)
Recalcitrant	Mn Oxides	3,170 µg/g (24%)	72,100 µg/g (70%)	462 µg/g (23%)
	Non Crystalline Fe Oxide	8,560 µg/g (65%)	29,600 µg/g (29%)	26 µg/g (1.3%)
	Crystalline Fe Oxide	*<372 µg/g (2.8%)	624 µg/g (0.61%)	12 µg/g (0.6%)
	Residual	55.3 µg/g (0.42%)	120 µg/g (0.12%)	7 µg/g (0.37%)

*Subtraction of residual extractant was not performed because high concentration of prior step results in negative value.

Within the biofilm matrix there were significant changes in the distribution of Mn with the addition of Cl_2 to the system (Fig. 13). A change in Cl_2 from the standard condition (to 0 or 2 mg/L) caused a decrease in Mn associated with exchangeable sites. In addition, an increase in Cl_2 (2 mg/L) caused a decrease in Mn associated with the carbonate phase. The loss of Mn from exchange sites and carbonate minerals with high Cl_2 dosage resulted in an increase in Mn associated with Mn oxides.

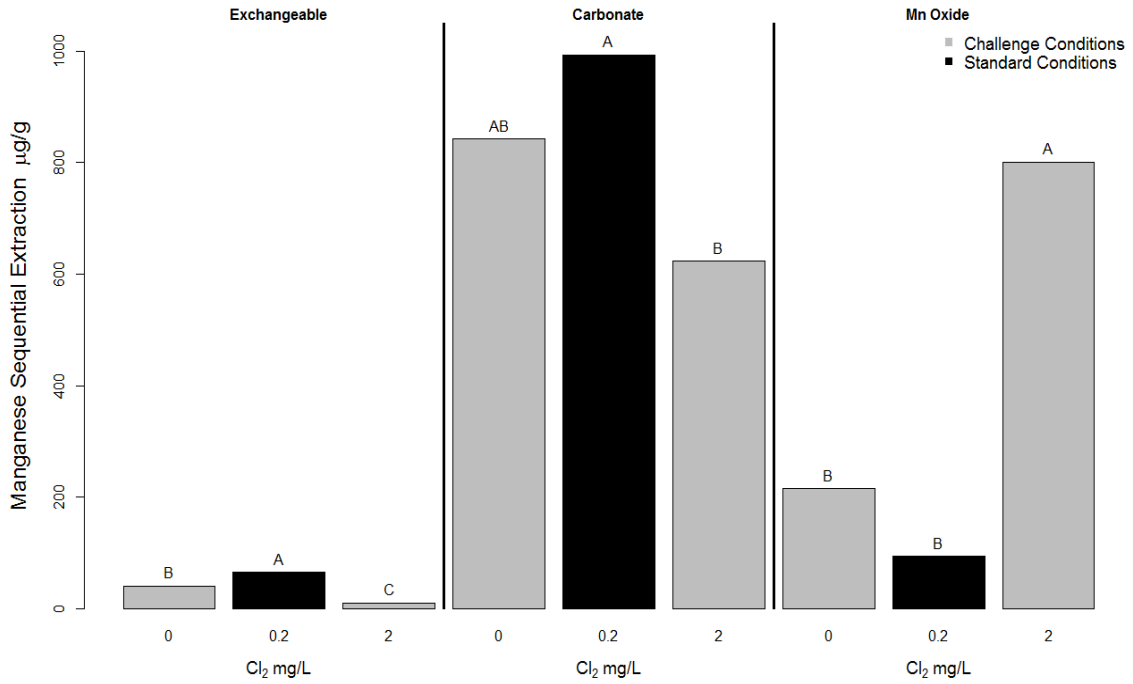

Fig. 13. Manganese associated with exchangeable, carbonate, and Mn oxide fractions affected by Cl_2 ($n_{challenge}$=12; $n_{standard\ condition}$=3). Bars connected by the same letter within factor group are not significantly different by Tukey HSD (α=0.05).

The Mn was added in the feed water as Mn^{2+} that was oxidized in the presence of Cl_2, forming Mn (III, IV) minerals, providing new surfaces for the retention of TICs. This was the accumulation mechanism that was also observed by (Peng et al. 2012). Mn(II) is the dominant form of Mn found entering DWDS (Crittenden et al. 2012) that could then be oxidized within the DWDS by abiotic and biotic processes. Ginige et al. (2011) reported increase Mn retention in laboratory produced biofilms with increased bioactivity. In this present study, the addition of Cl_2 decreased bioactivity but increased Mn retention, indicating abiotic oxidation of Mn via the addition of Cl_2.

Iron (Fe)

As with Mn, Fe was sorbed or precipitated within the column as demonstrated by the lower effluent concentration compared with the Fe added in the feed solution at 450 µg/L (Fig. 14). Under standard conditions (16°C, 0.2 mg/L Cl_2 and 1 mg/L DOC) the average Fe concentration in the effluent was 225 µg/L. The two-way interaction of Cl_2 and DOC factors affected Fe concentrations in the effluent of the columns. As observed with Mn, there was a decrease in Fe in the effluent with the addition of Cl_2 at 2 mg/L, compared to the standard condition. Unlike Mn, challenges did not impact the amount of Fe associated with suspended solids; both in the feed and the effluent, Fe remained ~99% suspended.

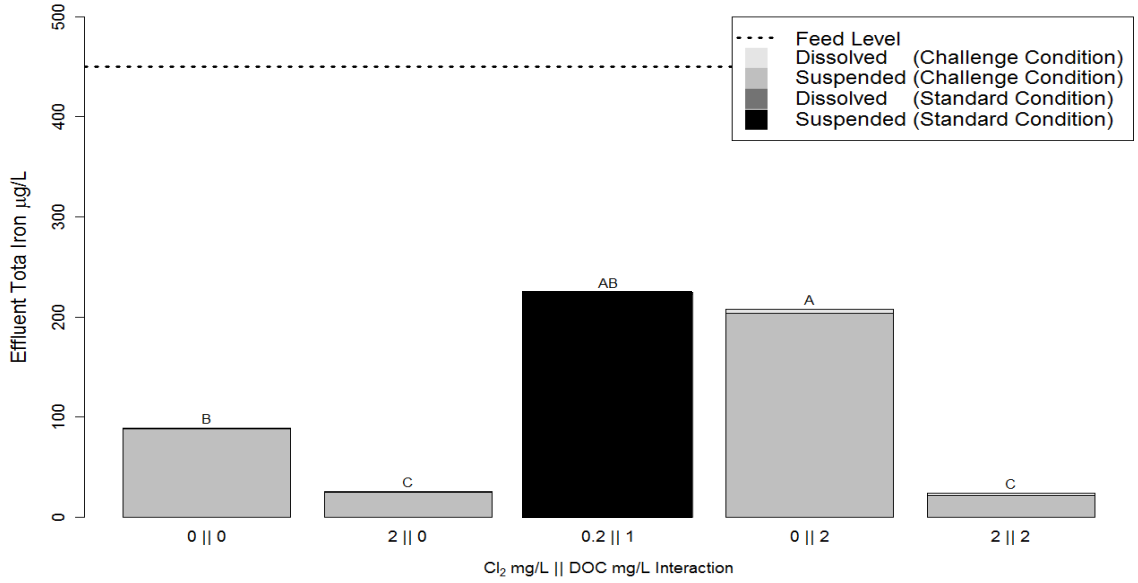

Fig. 14. Effluent Fe affected by two-way interaction of Cl_2||DOC ($n_{challenge}$=24; $n_{standard\ condition}$=12). The bars display the concentration of Fe associated with suspended solids and dissolved in solution. Bars connected by the same letter are not significantly different by Tukey HSD (α=0.05).

In the biofilm matrix there were no discernible differences in total Fe on the beads as a result of challenges. On average, across all columns about 55,000 µg/g ±1,300 µg/g of Fe sorbed or precipitated by the end of the study. The amount accumulated in the columns equaled 60% of the total mass of Fe added to the columns throughout the study. The majority of solid phase Fe (72%) (Fig. 15) accumulated in the organic fraction of the biofilm matrix at 30,000 µg/g.

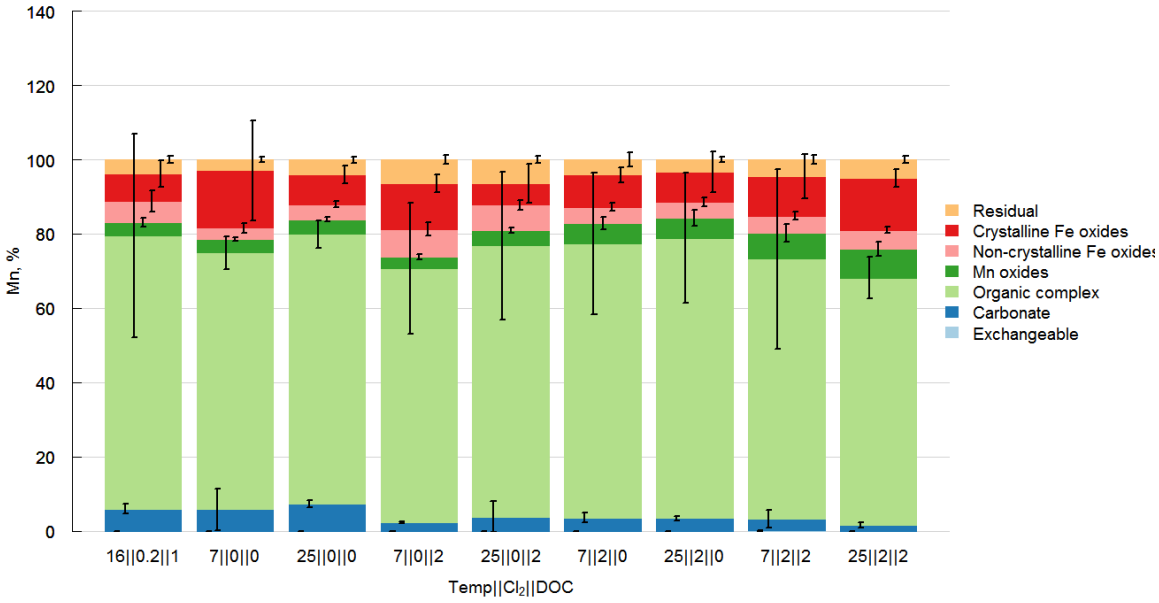

Fig. 15. Distribution of Fe as defined by sequential extractions. Units of x-axis for each challenge are °C ||mg/L Cl_2 ||mg/L DOC. Error bars equal one standard deviation (n=3).

The organic fraction of Fe in the AST and UPA solids was also considerable with a concentration of 19,400 µg/g (19%) and 20,100 µg/g (16%), respectively. But the majority of Fe was associated with the crystalline Fe oxides at 39,700 (40%) and 51,900 µg/g (42%) for AST and UPA, respectively (Table 13). Swab solids from both sites were similar. The greater association of Fe with the more recalcitrant fractions of the swab solids

could be a result of the legacy time frames experienced in the DWDS resulting in mineral transformations from non-crystalline to more crystalline structures (Lock and Janssen 2003).

Table 13: Fe sequential extraction comparison between swab and column solids.

	Fe Solid Fractions	Swab Solids AST (Fig. D-1)	Swab Solids UPA (Fig. D-2)	Column Solids (Fig. 15)
Labile	Exchangeable	<0.74 µg/g (0.0%)	<0.84 µg/g (0.0%)	4.42 µg/g (0.01%)
	Carbonate	11,200 µg/g (11%)	5,820 µg/g (4.7%)	1,750 µg/g (4.2%)
	Organic	19,400 µg/g (19%)	20,100 µg/g (16%)	30,200 µg/g (72%)
Recalcitrant	Mn Oxides	2,200 µg/g (2.2%)	*<179 µg/g (0.2%)	2,060 µg/g (4.9%)
	Non Cryst. Fe Oxide	26,500 µg/g (27%)	42,200 µg/g (34%)	2,100 µg/g (5.0%)
	Cryst. Fe Oxide	39,700 µg/g (40%)	51,900 µg/g (42%)	4,160 µg/g (9.9%)
	Residual	959 µg/g (0.96%)	3,110 µg/g (2.5%)	1,860 µg/g (4.4%)

*Subtraction of the concentration of Fe associated with the previous extractant from the indicated extraction step resulted in a negative value.

Within the column solids there were significant differences in the distribution of Fe in the biofilm matrix among challenges (Fig. 16). The carbonate phase showed a decrease in associated Fe with an increase in DOC. Iron associated with the Mn oxide phase increased significantly with an increase in Cl_2. Iron was added to the columns as Fe(III) and therefore was added to the columns in suspended form (Table 10). The increased Fe associated with the biofilm matrix was the result of the Mn(II) being oxidized by the additional Cl_2, adding additional surface area for the accumulation of Fe.

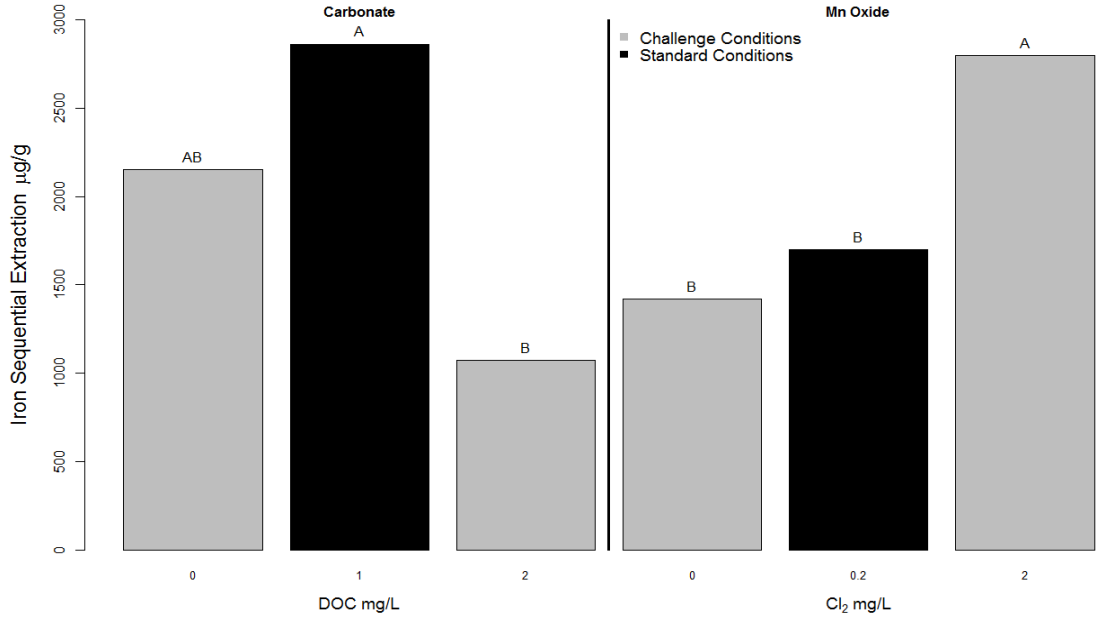

Fig. 16. Iron associated with carbonate and Mn oxide fractions affected by DOC and Cl_2 respectively ($n_{challenge}$=12; $n_{standard\ condition}$=3). Bars connected by the same letter within factor group are not significantly different by Tukey HSD (α=0.05).

TICs

As with the matrix elements, the solution concentrations were determined in the effluent using the last four sampling intervals (Appendix C). Data are presented for this steady-state solution concentration as well as the corresponding total concentration of each TIC element associated with the biofilm matrix extracted from the glass beads at the time of harvesting. Additional box and whisker plots are included in Appendix A to illustrate the distribution of data.

Arsenic (As)

Arsenic was fed into the columns at the MCL of 10 µg/L, and all columns showed sorption or precipitation of As (Fig.17 a) except for 7 °C, 0 mg/L, and 2 mg/L DOC which

demonstrated a release of As. Under standard conditions, effluent As levels occurred at 8.4 µg/L. Significant changes occurred when the columns were challenged with low temperature (7 °C) and low DOC (0 mg/L), resulting in a decrease in As in the effluent with or without Cl_2. Suspended As in the effluent of the columns was affected by challenges. An increase in Cl_2 caused a decrease in suspended As compared to the standard conditions from ~10% to ~3%. In the biofilm matrix, an increase in DOC to 2 mg/L decreased the concentration of As (Fig.17 b). At low DOC (0 mg/L or 1 mg/L) 20% of the total influent As was removed by the biofilm matrix. At high DOC (2 mg/L), the removal efficiency dropped to 13%.

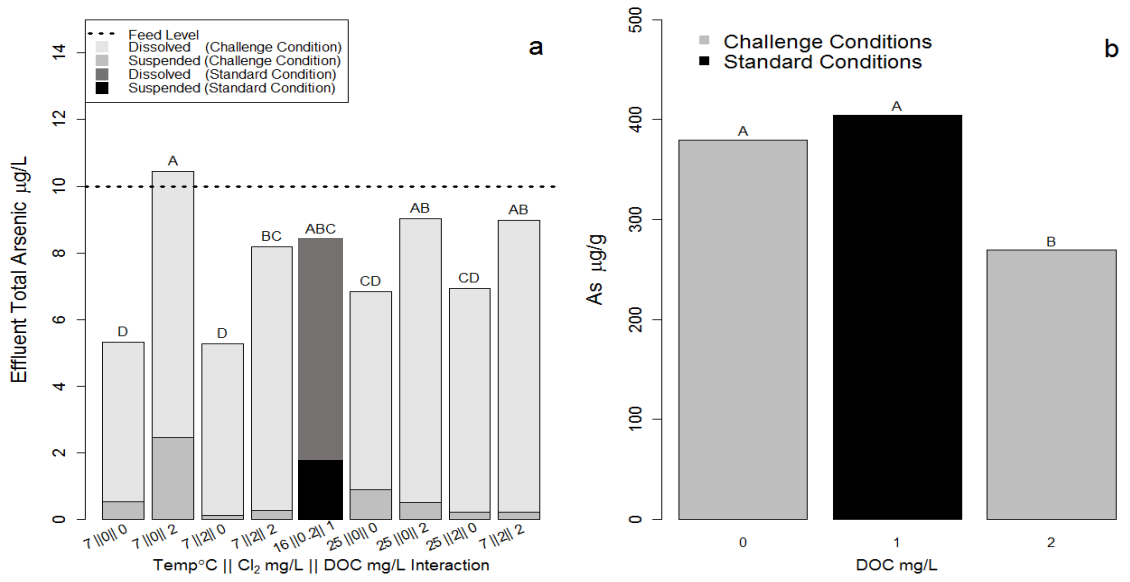

Fig. 17. (a) Effluent As affected by three way temperature||Cl_2||DOC interaction ($n_{challenge}$=12; $n_{standard\ condition}$=12). The bars display the concentration of As associated with suspended solids and dissolved in solution. The ANOVA was performed on the total concentration of As in the effluent. Challenge condition n = 36 Standard condition n=36. (b) Biofilm matrix As affected by DOC ($n_{challenge}$=12; $n_{standard\ condition}$=3). Bars connected by the same letter are not significantly different by Tukey HSD (α=0.05). Box and Whisker plot shown in Fig. A-5.

Arsenic in the biofilm matrix was positively correlated with both Fe and Mn (Fig. 18). Arsenic has been shown to sorb to both Fe and Mn oxides (Lytle and Liggett 2011; Watanabe et al. 2012).

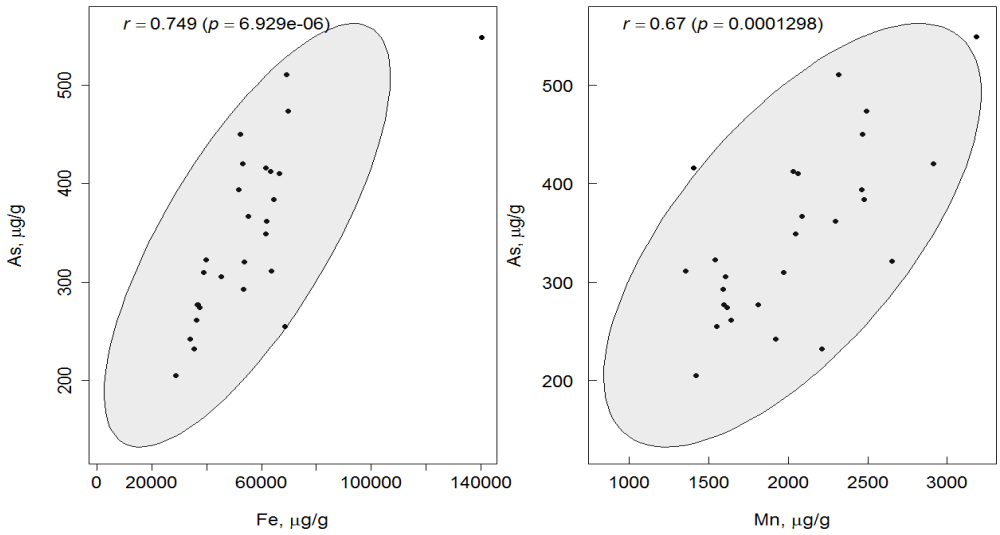

Fig. 18. Correlation analysis of As with matrix elements Fe and Mn within the biofilm matrix (n=27). Shaded ellipse is 95% joint confidence region.

Within the biofilm matrix the majority of As, defined by sequential extraction (Fig. 19) accumulated in the exchangeable, carbonate, and organic fractions, at 66.3 µg/g (20%), 66.1 µg/g (20%), and 184 µg/g (56%) respectively.

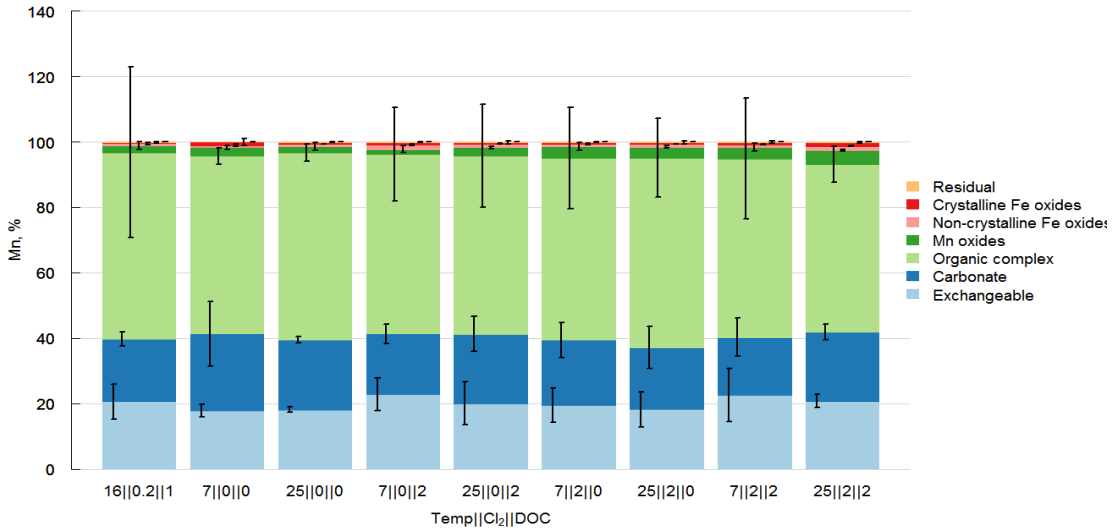

Fig. 19. Distribution of As as defined by sequential extractions. Units of x-axis for each challenge are °C ||mg/L Cl2 ||mg/L DOC. Error bars equal to standard deviation of mean (n=3).

The association of As with the organic fraction is also displayed in the AST and UPA swab solids making up approximately 50% of the total As at both swabbing sites (Table 14). Unlike the swab solids, the As in the column solids was associated with more labile fractions such that a combined 40% was associated with the exchangeable and carbonate fractions.

Table 14: As sequential extraction comparison between swab and column solids.

As Solid Fractions		Swab Solids AST (Fig. D-1)	Swab Solids UPA (Fig. D-2)	Column Solids (Fig. 19)
Labile	Exchangeable	59.0 µg/g (5.3%)	81.0 µg/g (12%)	66.3 µg/g (20%)
	Carbonate	50.6 µg/g (4.5%)	43.4 µg/g (6.5%)	66.1 µg/g (20%)
Recalcitrant	Organic	561 µg/g (50%)	311 µg/g (47%)	184 µg/g (56%)
	Mn Oxides	178 µg/g (16%)	72.2 µg/g (11%)	9.14 µg/g (2.7%)
	Non Cryst. Fe Oxide	247 µg/g (22%)	121 µg/g (18%)	2.93 µg/g (0.89%)
	Cryst. Fe Oxide	22.6 µg/g (2.0%)	34.8 µg/g (5.2%)	2.24 µg/g (0.68%)
	Residual	*<12.1µg/g (1.1%)	1.30 µg/g (0.20%)	0.494 µg/g (0.15%)

*Subtraction of the concentration of As associated with the previous extractant from the indicated extraction step resulted in a negative value.

Within the biofilm matrix, significant effects were observed in the exchangeable and organic fractions (Fig. 20), showing that an increase in both temperature and DOC resulted in a significant decrease in As associated with both the exchangeable and organic phase of the biofilm matrix.

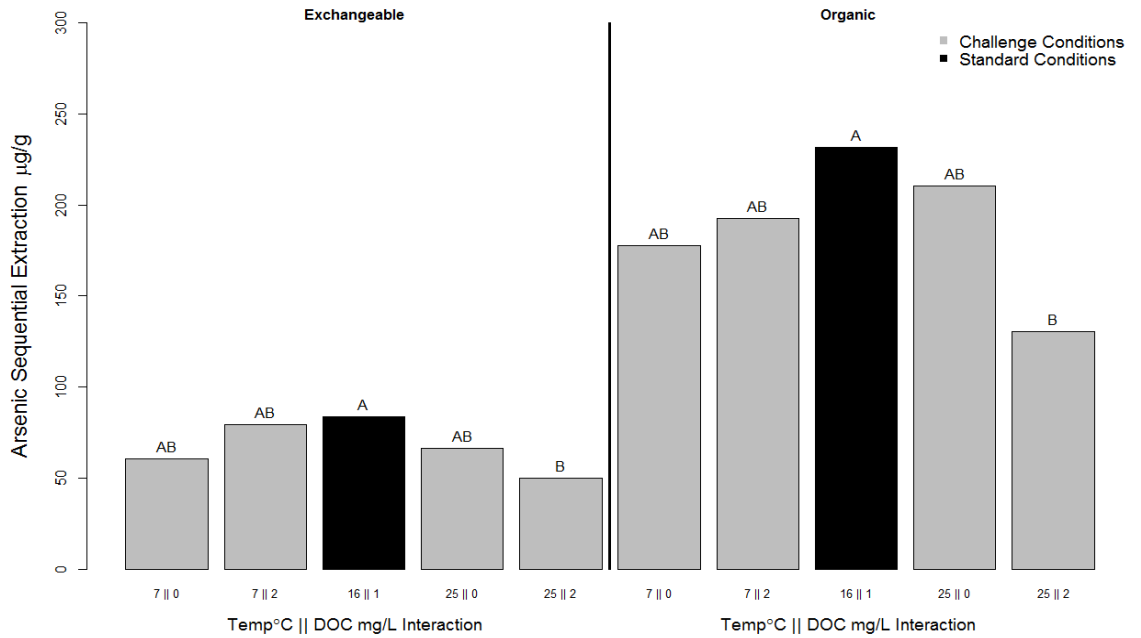

Fig. 20. Arsenic associated with exchangeable and organic sequential extraction fractions affected by two way temperature||DOC interaction ($n_{challenge}$=6; $n_{standard\ condition}$=3). Bars connected by the same letter within factor group are not significantly different by Tukey HSD (α=0.05).

The biofilm matrix showed a decrease in As with the addition of DOC in both the exchangeable and organic fractions, suggesting a competition for exchange sites and/or chelation mechanism, similar to the findings of Grafe et al. (2001) where the ability of DOC to increase As bioavailability was observed. However, no relationship of DOC and As was observed in the effluent of this study. It was also observed that As did not associate

with the Fe oxides as defined by the sequential extraction as was expected. This may have been due to the high inorganic carbon content of the feed water (203 mg/L HCO_3), inhibiting sorption of As to Fe oxides as observed by Holms (2002). However, a significant relationship of As with Fe and Mn was observed by correlation analysis in the biofilm matrix (Fig. 18). This suggests that As is associated with Fe and Mn. The sequential extraction is based on operationally defined mineral phases. Newly formed Fe and Mn oxides, over the time scale of this study compared to soil and sediment systems for which these extractions were developed, may be extracted with milder reagents. A more likely scenario is that As associated with Fe and Mn oxides are being sequestered within the biofilm matrix resulting in them being included in the organic fraction rather than any of the defined Mn or Fe fractions.

Lead (Pb)

Lead was fed into the columns at the regulated action level of 15 μg/L, and all columns showed sorption or precipitation of Pb across all challenges (Fig. 21 a). Under standard conditions (16°C, 0.2 mg/L Cl_2, and 1 mg/L DOC) the average Pb concentration in the effluent was 3.5 μg/L. More Pb was released from columns with a decrease in both temperature and Cl_2 along with an increase in DOC (7°C, 0 mg/L Cl_2, and 2 mg/L DOC). Suspended Pb in the effluent was impacted by the challenges as determined by significant ANOVA, with an increase in both Cl_2 and DOC causing a drop in suspended Pb from 95% to 83%. In the biofilm matrix an increase in DOC caused less accumulation of Pb (Fig. 21 b). Of the total added Pb in the influent over the duration of the study, 55% accumulated in the biofilm matrix under standard conditions. When the DOC was increased to 2 mg/L

this value dropped to 40%. No change occurred when the addition of DOC was decreased to 0 mg/L.

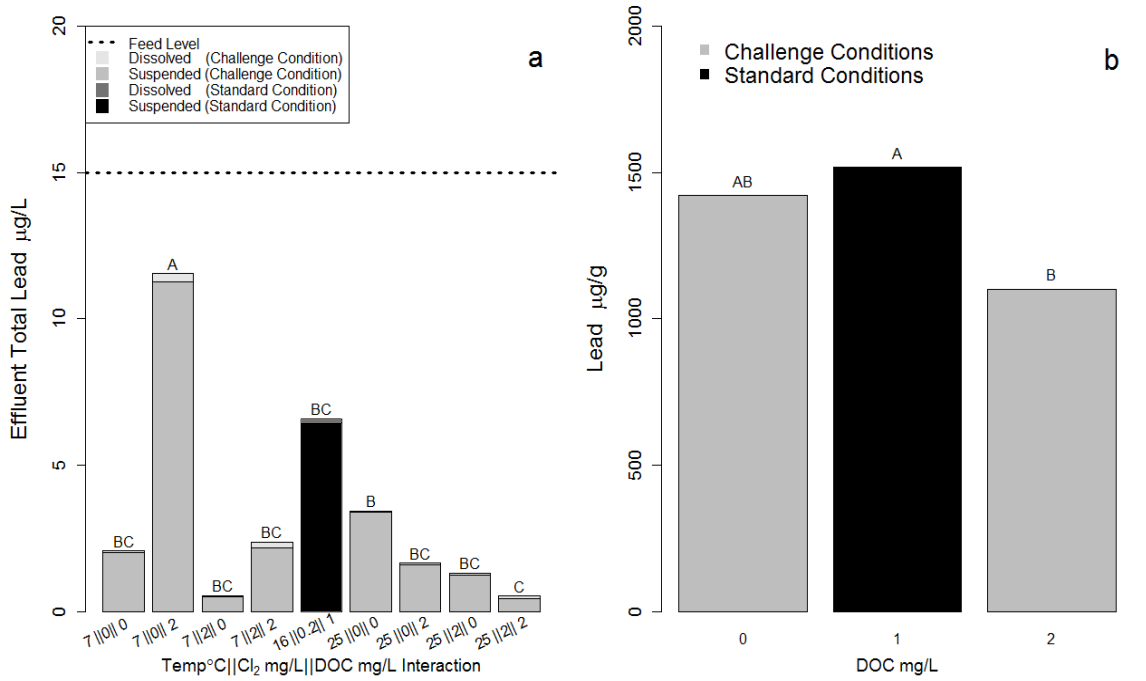

Fig. 21. (a) Effluent Pb affected by three way interaction of temperature||Cl_2||DOC ($n_{challenge}$=12; $n_{standard\ condition}$=12). The bars display the concentration of Pb associated with suspended solids and dissolved in solution. The ANOVA was performed on the total concentration of Pb in the effluent. Challenge condition n=12 Standard condition n=12. (b) Biofilm matrix Pb affected by DOC ($n_{challenge}$=12; $n_{standard\ condition}$=3). Bars connected by the same letter within factor group are not significantly different by Tukey HSD (α=0.05). Box and Whisker plot shown in Fig. A-6.

Correlation analysis shows Pb associating with both Fe and Mn solids (Fig. 22). Iron and Mn oxides have been shown in other studies to have a high affinity for Pb (Hua et al. 2012) with biogenically oxidized Mn having especially high adsorption capacity for Pb (Nelson et al. 2002).

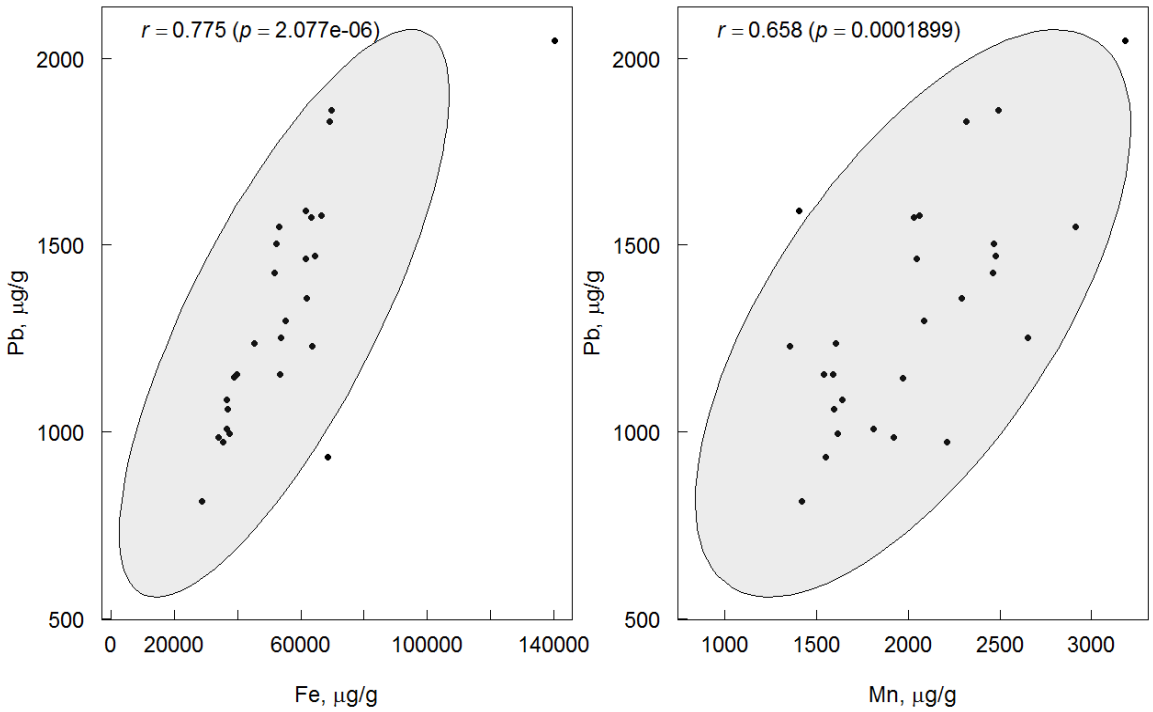

Fig. 22. Correlation analysis of Pb with matrix elements Fe and Mn within the biofilm matrix (n=27). Shaded ellipse is 95% joint confidence region.

The majority of Pb was associated with the carbonate and organic fractions of the biofilm matrix at 743 µg/g (62%) and 409 µg/g (34%) respectively (Fig. 23) and not Mn or Fe as described by the correlation analysis. This was due to Fe and Mn associated Pb being included in the carbonate and organic fractions solids, as discussed under As behavior.

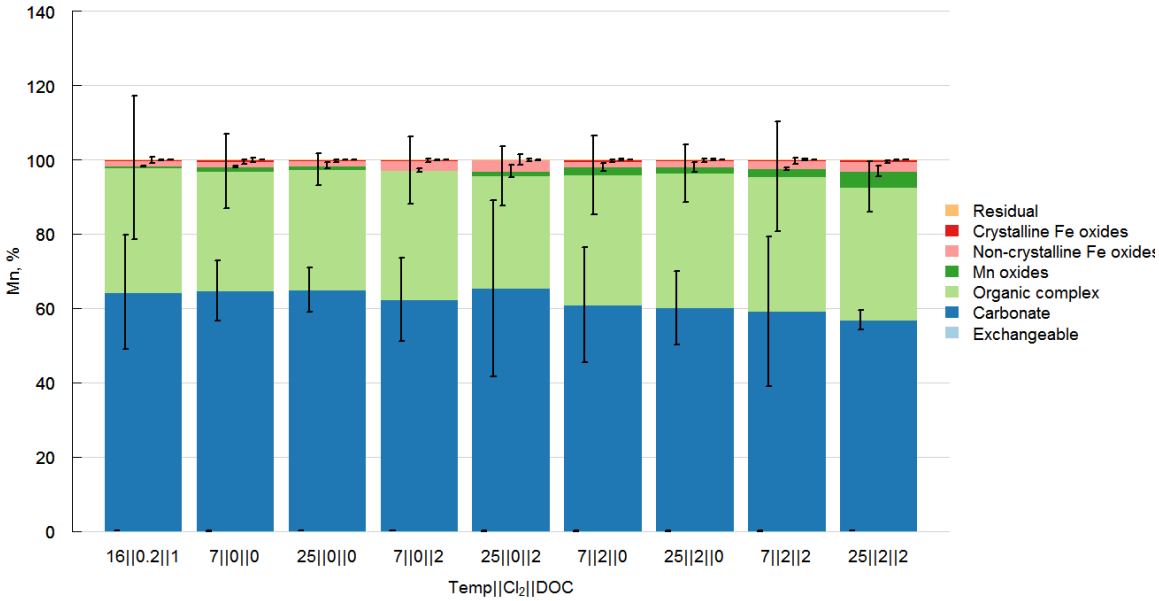

Fig. 23. Distribution of Pb as defined by sequential extractions. Units of x-axis for each challenge are °C ||mg/L Cl_2||mg/L DOC. Error bars equal to standard deviation of mean (n=3).

In the AST swab solids these same fractions were observed to hold significant concentrations of Pb at 220 µg/g and 151 µg/g respectively, though together they only account for 15% of the total Pb (Table 15). The majority of Pb in the swab solids at AST and UPA (~80%) was found in the more recalcitrant non-crystalline Fe oxide fraction at 1,880 µg/g and 5,500 µg/L, respectively. This is due to the legacy time frames experienced in the DWDS and also the aggressive nature of the swab cleaning trial.

Table 15: Pb sequential extraction comparison between swab and column solids.

Pb Solids Fraction		Swab Solids AST (Fig. D-1)	Swab Solids UPA (Fig. D-2)	Column Solids (Fig. 23)
Labile	Exchangeable	<0.40 µg/g (0.0%)	<0.40 µg/g (0.0%)	<0.41 µg/g (0.0%)
	Carbonate	220 µg/g (9.3%)	575 µg/g (8.8%)	743 µg/g (62%)
	Organic	151µg/g (6.4%)	115 µg/g (1.7%)	409 µg/g (34%)
Recalcitrant	Mn Oxides	19.4 µg/g (0.8%)	8.67 µg/g (0.13%)	17.9 µg/g (1.5%)
	Non Cryst. Fe Oxide	1,880 µg/g (79%)	5,500 µg/g (85%)	23.0 µg/g (1.9%)
	Cryst. Fe Oxide	102 µg/g (4.3%)	301 µg/g (4.6%)	3.13 µg/g (0.26%)
	Residual	0.50 µg/g (0.0%)	6.42 µg/g (0.1%)	0.52 µg/g (0.04%)

Within the biofilm matrix, significant effects due to challenges occurred in the carbonate and Mn oxide fractions (Fig. 24), where an increase in temperature and DOC resulted in less Pb associated with the carbonate fraction. An increase in Cl_2 however, resulted in an increase in the Mn oxide fraction.

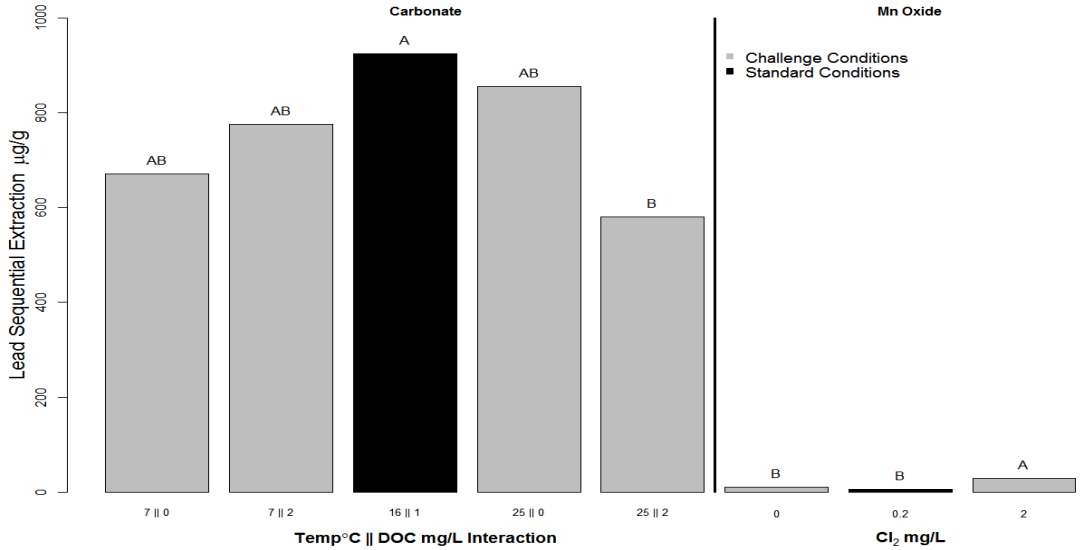

Fig. 24. Lead associated with carbonate and Mn oxide sequential extraction fractions affected by two-way interaction of temperature||DOC ($n_{challenge}$=6; $n_{standard\ condition}$=3) and one way interaction of Cl_2 respectively ($n_{challenge}$=12; $n_{standard\ condition}$=3). Bars connected by the same letter within factor group are not significantly different by Tukey HSD (α=0.05).

In a study conducted by Kim and Herrera (2010) the researchers observed that a Cl_2 residual of 0.5-1 mg/L was enough to provide favorable conditions for the formation of PbO_2 scale. In another study by Lin and Valentine (2009), the researchers observed that the addition of natural organic matter (NOM) could reduce PbO_2 to Pb(II) resulting in release of Pb from the scale. In this present study, an increase in effluent Pb was observed with decreased temperature, Cl_2, and high DOC (Fig. 21 a). A release of Pb from the biofilm matrix was observed with increased DOC at 25°C in the carbonate fraction compared to the standard condition (Fig. 24). It was also observed that increasing both DOC and Cl_2 resulted in less suspended Pb. Correlation analysis (Fig. 22) demonstrated a relationship between Pb and both Fe and Mn. Though the results are mixed, they do show the possible interactions described by Kim and Herrera (2010) and Lin and Valentine (2009), where the addition of Cl_2 increased retention of Pb, while the addition of DOC caused a decrease of Pb in the solids. Additionally, an increase in the Mn oxide fraction was also observed. This is likely the result of additional surface sites caused by the formation of Mn oxides as a result of the addition of Cl_2 (Fig. 24).

Thallium (Tl)

The concentration of Tl in the feed solution was 2.25 µg/L (MCL = 2.0 µg/L); all columns showed sorption or precipitation of Tl (Fig. 25 a). Under standard conditions (16°C, 0.2 mg/L Cl_2 and 1 mg/L DOC) the average Tl concentration in the effluent was 2.00 µg/L. Only single factor effects were observed for Tl; there were no interactions. A change in temperature from 16°C to either 7°C or 25°C or a change in DOC from 1 mg/L

to either 0 or 2 mg/L decreased Tl in the effluent. The largest difference from the standard condition was the addition of 2 mg/L Cl_2, causing an effluent concentration of 0.5 µg/l. Only 13% of the Tl was associated with suspended solids in the effluent and the challenges did not affect this distribution. Compared with the standard condition, adding Cl_2 increased the total Tl on the biofilm matrix in the columns (Fig. 25 b) from 6% of total influent Tl added to 12%.

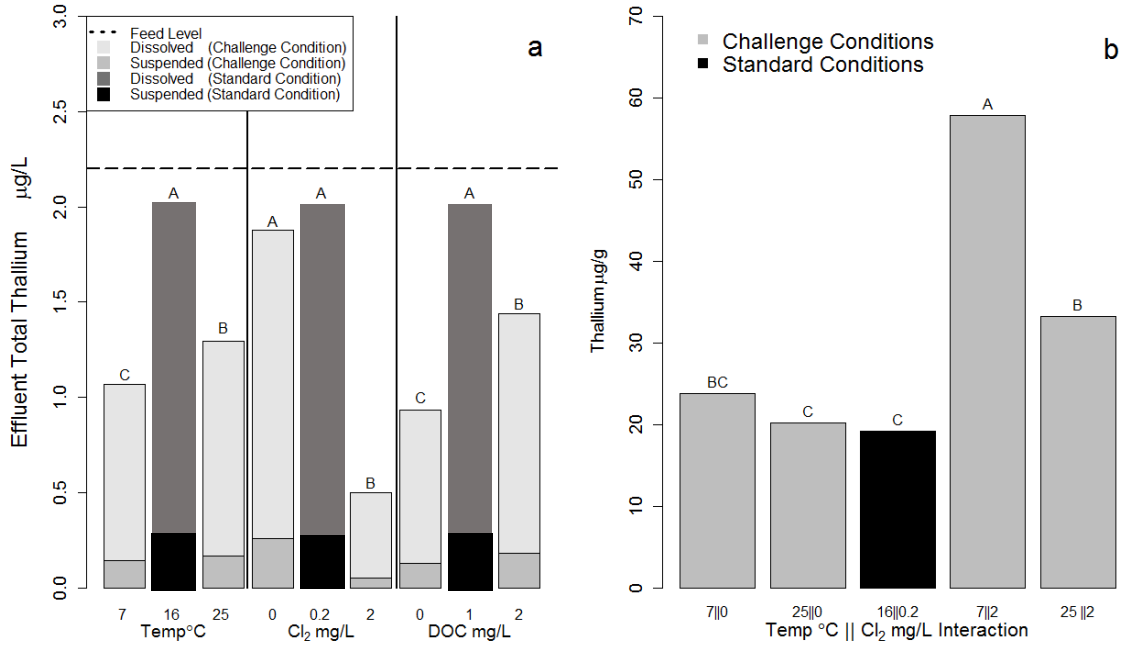

Fig. 25. (a) Effluent Tl affected by Temperature & Cl2 & DOC ($n_{challenge}$=48; $n_{standard\ condition}$=12). The bars display the concentration of Tl associated with suspended solids and dissolved in solution. The ANOVA was performed on the total concentration of Tl in the effluent. (b) Biofilm matrix Tl affected by two-way interaction of temperature||Cl_2 ($n_{challenge}$=6; $n_{standard\ condition}$ = 3). Bars connected by the same letter within factor group are not significantly different by Tukey HSD (α = 0.05). Box and Whisker plot shown in Fig. A-7.

Correlation analysis of Tl (Fig. 26), unlike as observed for As and Pb, showed no correlation with Fe. A weak albeit significant relationship with Mn was observed. Jacobson

et al. (2005) observed similar results, observing a strong association of Tl with Mn oxides and a poor association with Fe oxides.

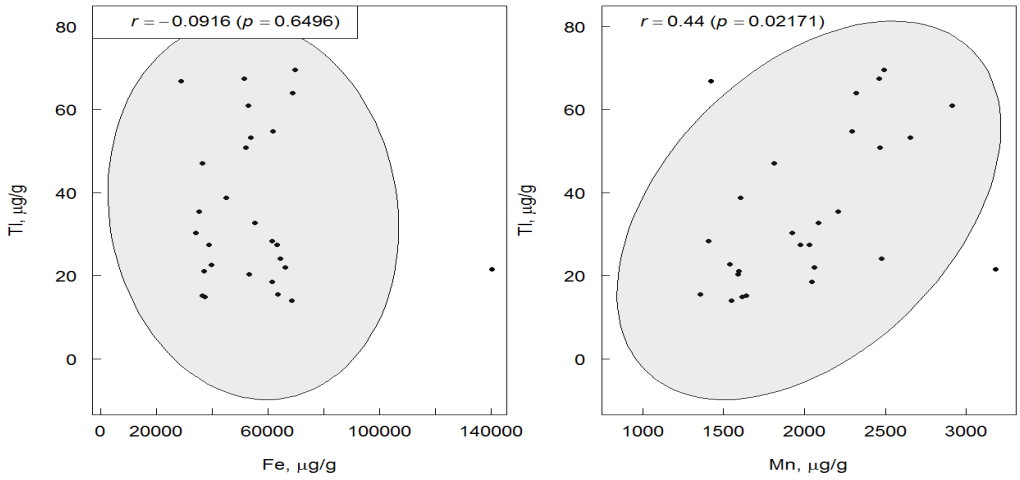

Fig. 26. Correlation analysis of Tl with matrix elements Fe and Mn within the biofilm matrix (n=27). Shaded ellipse is 95% joint confidence region.

The majority of Tl in the biofilm matrix (Fig. 27) accumulated in the exchangeable fraction at 11.5 µg/g (34%), carbonate at 13.1 µg/g (39%), organic at 4.79 µg/g (14%), and Mn oxide fractions at 2.75 µg/g (8.1%).

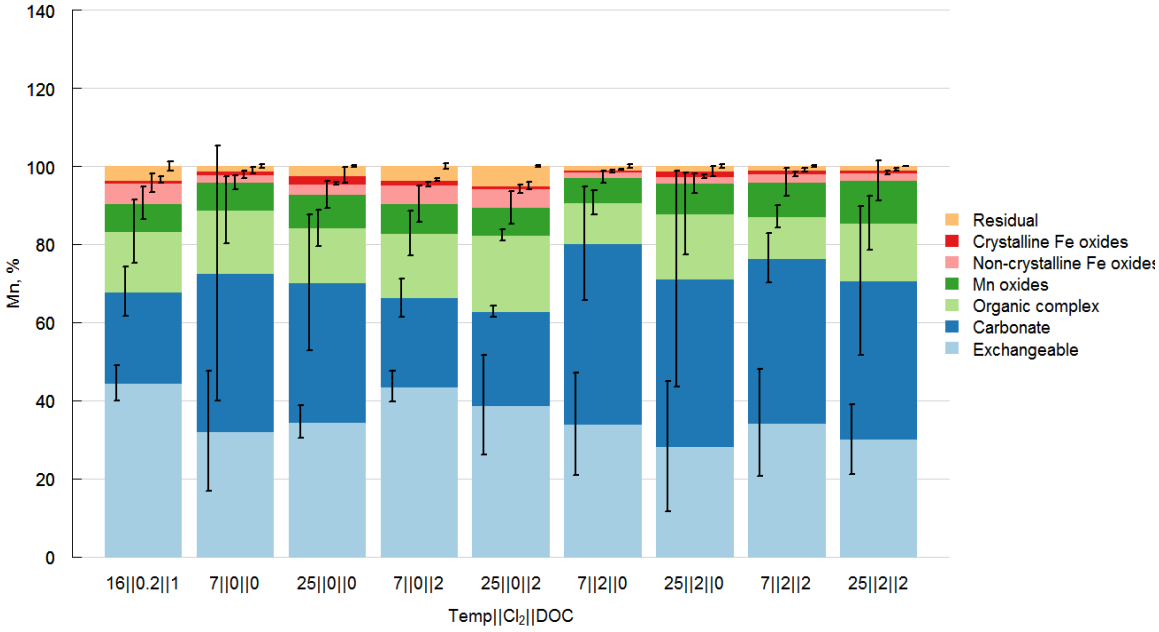

Fig. 27. Distribution of Tl as defined by sequential extractions. Units of x-axis for each challenge are °C ||mg/L Cl_2 ||mg/L DOC. Error bars equal to standard deviation of mean (n=3).

This distribution is similar to what was observed in the AST pipe solids (Table 16), with the majority of Tl being associated with the same fractions as those seen in the AST swab solids at 81.7 µg/g (7.4%), 315 4g/g (28%), 93.7 µg/g (8.5%), and 253 µg/g (23%) respectively. These results are also similar to the major fractions of Tl in the UPA swab solids though with considerable more Tl associated with the carbonate fraction making up 61% of the total Tl in the UPA solids compared to only 28% in AST.

Table 16: Tl sequential extraction comparison between swab and column solids.

	Tl Solid Fractions	Swab Solids AST (Fig. D-1)	Swab Solids UPA (Fig. D-2)	Column Solids (Fig. 27)
Labile	Exchangeable	81.7 µg/g (7.4%)	85.8 µg/g (11%)	11.5 µg/g (34%)
	Carbonate	314 µg/g (28%)	485 µg/g (61%)	13.1 µg/g (39%)
	Organic	93.7 µg/g (8.5%)	*<8.71 µg/g (1.1%)	4.79 µg/g (14%)
Recalcitrant	Mn Oxides	253 µg/g (23%)	136 µg/g (17%)	2.75 µg/g (8.1%)
	Non Cryst. Fe Oxide	321 µg/g (29%)	80.2 µg/g (10%)	0.829 µg/g (2.4%)
	Cryst. Fe Oxide	40.3 µg/g (3.6%)	6.17 µg/g (0.8%)	0.342 µg/g (1.0%)
	Residual	1.98 µg/g (0.2%)	0.7 µg/g (0.1%)	0.554 µg/g (1.6%)

*Subtraction of the concentration of Tl associated with the previous extractant from the indicated extraction step resulted in a negative value.

In the biofilm matrix, Tl associated with exchange sites, carbonate minerals, and organic matter increased relative to the standard condition when Cl_2 levels were raised to 2 mg/L Cl_2. An interaction between Cl_2 and DOC was observed in the Mn oxide phase where the addition of DOC and Cl_2 caused an increase in Tl.

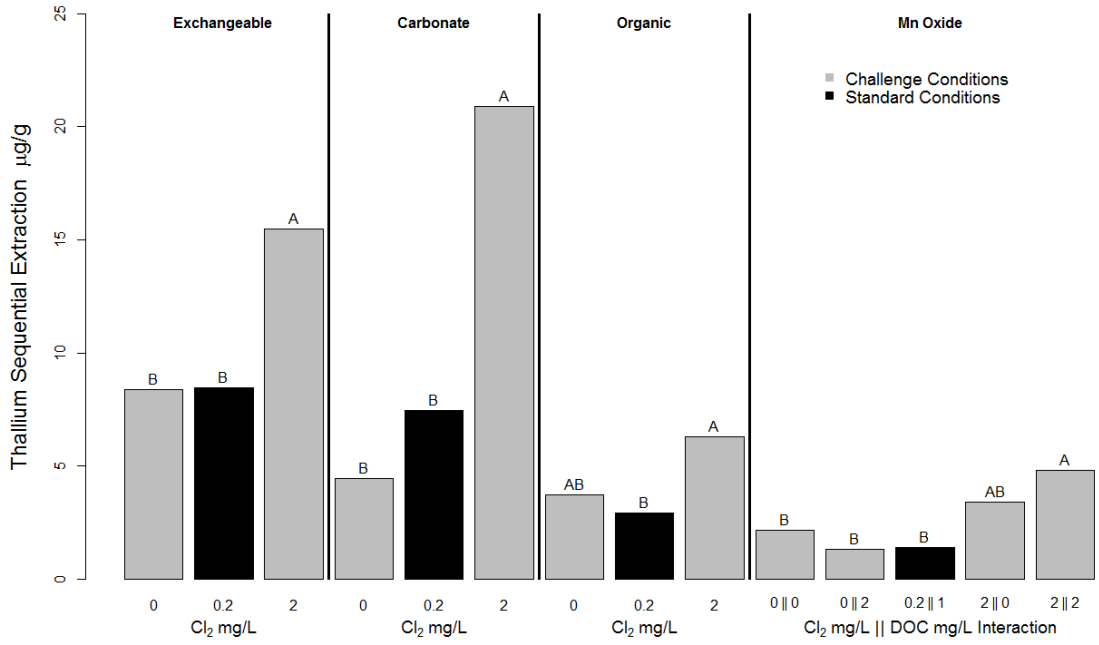

Fig. 28. Thallium associated with exchangeable, carbonate, and organic sequential extraction fractions affected by Cl_2 ($n_{challenge}$=12; $n_{standard\ condition}$=3). Additionally Mn oxide fraction affected by two way Cl_2||DOC interaction ($n_{challenge}$=6; $n_{standard\ condition}$=3). Bars connected by the same letter within factor group are not significantly different by Tukey HSD (α=0.05).

Tl is known to associate with Mn oxides (Jacobson et al. 2005) on exchange sites. There was an increase of Mn oxides with Cl_2 addition (Fig. 28) and an increase in exchangeable Tl and other more easily extractable solid phases such as the carbonate and organic fractions. Peng et al. (2011) stated that these phases are the most easily released with changes in conditions. Correlation analysis demonstrated that total Tl concentration in the biofilm solids across all treatments was correlated with total Mn, but not Fe (Fig. 26). From the sequential extraction results and the relationship demonstrated by correlation, Tl is associated with Mn in these solids.

The redox potential of Mn ($MnO_2 + 4H^+ + 2\ e^- = Mn^{2+} + 2H_2O$; $E^o = 1.23V$) and Tl ($Tl^{3+} + 2e^- = Tl^+$; $E^o = 1.25V$) are similar. The oxidation and precipitation of Mn was observed with Cl_2 addition. However the addition of Cl_2 did not impact the suspended Tl in the effluent, though Tl retention in the columns increased. These results may indicate that the retention of Tl occurred only when continually oxidized by Cl_2 in the columns. This may explain why Cl_2 did not impact effluent suspended Tl because the oxidized Tl in the effluent was given enough time to be reduced back to the Tl(I), unlike Mn which remained oxidized. Tl(III) is relatively unstable; therefore Tl(I) is the preferred oxidation state (USEPA 2012). These results indicate that Tl was retained in the columns mainly through precipitation by continuous oxidation of Tl(I) to Tl(III) by Cl_2.

Copper (Cu)

Cu was fed into the columns at 30 μg/L (action level = 1,300 μg/L), and all columns showed sorption or precipitation of Cu (Fig. 29). Under the standard conditions (16°C, 0.2 mg/L Cl_2 and 1 mg/L DOC) the average Cu concentration in the effluent was 14.8 μg/L. Significant changes occurred when the DOC was decreased to 0 mg/L, regardless of temperature (7 or 25°C), resulting in a decrease of Cu in the effluent. Adding DOC at 2 mg/L at 7°C caused an increase in Cu in the effluent. The suspended Cu in the effluent was about 45% with no impact from challenges. The biofilm matrix showed no significant change with challenge, containing on average across all columns 1980 μg/g ± 460 μg/g Cu. This equates to about 33% of the total Cu added during the entire study.

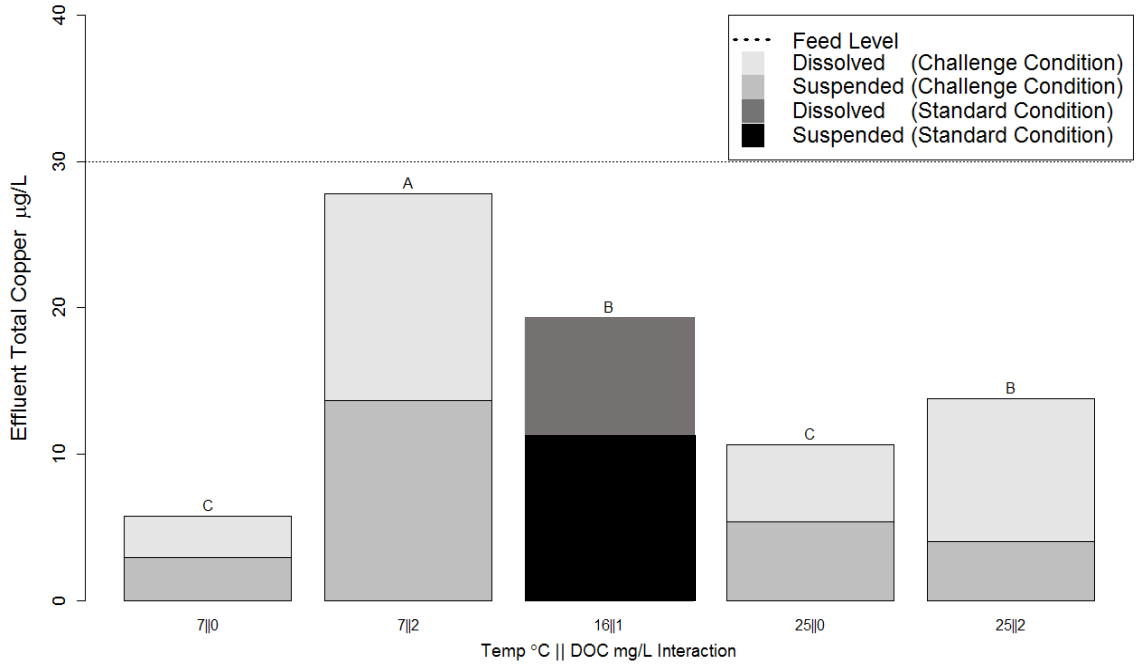

Fig. 29. Effluent Cu affected by two way interaction of temperature||DOC ($n_{challenge}$= 24; $n_{standard\ condition}$=12). Bars connected by the same letter within factor group are not significantly different by Tukey HSD (α=0.05). The bars display the concentration of Cu associated with suspended solids and dissolved in solution. The ANOVA was performed on the total concentration of Cu in the effluent. Box and Whisker plot shown in Fig. A-8.

Correlation analysis demonstrated a relationship or association of Cu to Fe and Mn oxides (Fig. 30). An affinity for Cu to Fe and Mn oxides was also observed in other studies (Hua et al. 2012; Li et al. 2009), though these studies demonstrated higher affinity for Mn oxides over Fe oxides. This preferential affinity for Mn over Fe oxides was not observed here in the correlation analysis.

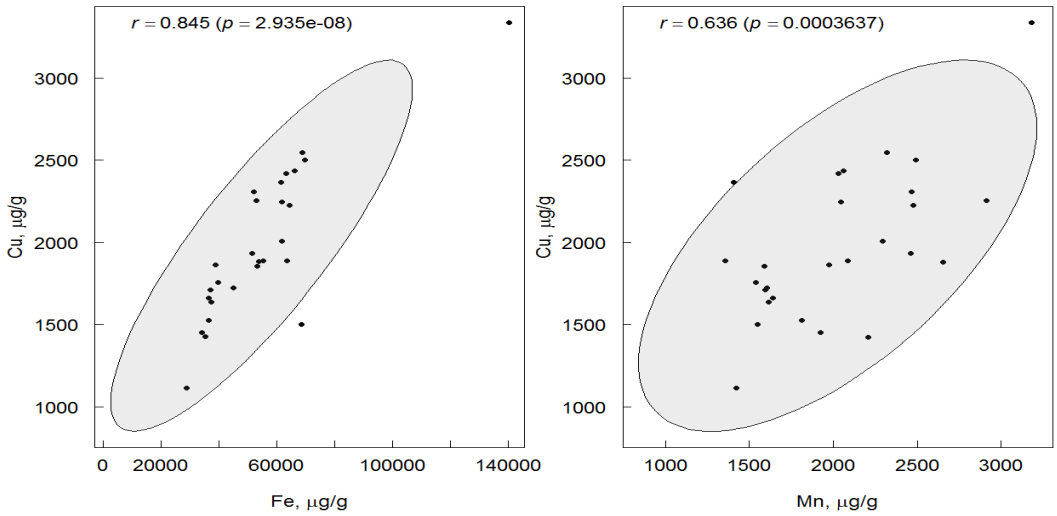

Fig. 30. Correlation analysis of Cu with matrix elements Fe and Mn within the biofilm matrix (n=27). Shaded ellipse is 95% joint confidence region.

The majority of Cu in the biofilm matrix was associated with the exchangeable, carbonate, and organic fractions at 255 µg/g (14%), 1190 µg/g (66%), and 310 (17%) µg/g respectively (Fig. 31).

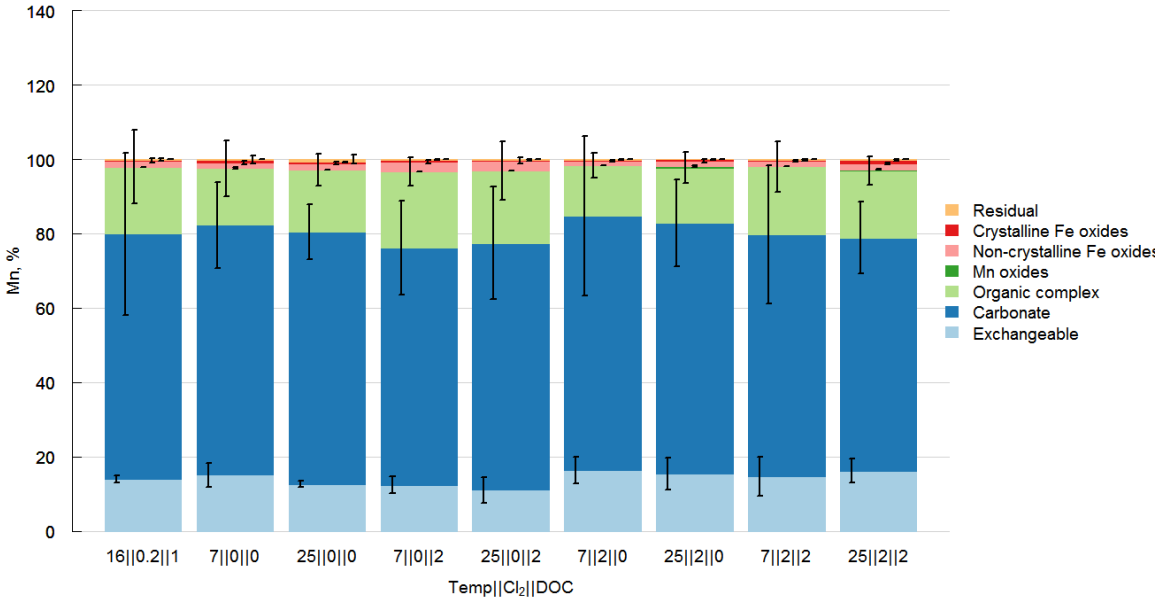

Fig. 31. Distribution of Cu as defined by sequential extractions. Units of x-axis for each challenge are °C ||mg/L Cl2 ||mg/L DOC. Error bars equal to standard deviation of mean (n=3).

This is similar to the major fractions of Cu observed in the AST swab solids with Cu associated mainly with the carbonate, organic, and non-crystalline oxide fractions at 964 µg/g (58%), 324 µg/g (19%), 287 µg/g (17%) respectively (Table 17). These fractions closely resemble those seen in the UPA solids, though with considerable more Cu accumulating in each fraction compared to AST.

Table 17: Cu sequential extraction comparison between swab and column solids.

Cu Solids Fraction		Swab Solids AST (Fig. D-1)	Swab Solids UPA (Fig. D-2)	Column Solids (Fig. 31)
Labile	Exchangeable	27.7 µg/g (1.6%)	55.3 µg/g (0.4%)	255 µg/g (14%)
	Carbonate	964 µg/g (58%)	8,610 µg/g (56%)	1,190 µg/g (66%)
	Organic	324 µg/g (19%)	3,990 µg/g (26%)	310 µg/g (17%)
Recalcitrant	Mn Oxides	34.0 µg/g (2.0%)	19.8 µg/g (0.1%)	1.59 µg/g (0.1%)
	Non Cryst. Fe Oxide	287 µg/g (17%)	2,650 µg/g (17%)	31.3 µg/g (1.7%)
	Cryst. Fe Oxide	19.3 µg/g (1.2%)	10.6 µg/g (0.1%)	7.98 µg/g (0.4%)
	Residual	21.4 µg/g (1.3%)	37.9 µg/g (0.3%)	4.10 µg/g (0.2%)

Cu was affected by challenges in the Mn oxide and non-crystalline Fe oxide fractions of the biofilm matrix (Fig. 32). Increasing the temperature and DOC to 25°C and 2 mg/L Cl_2 resulted an increase of Cu in the Mn oxide fraction. Challenges had no effect on the non-crystalline Fe oxide fraction compared to the standard condition. There were however significant changes when making comparisons between challenges. For example, the 0 mg/L Cl_2 || 2 mg/L DOC interaction demonstrated more retention of Cu than the 2 mg/L Cl_2 challenges.

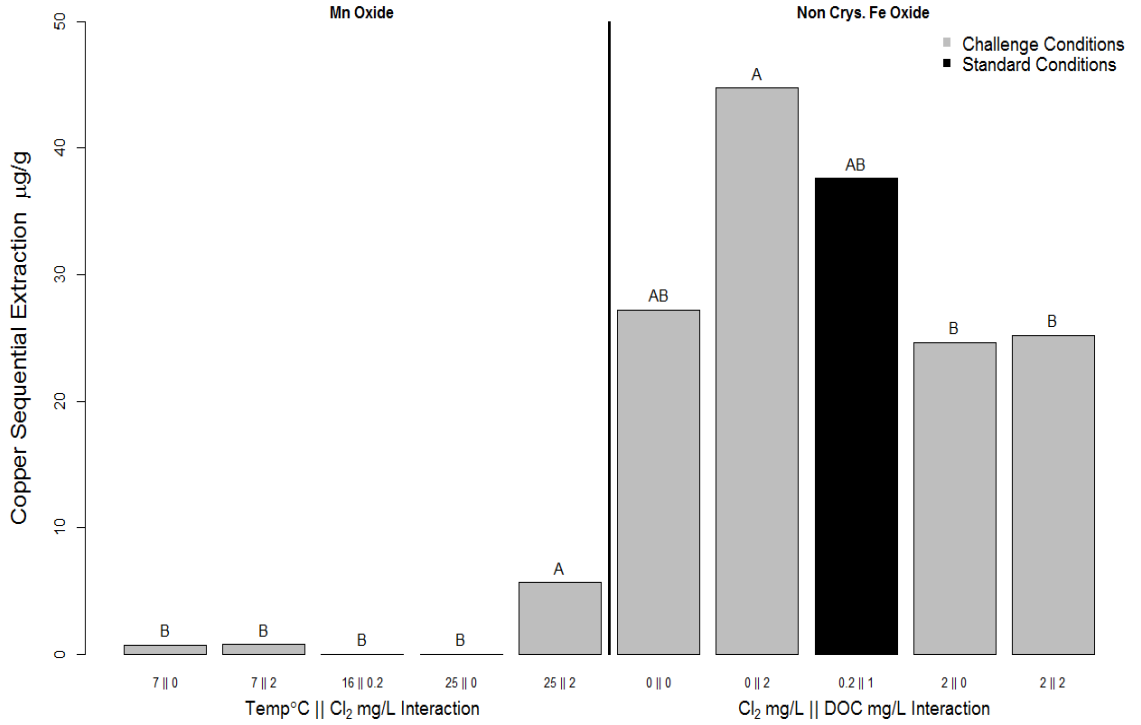

Fig. 32. Cu Mn oxide and non crystalline Fe oxide fractions affected by two way interaction of temperature||Cl_2 and Cl_2||DOC respectively ($n_{challenge}$=6; $n_{standard\ condition}$=3).

Copper accumulated more within the biofilm matrix with the addition of surface sites resulting from the oxidation of Mn(II) in the feed with the addition of Cl_2. This is evident due to the increase of Cu in the Mn oxide fraction with high Cl_2 dose and the correlation analysis suggesting an association of Cu with Fe and Mn solids.

Chromium (Cr)

Hexavalent Cr was fed into the columns at 10 µg/L (MCL = 100 µg/L). The average effluent concentration of all columns was ~10 µg/L Cr, indicating little sorption was occurring in the columns regardless of challenge. No significant changes related to challenges occurred in the effluent or in the biofilm matrix, and on average across all

columns the biofilm matrix contained 35.9 µg/g ± 6.66 µg/g Cr. This equates to about 2% of the total Cr added during the entire study. Correlation analysis shows an association of Cr with both Fe and Mn solids (Fig. 33). Cr(VI) has been observed in other studies to associate with Fe hydroxides (Richard and Bourg 1991), as was the case here.

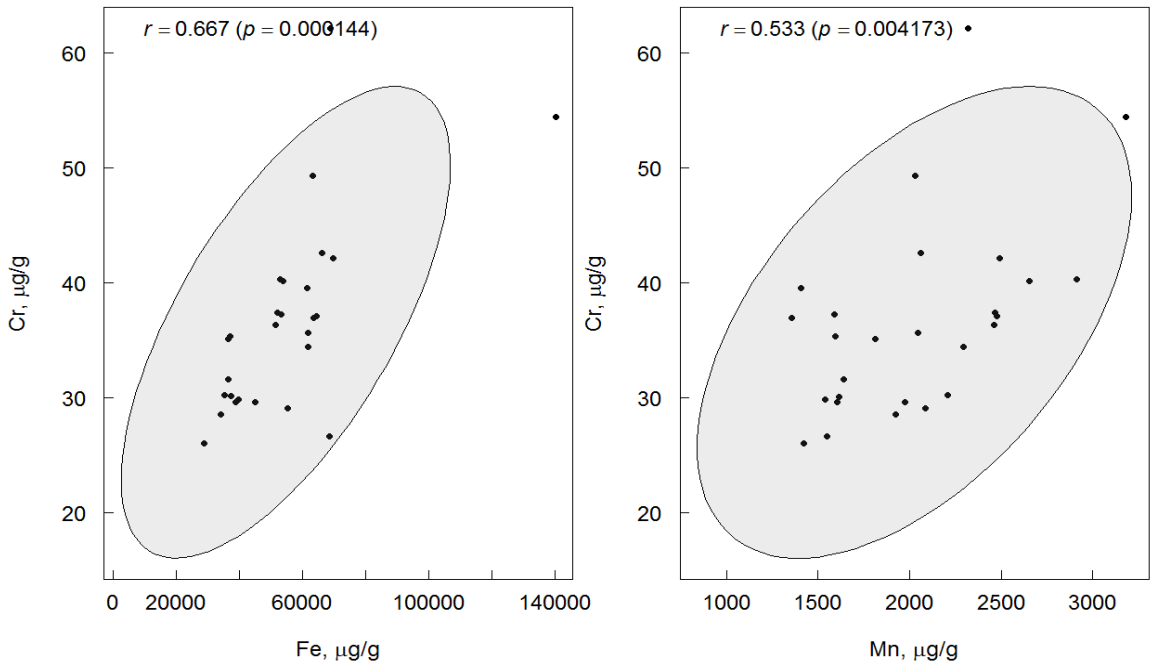

Fig. 33. Correlation analysis of Cr with matrix elements Fe and Mn within the biofilm matrix (n=27). Shaded ellipse is 95% joint confidence region.

The majority of Cr (Fig. 34) in the biofilm matrix was associated with the carbonate, organic, and the more recalcitrant crystalline Fe oxide fractions at 7.12 µg/g (15%), 8.70 µg/g (19%), 19.2 µg/g (41%) respectively. This more recalcitrant association with the biofilm matrix is unique compared to the other TICs.

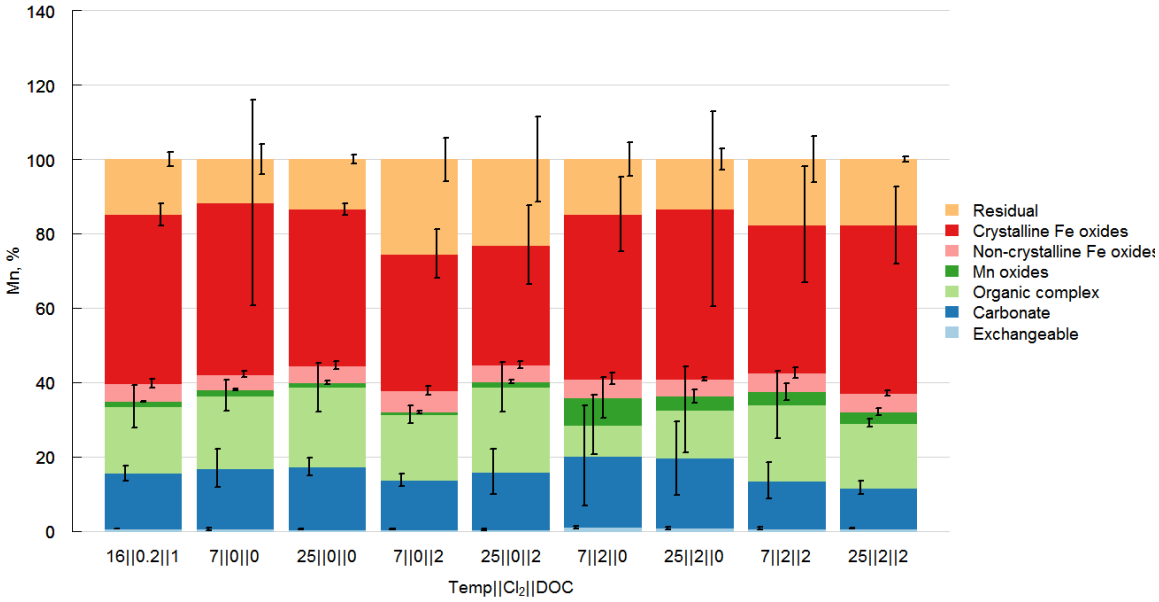

Fig. 34. Distribution of Cr as defined by sequential extractions. Units of x-axis for each challenge are °C ||mg/L Cl_2 ||mg/L DOC. Error bars equal to standard deviation of mean (n=3).

The distribution of Cr in the column solids is similar to the swab solids (Table 18), where the majority of Cr makes up the more recalcitrant fractions. The oxidation state of Cr was not determined in either the swab or column solids. Cr(VI) was added to the columns in this study and is known to be highly soluble and mobile compared to Cr(III) (Richard and Bourg 1991). Some of the Cr(VI) added to the columns could have been reduced to Cr(III) by the biofilm. This might explain the Cr behavior observed, where Cr(III) was associated with the recalcitrant fraction of the solids and Cr(VI) with the more labile fractions.

Table 18: Cr sequential extraction comparison between swab and column solids.

Cr Solids Fraction		Swab Solids AST (Fig. D-1)	Swab Solids UPA (Fig. D-2)	Column Solids (Fig. 34)
Labile	Exchangeable	<0.01 µg/g (0.01%)	0.33 µg/g (0.62%)	0.282 µg/g (0.6%)
	Carbonate	2.07 µg/g (6.5%)	2.68 µg/g (5.0%)	7.12 µg/g (15%)
	Organic	1.67 µg/g (5.3%)	1.79 µg/g (3.4%)	8.70 µg/g (19%)
Recalcitrant	Mn Oxides	0.19 µg/g (0.62%)	<0.01 µg/g (0.01%)	1.19 µg/g (2.6%)
	Non Cryst. Fe Oxide	7.10 µg/g (22%)	6.96 µg/g (13%)	2.23 µg/g (4.8%)
	Cryst. Fe Oxide	7.37 µg/g (23%)	9.94 µg/g (19%)	19.2 µg/g (41%)
	Residual	13.4 µg/g (42%)	31.5 µg/g (59%)	7.62 µg/g (16%)

In the column solids, significant changes due to challenges occurred in the exchangeable and Mn oxide fractions (Fig. 35). An increase in Cl_2 from the 0.2 mg/L to 2 mg/L caused an increase in Cr in both solids fractions.

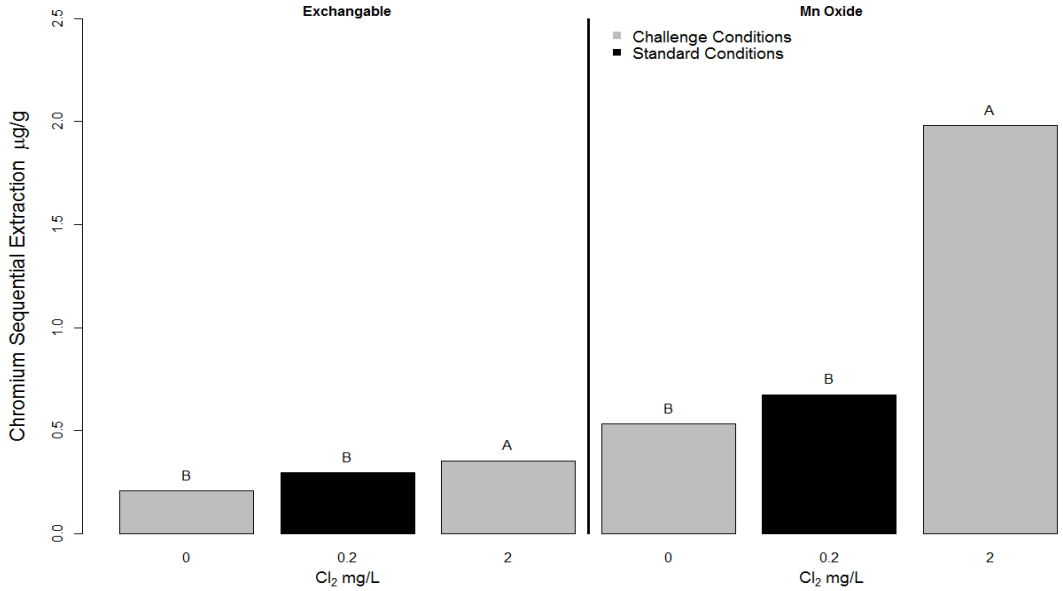

Fig. 35. Hexavalent chromium associated with exchangeable and Mn oxide sequential extraction fractions affected by Cl_2 ($n_{challenge}$=12; $n_{standard\ condition}$=3). Bars connected by the same letter within factor group are not significantly different by Tukey HSD (α=0.05).

The increase in Cr in the exchangeable and Mn oxide fraction of the biofilm matrix with the addition of Cl_2 suggests that Cr accumulated more within the biofilm matrix with the addition of surface sites that resulted from Mn^{+2} in the feed water being oxidized as a result of the addition of Cl_2. This is also supported by the correlation analysis showing a relationship between Cr and the matrix elements Fe and Mn.

CHAPTER VIII

SUMMARY AND CONCLUSIONS

A biofilm matrix was formed within the columns as evidenced by the presence of ATP and DNA on the surface of the glass beads at the end of the study. Additionally, accumulation of matrix elements (Mn and Fe) along with TICs (Tl, As, Pb, Cu, and Cr) occurred within the columns. Challenges, assessed under steady-state conditions, caused only an increase or decrease in the extent that TICs accumulated in the biofilm matrix and not a net release of TICs. The sequential extraction fractions between the swab and column solids compared relatively well though much of the matrix elements and TICs were more recalcitrant in the swab solids than the more labile column solids. This is due in part to the legacy time frames experienced in a DWDS rather than the 6 months used in this study.

Correlation analysis showed an association of all TICs with Fe and Mn, with the exception of Tl, which was observed to only associate with Mn in the solids. A major fraction of Fe and Mn accumulated in the organic defined fraction of the biofilm, demonstrating the roles that both the biofilm structure and these matrix elements play in the accumulation of TICs.

Challenges that caused significant changes in TIC behavior are summarized in Table 19; % accumulated is defined as the % of TIC that accumulated within the biofilm matrix over the duration of the experiment. An increase in Cl_2 resulted in an increase in Mn oxide surfaces within the biofilm matrix due to oxidation and precipitation of the added Mn^{2+}. This in turn led to the additional accumulation of Tl, Pb, Cu, Cr, and Fe. The extraction step for Mn oxides is hydroxylamine hydrochloride at pH 2. This reducing agent

may also dissolve freshly precipitated Fe oxides. Regardless, the addition of Cl_2 increased surfaces for retention of TICs.

The majority of Tl behavior was controlled by Cl_2 concentrations. This was likely due to the continuous oxidation and precipitation of Tl(I) to Tl(III) by Cl_2, resulting in retention and accumulation of Tl onto Mn oxides that were sequestered in the biofilm matrix. This is in line with the results observed in the monitoring study at Park City (Friedman et al. 2015), where Tl release from the DWDS was related to low Cl_2 residual. It is also consistent with the desorption experiment using the AST and UPA swab solids (Friedman et al. 2015), where the addition of Cl_2 decreased Tl desorption from the swab solids.

Unlike the other TICs, As was only affected by the concentration of DOC in the challenges and not Cl_2. DOC was observed to compete for sorption sites resulting in less As in the biofilm matrix with increased DOC, suggesting a possible release mechanism.

Addition of Cl_2 at 2 mg/L did increase Pb association with Mn oxide but the main effect of Pb behavior was the addition of 2 mg/L DOC, causing an increase in the concentration in the effluent at 7°C and a decrease in the carbonate fraction of the biofilm matrix at 25°C. These mixed results suggests possible interactions occurring that were observed in other studies. Kim and Herrera (2010) observed the ability of Cl_2 to create PbO_2 scales while Lin and Valentine (2009) observed the ability of NOM to dissolve those scales by reducing Pb(IV) to Pb(II).

The results of this laboratory study demonstrate the ease by which TICs accumulate on surfaces affected by biological systems. The amount accumulated observed at the end

of the study depended on the concentration of Cl_2 and DOC in the system. The highly concentrated solids were sensitive to hydraulic and physical disturbance, as evident when moving the columns. Relocating the columns to their respective constant temperature rooms resulted in significant disturbance and so analysis on the effluent to determine response to challenges was done only when the columns reached steady-state. Though not the focus of this study, hydraulic disturbance could be a major factor in releasing these highly concentrated TICs, showing the importance of regular pipe cleaning activities and striving for conditions within the pipe that reduce the amount of accumulation of matrix elements and TICs.

Table 19: Summary Table

Element	% Accumulated Under Standard Conditions	Major Factor: Impact of Challenge on % Accumulated	Description
Mn	33%	Cl_2: No net impact on % accumulated of Mn observed	Manganese in the biofilm matrix increased with increased Cl_2 within the Mn oxide fraction indicating oxidation of Mn(II).
Fe	60%	Cl_2: No net impact on % accumulated of Fe observed	Fe in the biofilm matrix increased in the Mn oxide fraction with increased Cl_2 as a result of the additional surfaces proved by the oxidation of Mn.
As	20%	DOC: Increased DOC caused % accumulated to decrease to 13%	Arsenic in the biofilm matrix decreased with increased DOC. This decrease was observed to occur in the exchangeable and organic fractions of the biofilm matrix.
Pb	50%	DOC and Cl_2: Increased DOC caused % accumulated to drop to 40%. No net impact on % accumulated of Pb was observed with change in Cl_2.	The addition of DOC decreased retention of Pb in the carbonate fraction of the biofilm matrix while the addition of Cl_2 increased retention of Pb in the Mn oxide fraction.
Tl	6%	Cl_2: Increase in Cl_2 caused % accumulated to increase to 12%.	Thallium increased in the biofilm matrix with increased Cl_2. The majority of the increase was observed to occur in the exchangeable and carbonate fractions.
Cu	33%	Cl_2: No net impact on % accumulated of Cu observed.	Copper increased within the Mn oxide fraction of the biofilm matrix with increased Cl_2, indicating retention of Cu by the addition of Mn oxide surfaces.
Cr	2%	Cl_2: No net impact on % accumulated of Cr observed.	Very little accumulation of Cr occurred but was still affected by chlorine. Increased Cl_2 caused more retention of Cr in the exchangeable and Mn oxide fractions of the biofilm matrix indicating retention by Mn oxide formation.

CHAPTER X

ENGINEERING SIGNIFICANCE

The outcome of this investigation was the identification of conditions that cause accumulation of TICs to biofilm matrices under DWDS conditions. The knowledge provides engineers the opportunity to reduce the risk of TIC accumulation and subsequent release in DWDS by modifying treatment practices of their source water and also secondary disinfection practices.

Minimizing the amounts of matrix elements in the feed water is especially important in reducing the amount of TIC accumulation downstream in the DWDS. However, even a large reduction in the accumulation of TICs can still lead to problems when considering the legacy timeframes experienced by DWDS, demonstrating the importance of returning the system to a "clean pipe condition" using cleaning techniques such as swabbing, ice pigging, and unidirectional flushing. Because downstream reactions within the DWDS are complex and site specific, knowing the chemistry of the feed water in anticipation for DWDS pipe reactions may also help to provide insight in how to treat the source water to maintain a clean pipe and avoid subsequent release. The results and conclusions provided here demonstrate a high potential for accumulation when the DWDS is sourced with Fe/Mn and TICs at secondary and primary MCLs.

Secondary disinfection practices were also shown to have a high impact on TIC accumulation, with Cl_2 as low as 0.2 mg/L causing accumulation. Increasing Cl_2 residual levels to 2 mg/L resulted in even more accumulation of TICs. In some states such Louisiana and Colorado revisions have been proposed to ensure control of pathogens in their DWDS.

These rules require an increase in Cl_2 residual in the DWDS to 0.5 mg/L 100% of the time. According to the observations in this study the new rules may be more effective in biological control but may also impact TIC adsorption, resulting in increased accumulation of some TICs. These unforeseen impacts of increasing residual Cl_2 could impact future decision processes related to new secondary disinfection rules.

REFERENCES

Amacher, M.C., 1996. Nickel, cadmium, and lead. In: Sparks, D. et al. (Eds.), Methods of soil analysis. Part 3-chemical methods., pp. 739-768.

Batté, M., Appenzeller, B. M. R., Grandjean, D., Fass, S., Gauthier, V., Jorand, F., Mathieu, L., Boualam, M., Saby, S., and Block, J. C. (2003). "Biofilms in drinking water distribution systems." *Re/Views in Environmental Science and Bio/Technology*, 2(2-4), 147-168.

Beech, W. B., and Sunner, J. (2004). "Biocorrosion: towards understanding interactions between biofilms and metals." *Curr. Opin. Biotechnol.*, 15(3), 181-186.

Boe-Hansen, R., Albrechtsen, H.-J., Arvin, E., and Jørgensen, C. (2002). "Bulk water phase and biofilm growth in drinking water at low nutrient conditions." *Water Res.*, 36(18), 4477-4486.

Camper, A., Butterfield, P., Ellis, B., Jones, W., Anderson, W., Huck, P., Slawson, R., Volk, C., Welch, N., and Lechevallier, M. (2000). "Investigation of the biological stability of water in treatment plants and distribution systems." AWWA Research Foundation, Denver.

Camper, A. K., Brastrup, K., Sandvig, A., Clement, J., Spencer, C., and Capuzzi, A. J. (2003). "Effect of distribution system materials on bacterial regrowth." *J Am Water Works Assn*, 95(7), 107-121.

Cerrato, J. M., Falkinham, J. O., Dietrich, A. M., Knocke, W. R., McKinney, C. W., and Pruden, A. (2010). "Manganese oxidizing and reducing microorganisms isolated from biofilms in chlorinated drinking water systems." *Water Res.*, 44(13), 3935-3945.

Costa, M., and Klein, C. B. (2006). "Toxicity and carcinogenicity of chromium compounds in humans." *Crit. Rev. Toxicol.*, 36(2), 155-163.

Critchley, M. M., Cromar, N. J., McClure, N., and Fallowfield, H. J. (2001). "Biofilms and microbially influenced cuprosolvency in domestic copper plumbing systems." *J. Appl. Microbiol.*, 91(4), 646-651.

Crittenden, J.C., Trussell, R.R., Hand, D.W., Howe, K.J., Tchobanoglous, G. 2012. MWH's Water Treatment: Principles and design, 3rd Ed. John Wiley and Sons, Inc. Hobken, NJ 1920 p

Dong, D. M., Hua, X. Y., Li, Y., and Li, Z. H. (2002). "Lead adsorption to metal oxides and organic material of freshwater surface coatings determined using a novel selective extraction method." *Environ. Pollut.*, 119(3), 317-321.

Dong, D. M., Li, Y., Zhang, B. Y., Hua, X. Y., and Yue, B. H. (2001). "Selective chemical extraction and separation of Mn, Fe oxides and organic material in natural surface coatings: application to the study of trace metal adsorption mechanism in aquatic environments." *Microchem. J.*, 69(1), 89-94.

Filella, M., Belzile, N., and Chen, Y. W. (2002). "Antimony in the environment: a review focused on natural waters I. Occurrence." *Earth-Sci. Rev.*, 57(1-2), 125-176.

Flemming, H.-C. (2002). "Biofouling in water systems, cases, causes and countermeasures." *Appl. Microbiol. Biotechnol.*, 59(6), 629-640.

Flemming, H. C. (2011). "The perfect slime." *Colloid Surface B*, 86(2), 251-259.

Friedman, M., Hill, A., Booth, S., Hallett, M., McNeill, L. M., J., Stevens, D., Sorensen, D., Hammer, T., Kent, W., De Haan, M., MacArthur, K., and Mitchell, K. (2015). "Metals accumulation and release within the distribution system: evaluation and mitigation." Water Research Foundation, 449.

Friedman, M. J., Hill, A. S., Reiber, S. H., Valentine, R. L., Larson, G., Young, A., Korshin, G. V., and Peng, C. Y. (2010). "Assessment of inorganics accumulation in drinking water system scales and sediments." *AWWA Research Foundation*, 1-311.

Giddings, E. M., Hornberger, M.I., and Hadley, H.K. (2001). "Trace metal concentrations in sediment and water and health of aquatic macroinvertebrate communities of streams near Park City, Summit County, Utah." U.S. Geological Survey, Salt Lake City.

Ginige, M. P., Wylie, J., and Plumb, J. (2011). "Influence of biofilms on iron and manganese deposition in drinking water distribution systems." *Biofouling*, 27(2), 151-163.

Grafe, M., Eick, M. J., and Grossl, P. R. (2001). "Adsorption of arsenate (V) and arsenite (III) on goethite in the presence and absence of dissolved organic carbon." *Soil Sci. Soc. Am. J.*, 65(6), 1680-1687.

Holm, T. R. (2002). "Effects of CO_3^{2-}/bicarbonate, Si, and PO_4^{3-} on arsenic sorption to HFO." *J Am Water Works Assn*, 94(4), 174-181.

Hua, X. Y., Dong, D. M., Liu, L., Gao, M., and Liang, D. P. (2012). "Comparison of trace metal adsorption onto different solid materials and their chemical components in a natural aquatic environment." *Appl. Geochem.*, 27(5), 1005-1012.

Huang, J. H., and Kretzschmar, R. (2010). "Sequential extraction method for speciation of arsenate and arsenite in mineral soils." *Anal. Chem.*, 82(13), 5534-5540.

Jacobson, A. R., McBride, M. B., Baveye, P., and Steenhuis, T. S. (2005). "Environmental factors determining the trace-level sorption of silver and thallium to soils." *Sci. Total Environ.*, 345(1-3), 191-205.

John, D. A. (1998). "Geologic setting and characteristics of mineral deposits in the central Wasatch Mountains, Utah." *Society of Economic Geologists Field Guidebook* 29, 11-33.

Kim, E. J., and Herrera, J. E. (2010). "Characteristics of lead corrosion scales formed during drinking water distribution and their potential influence on the release of lead and other contaminants." *Environ. Sci. Technol.*, 44(16), 6054-6061.

Lautenschlager, K., Hwang, C., Liu, W.-T., Boon, N., Köster, O., Vrouwenvelder, H., Egli, T., and Hammes, F. (2013). "A microbiology-based multi-parametric approach towards assessing biological stability in drinking water distribution networks." *Water Res.*, 47(9), 3015-3025.

Lechevallier, M. W., Babcock, T. M., and Lee, R. G. (1987). "Examination and characterization of distribution-system biofilms." *Appl. Environ. Microbiol.*, 53(12), 2714-2724.

Li, Y., Wang, X. L., Huang, G. H., Zhang, B. Y., and Guo, S. H. (2009). "Adsorption of Cu and Zn onto Mn/Fe oxides and organic materials in the extractable fractions of river surficial sediments." *Soil Sediment Contam*, 18(1), 87-101.

Lin, Y. P., and Valentine, R. L. (2009). "Reduction of lead oxide (PbO_2) and release of Pb(II) in mixtures of natural organic matter, free Chlorine and monochloramine." *Environ. Sci. Technol.*, 43(10), 3872-3877.

Lock, K., and Janssen, C. R. (2003). "Influence of aging on metal availability in soils." *Rev Environ Contam T*, 178, 1-21.

Lytle, D. A., and Liggett, J. (2011). "Arsenic accumulation and release studies using a cast iron pipe section." *Water Quality Technology Conference*, AWWA, Phoenix, AZ.

Mann, E. E., and Wozniak, D. J. (2012). "Pseudomonas biofilm matrix composition and niche biology." *FEMS Microbiol. Rev.*, 36(4), 893-916.

McAffee, C. (2012). "2012 Consumer confidence report." (July. 31, 2012).

McAffee, C. (2012). "Thaynes Canyon neighborhood water quality meeting." Park City Utility.

Momba, M. N. B., Kfir, R., Venter, S. N., and Cloete, T. E. (2000). "An overview of biofilm formation in distribution systems and its impact on the deterioration of water quality." *Water Sa*, 26(1), 59-66.

Nelson, Y. M., Lion, L. W., Shuler, M. L., and Ghiorse, W. C. (2002). "Effect of oxide formation mechanisms on lead adsorption by biogenic manganese (hydr)oxides, iron (hydr)oxides, and their mixtures." *Environ. Sci. Technol.*, 36(3), 421-425.

Payment, P., and Robertson, W. (2004). "The microbiology of piped distribution systems and public health." *Safe Piped Water: Managing Microbial Water Quality in Piped Distribution Systems*, 1-18.

Peng, C. Y., Hill, A. S., Friedman, M. J., Valentine, R. L., Larson, G. S., Romero, A. M. Y., Reiber, S. H., and Korshin, G. V. (2012). "Occurrence of trace inorganic contaminants in drinking water distribution systems." *J Am Water Works Assn*, 104(3), 53-54.

Peng, C. Y., and Korshin, G. V. (2011). "Speciation of trace inorganic contaminants in corrosion scales and deposits formed in drinking water distribution systems." *Water Res.*, 45(17), 5553-5563.

Peter, A. L. J., and Viraraghavan, T. (2005). "Thallium: a review of public health and environmental concerns." *Environ. Int.*, 31(4), 493-501.

Priester, J. H., Olson, S. G., Webb, S. M., Neu, M. P., Hersman, L. E., and Holden, P. A. (2006). "Enhanced exopolymer production and chromium stabilization in Pseudomonas putida unsaturated biofilms." *Appl. Environ. Microbiol.*, 72(3), 1988-1996.

R Core Team. (2013). R: A Language and Environment for Statistical Computing. R Foundation for Statistical Computing, Vienna, Austria.

Richard, F. C., and Bourg, A. C. M. (1991). "Aqueous geochemistry of chromium - a review." *Water Res.*, 25(7), 807-816.

Sarin, P., Snoeyink, V. L., Bebee, J., Jim, K. K., Beckett, M. A., Kriven, W. M., and Clement, J. A. (2004). "Iron release from corroded iron pipes in drinking water

distribution systems: effect of dissolved oxygen." *Water Res.*, 38(5), 1259-1269 0043-1354.

Sarin, P., Snoeyink, V. L., Bebee, J., Kriven, W. M., and Clement, J. A. (2001). "Physico-chemical characteristics of corrosion scales in old iron pipes." *Water Res.*, 35(12), 2961-2969.

Schock, M. R., Hyland, R. N., and Welch, M. M. (2008). "Occurrence of contaminant accumulation in lead pipe scales from domestic drinking-water distribution systems." *Environ. Sci. Technol.*, 42(12), 4285-4291.

Shelby, J. E. (2005). *Introduction to glass science and technology*, Royal Society of Chemistry, Cambridge.

Shrout, J. D., and Nerenberg, R. (2012). "Monitoring bacterial twitter: Does quorum sensing determine the behavior of water and wastewater treatment biofilms?" *Environ. Sci. Technol.*, 46(4), 1995-2005.

Sly, L. I., Hodgkinson, M. C., and Arunpairojana, V. (1990). "Deposition of manganese in a drinking-water distribution-system." *Appl. Environ. Microbiol.*, 56(3), 628-639.

Smedley, P. L., and Kinniburgh, D. G. (2002). "A review of the source, behaviour and distribution of arsenic in natural waters." *Appl. Geochem.*, 17(5), 517-568.

Smeets, P., Medema, G. J., and Van Dijk, J. C. (2009). "The Dutch secret: how to provide safe drinking water without chlorine in the Netherlands." *Drinking Water Engineering and Science*, 2(1), 1-14 1996-9457.

Toner, B., Fakra, S., Villalobos, M., Warwick, T., and Sposito, G. (2005). "Spatially resolved characterization of biogenic manganese oxide production within a bacterial biofilm." *Applied and Environmental Microbiology*, 71(3), 1300-1310.

Toner, B., Manceau, A., Webb, S. M., and Sposito, G. (2006). "Zinc sorption to biogenic hexagonal-birnessite particles within a hydrated bacterial biofilm." *Geochim. Cosmochim. Acta*, 70(1), 27-43.

Tuovinen, O. H., Button, K. S., Vuorinen, A., Carlson, L., Mair, D. M., and Yut, L. A. (1980). "Bacterial, chemical, and mineralogical characteristics of tubercles in distribution pipelines." *J Am Water Works Assn*, 72(11), 626-635.

US Census Bureau (2013). "2013 population estimate (as of July 1, 2013)." Population Division, US Census Bureau, Washington.

USEPA (2011a). "Surface water treatment rules what do they mean to you?" < http://www.epa.gov/dwreginfo/surface-water-treatment-rules>. (December 2, 2015).

USEPA(2011b). "USEPA SW-846." <http://www.epa.gov/osw/hazard/testmethods/sw846/>. (July 27, 2015).

USEPA (2012). "2012 Edition of the drinking water standards and health advisories." U.S. Environmental Protection Agency.

Vanderkooij, D. (1992). "Assimilable organic-carbon as an indicator of bacterial regrowth." *J Am Water Works Assn*, 84(2), 57-65.

Vanderkooij, D., Veenendaal, H. R., Baarslorist, C., Vanderklift, D. W., and Drost, Y. C. (1995). "Biofilm formation on surfaces of glass and teflon exposed to treated water." *Water Res.*, 29(7), 1655-1662.

Wan, S., Ma, M., Lv, L., Qian, L., Xu, S., Xue, Y., and Ma, Z. (2014). "Selective capture of thallium (I) ion from aqueous solutions by amorphous hydrous manganese dioxide." *Chem. Eng. J.*, 239, 200-206.

Watanabe, J., Tani, Y., Miyata, N., Seyama, H., Mitsunobu, S., and Naitou, H. (2012). "Concurrent sorption of As(V) and Mn(II) during biogenic manganese oxide formation." *Chem. Geol.*, 306, 123-128.

APPENDICES

APPENDIX A Box and Whisker Plots of Effluent and Solids Data

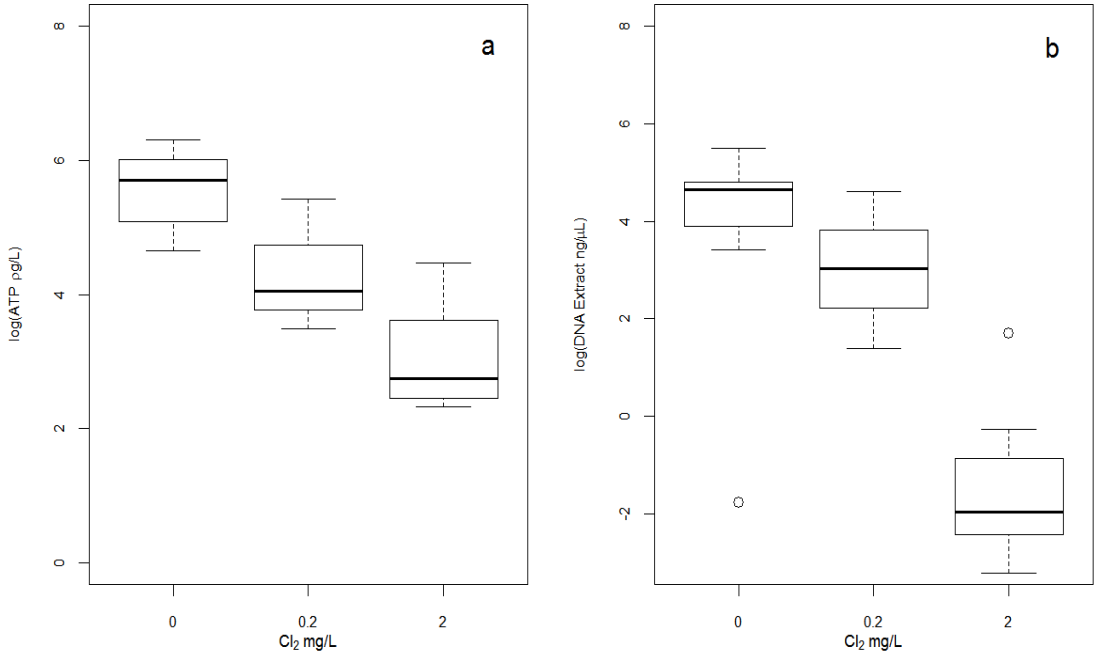

Fig. A-1. a) ATP on surface of glass beads affected by Cl2; b) DNA on surface of glass beads affected by Cl_2. ($n_{challenge}$=12; $n_{standard\ condition}$= 3). Data also shown in Fig. 9.

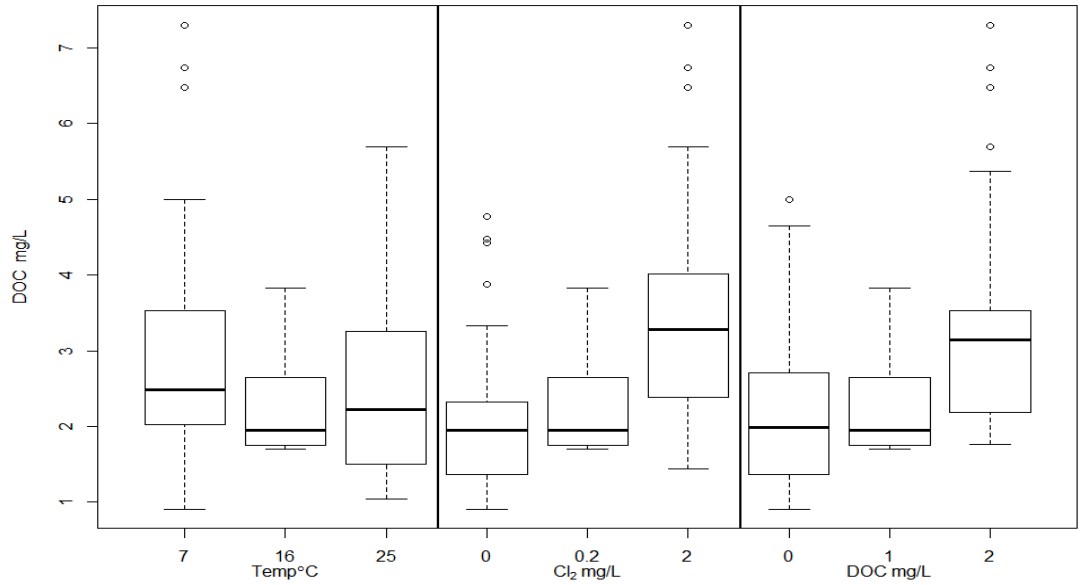

Fig. A-2. Effluent DOC affected by temperature & Cl_2 & DOC ($n_{challenge}$=48; $n_{standard\ condition}$= 12). Data also shown in Fig. 10.

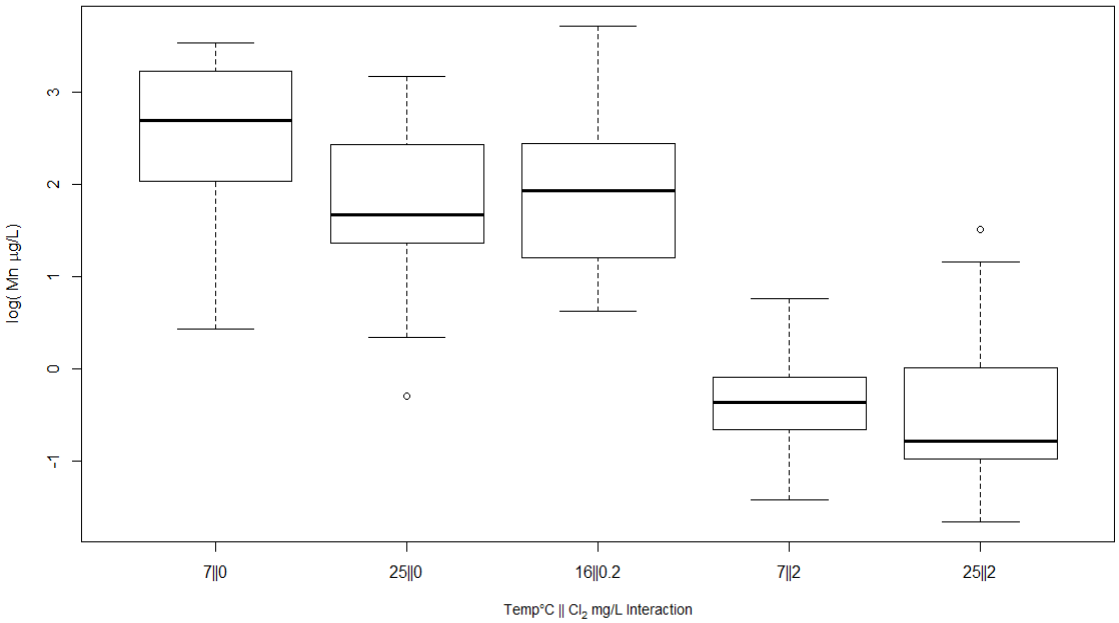

Fig. A-3. Significant two way interaction of temperature||Cl2 for effluent Mn ($n_{challenge}$= 24; $n_{standard\ condition}$ = 12). The bars display the concentration of Mn associated with suspended solids and dissolved in solution. Data also shown in Fig. 11.

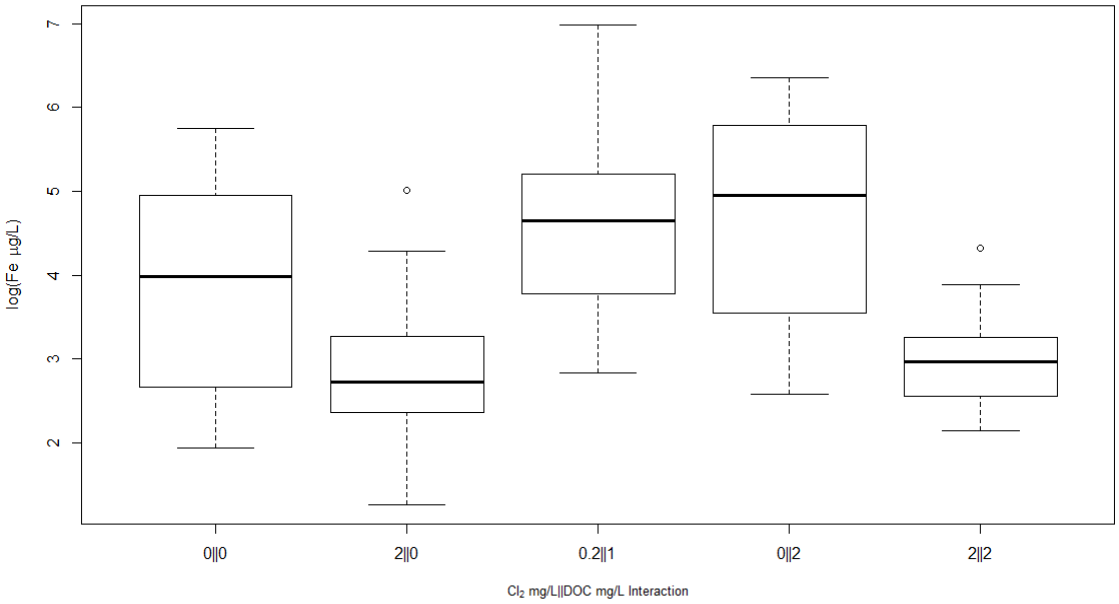

Fig. A-4. Significant two way interaction of temperature||Cl2 for effluent Fe ($n_{challenge}$= 24; $n_{standard\ condition}$= 12). The bars display the concentration of Fe associated with suspended solids and dissolved in solution. Data also shown in Fig. 14.

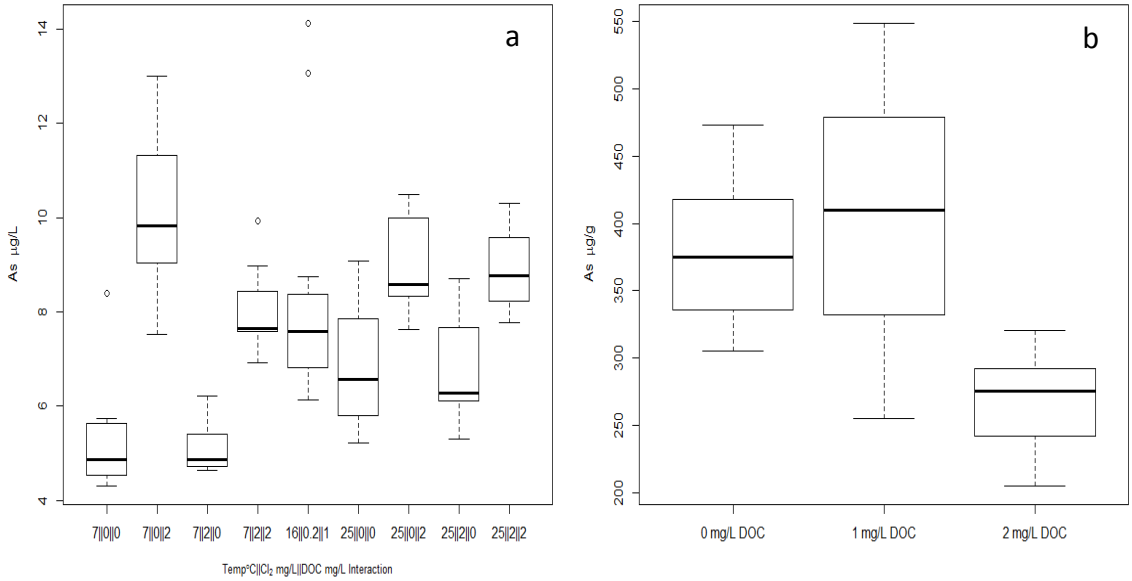

Fig. A-5. (a) Effluent As affected by three way interaction of temperature||Cl2||DOC ($n_{challenge}$=12; $n_{standard\ condition}$=12). (b) Biofilm matrix As affected by DOC ($n_{challenge}$=12; $n_{standard\ condition}$=3). Data also shown in Fig. 17.

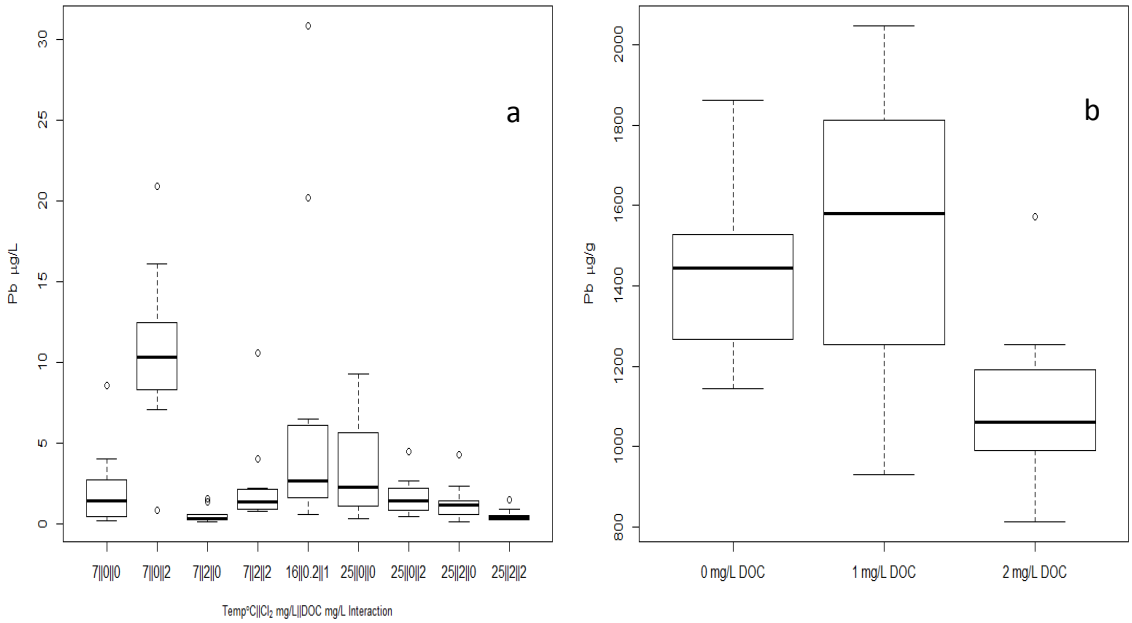

Fig. A-6. (a) Effluent Pb affected by three way interaction of temperature||Cl2||DOC ($n_{challenge}$=12; $n_{standard\ condition}$=12). (b) Solids Pb affected by DOC ($n_{challenge}$=12; $n_{standard\ condition}$=3). Data also shown in Fig. 21.

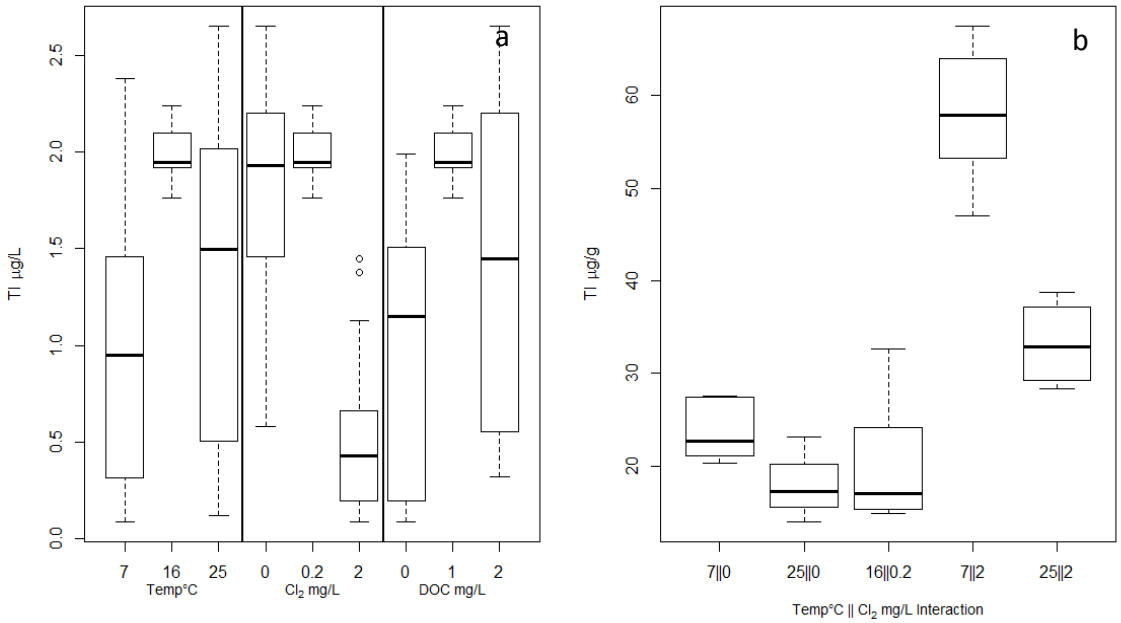

Fig. A-7. (a) Effluent Tl affected by Temperature & Cl_2 & DOC ($n_{challenge}$=48; $n_{standard\ condition}$=12). The bars display the concentration of Tl associated with suspended solids and dissolved in solution. (b) Biofilm solids Tl affected by two way interaction of temperature||Cl_2 ($n_{challenge}$=6; $n_{standard\ condition}$=3. Data also shown in Fig. 25.

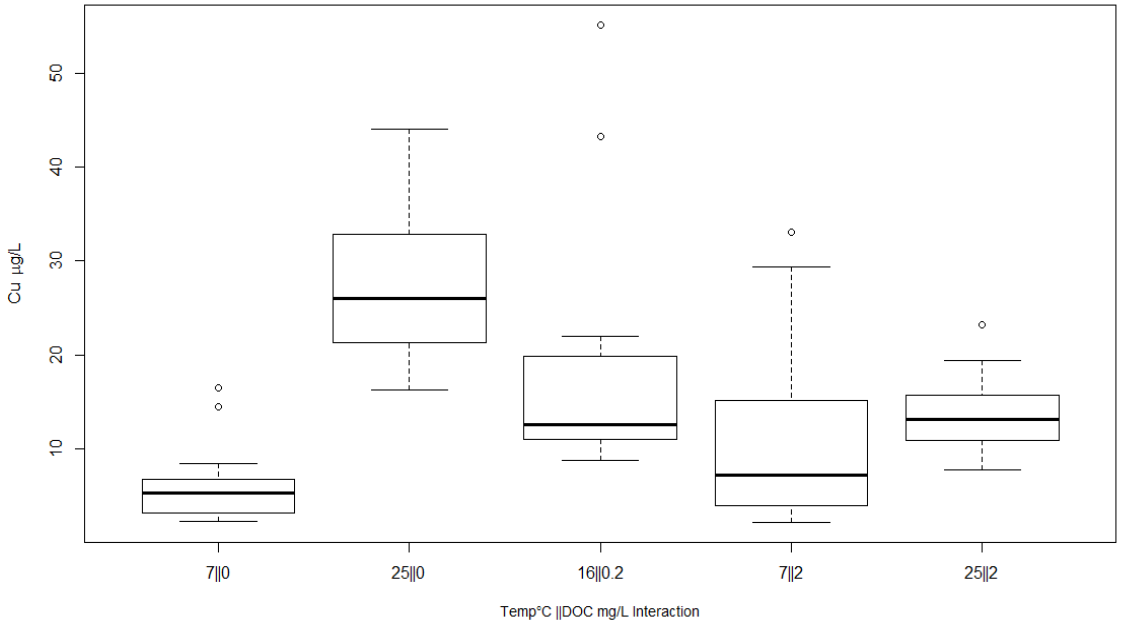

Fig. A-8. Effluent Cu affected by two way interaction of temperature||DOC ($n_{challenge}$= 24; $n_{standard\ condition}$=12). Data also shown in Fig. 29.

APPENDIX B Additional Side Studies

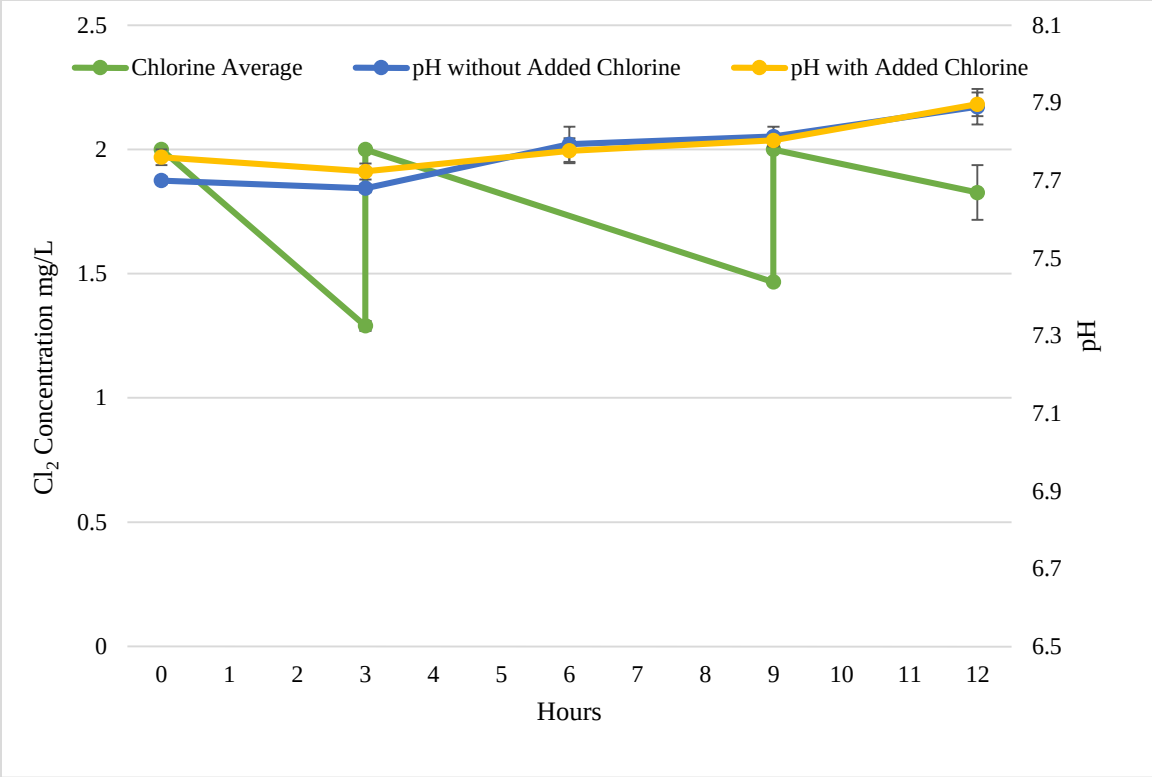

Fig. B-1. Feed solution with and without Cl_2 added and maintained over 12 hours to determine effect on pH. Replicated in triplicate.

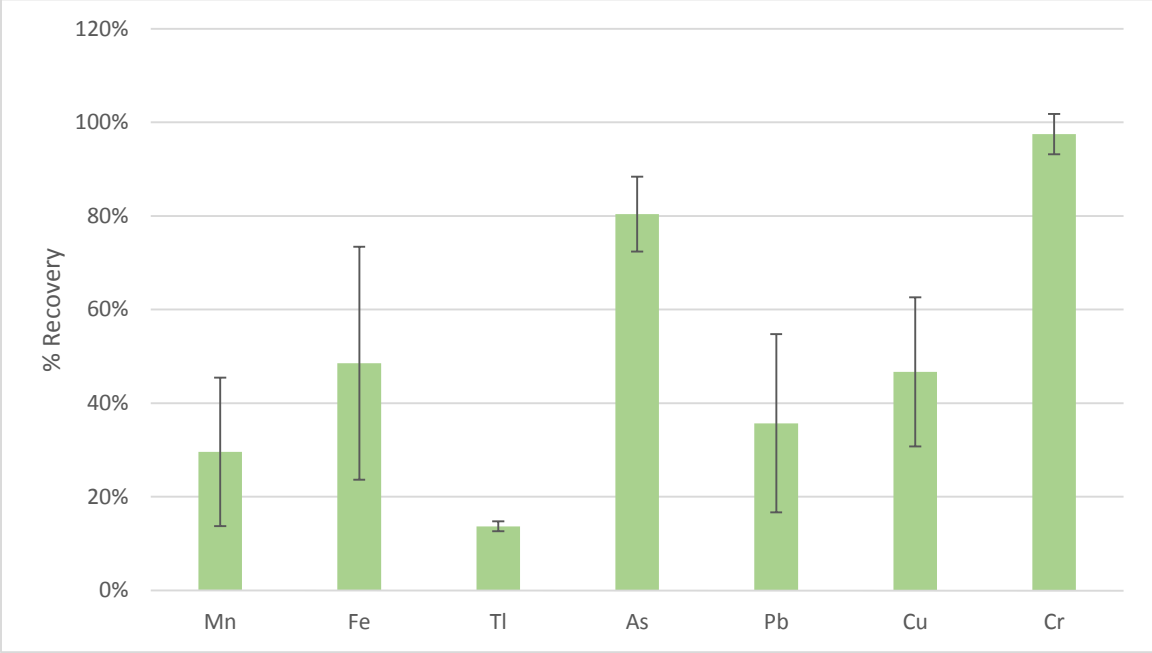

Fig. B-2. Sorption test on glass beads over 2 days. Percentages represent % recovery of matrix element or TICs when glass beads are present.

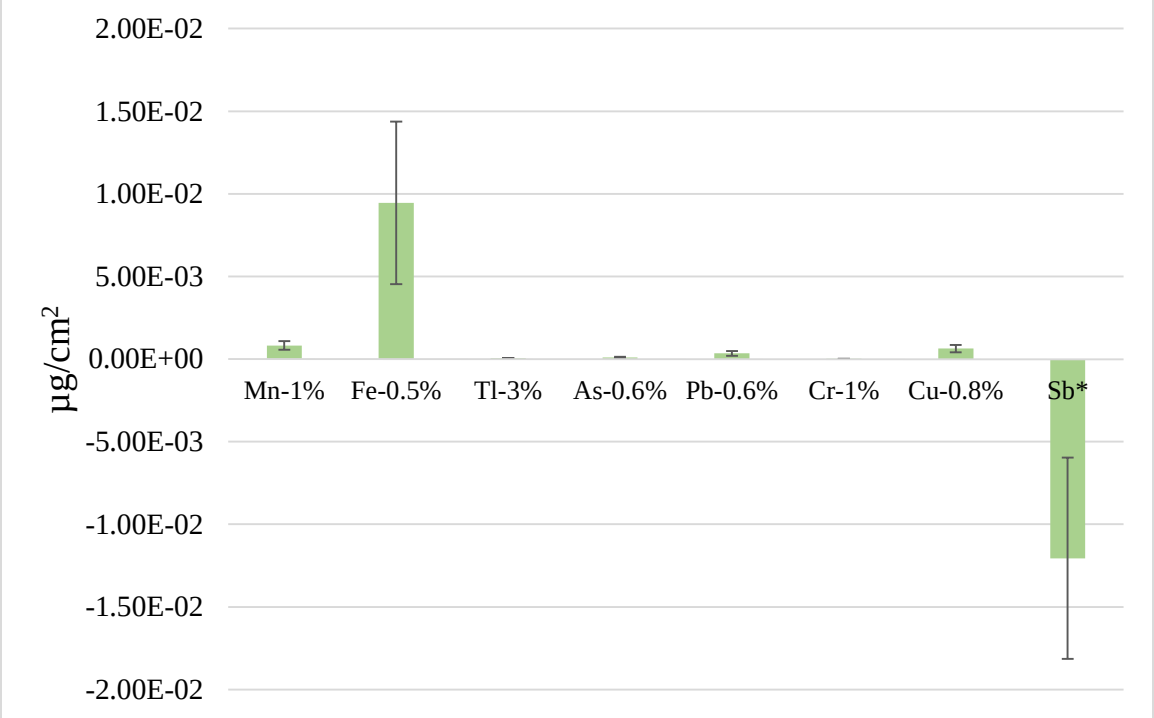

Fig. B-3. Sorption test on glass beads over 2 days. Positive values show sorption. Negative values indicate desorption. Percentages represent percentage of total mass of element on beads at end of study. *Data not shown due to Sb contamination on beads.

APPENDIX C Effluent Plots

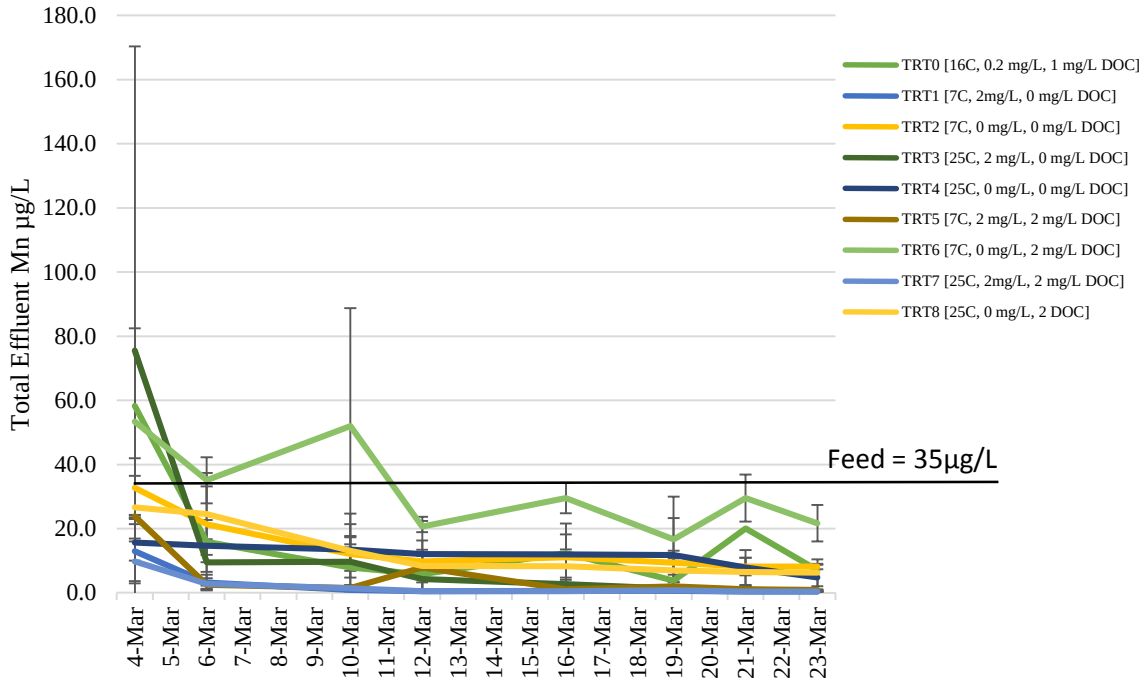

Fig. C-1. Total effluent Mn during challenge phase. Error bars refer to standard deviation of triplicate mean.

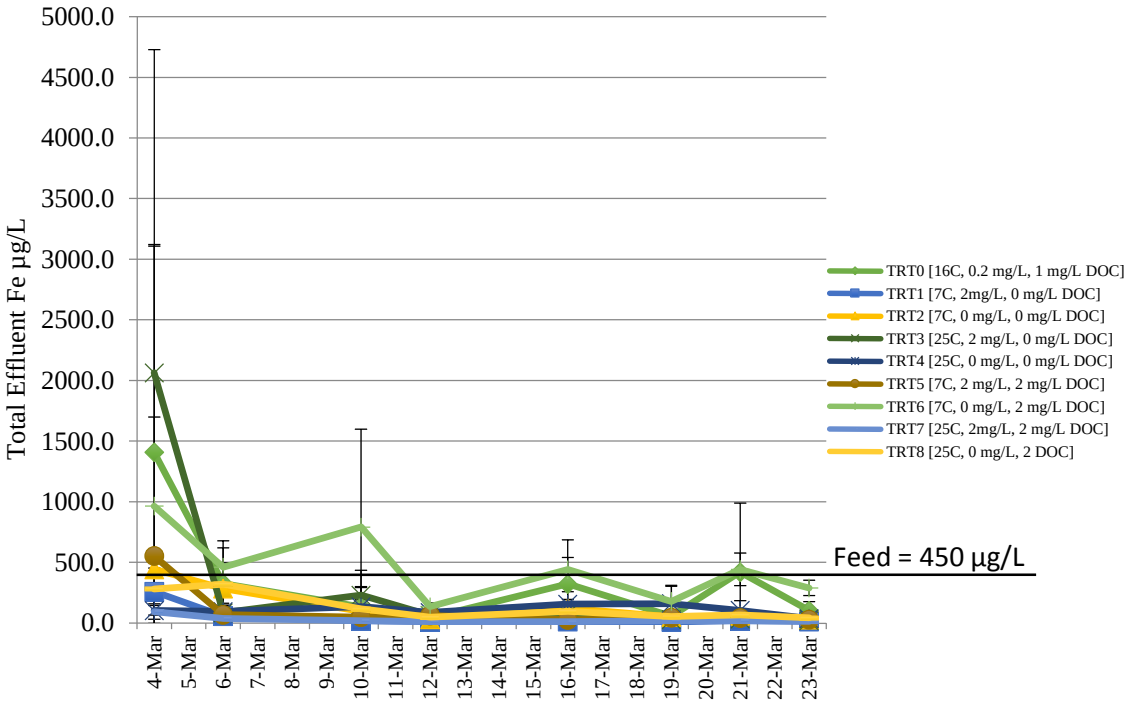

Fig. C-2. Total effluent Fe during challenge phase. Error bars refer to standard deviation of triplicate mean.

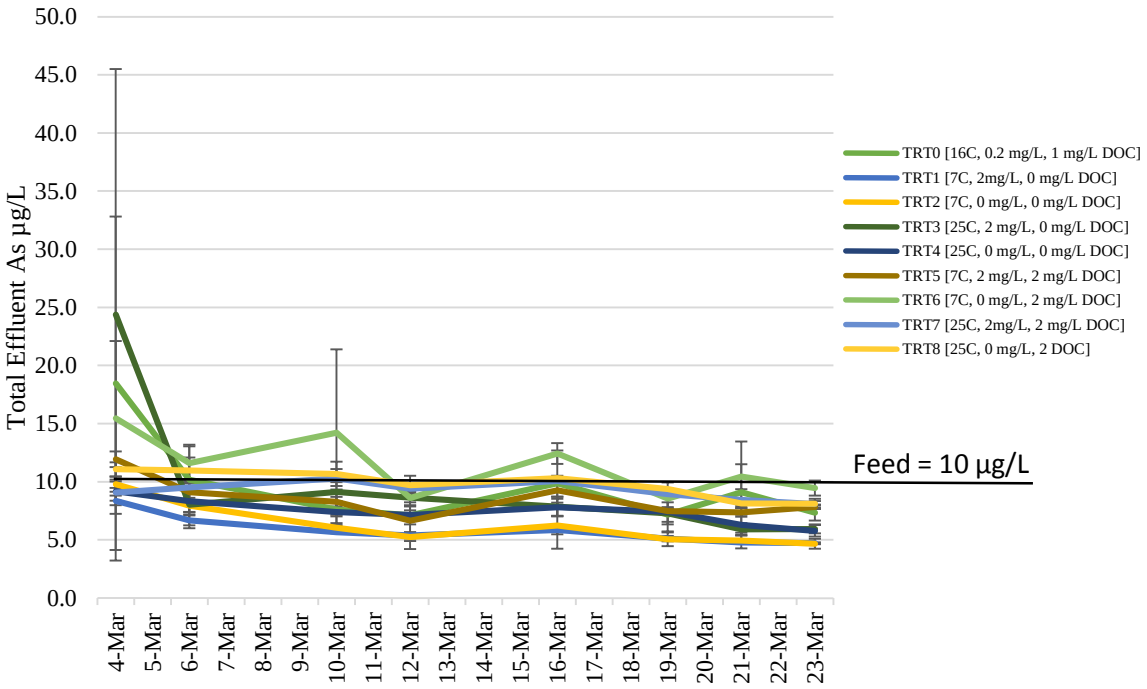

Fig. C-3. Total Effluent As during challenge phase. Error bars refer to standard deviation of triplicate mean.

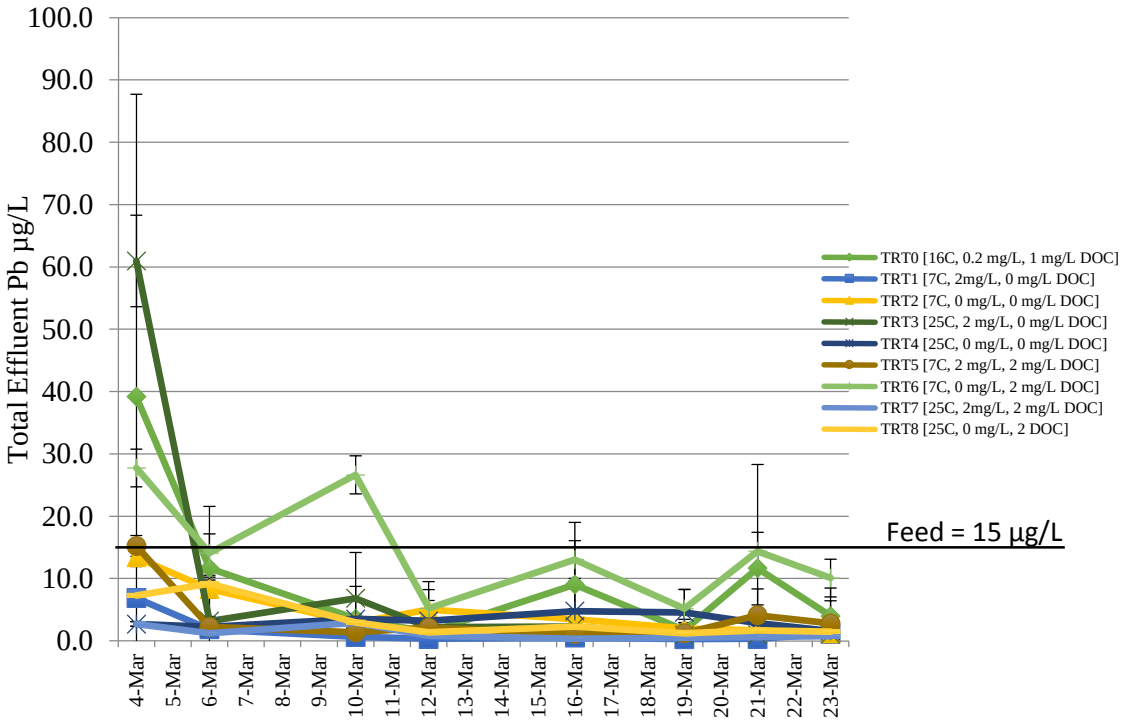

Fig. C-4. Total Effluent Pb during challenge phase. Error bars refer to standard deviation of triplicate mean.

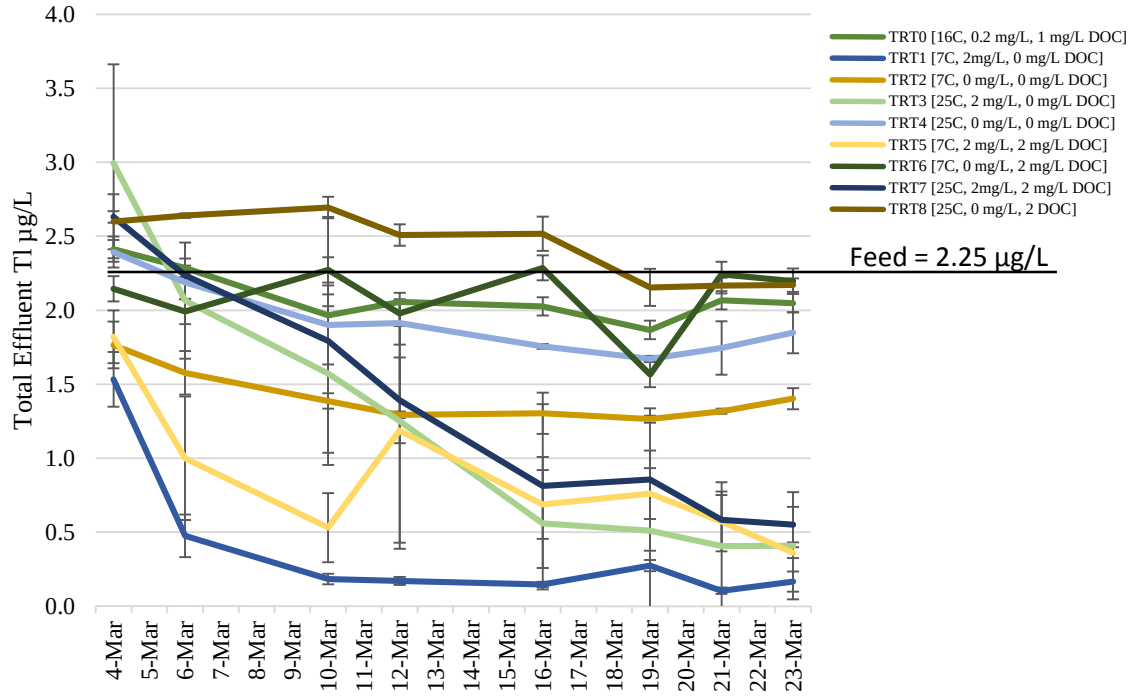

Fig. C-5. Total Effluent Tl during challenge phase. Error bars refer to standard deviation of triplicate mean.

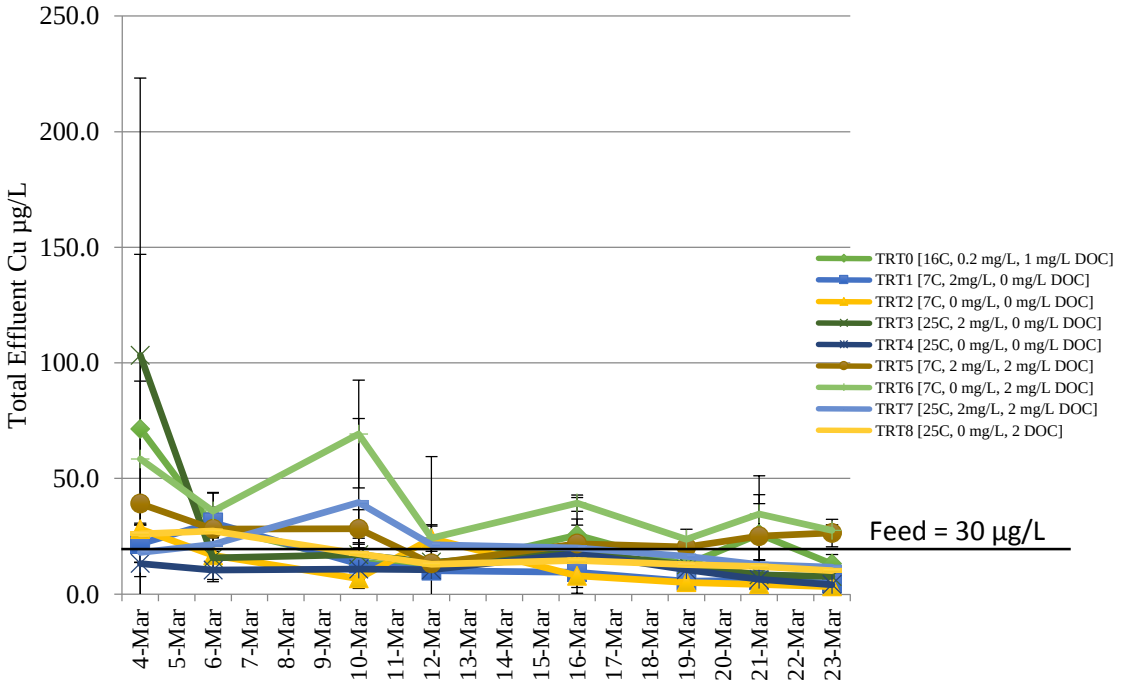

Fig. C-6. Total Effluent Cu during challenge phase. Error bars refer to standard deviation of triplicate mean.

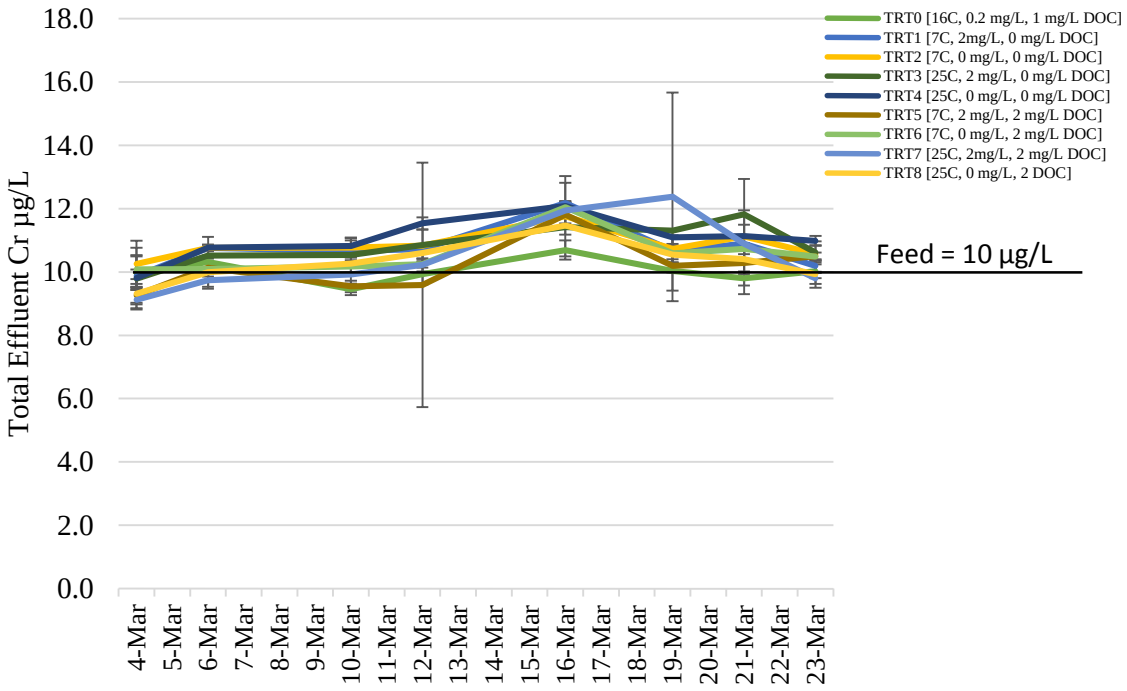

Fig. C-7. Total Effluent Cr during challenge phase. Error bars refer to standard deviation of triplicate mean.

APPENDIX D Swab Solids Sequential Extraction Plots

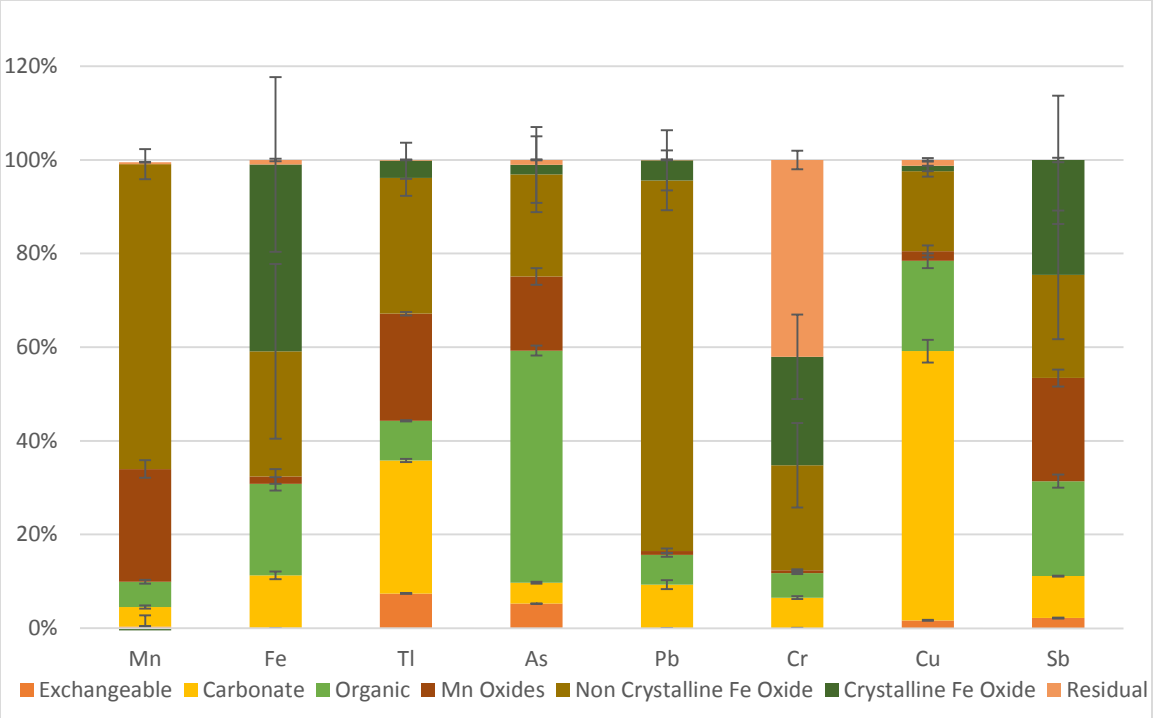

Fig. D-1. Distribution of TICs as defined by sequential extractions for AST Swab Cleaning Trial.

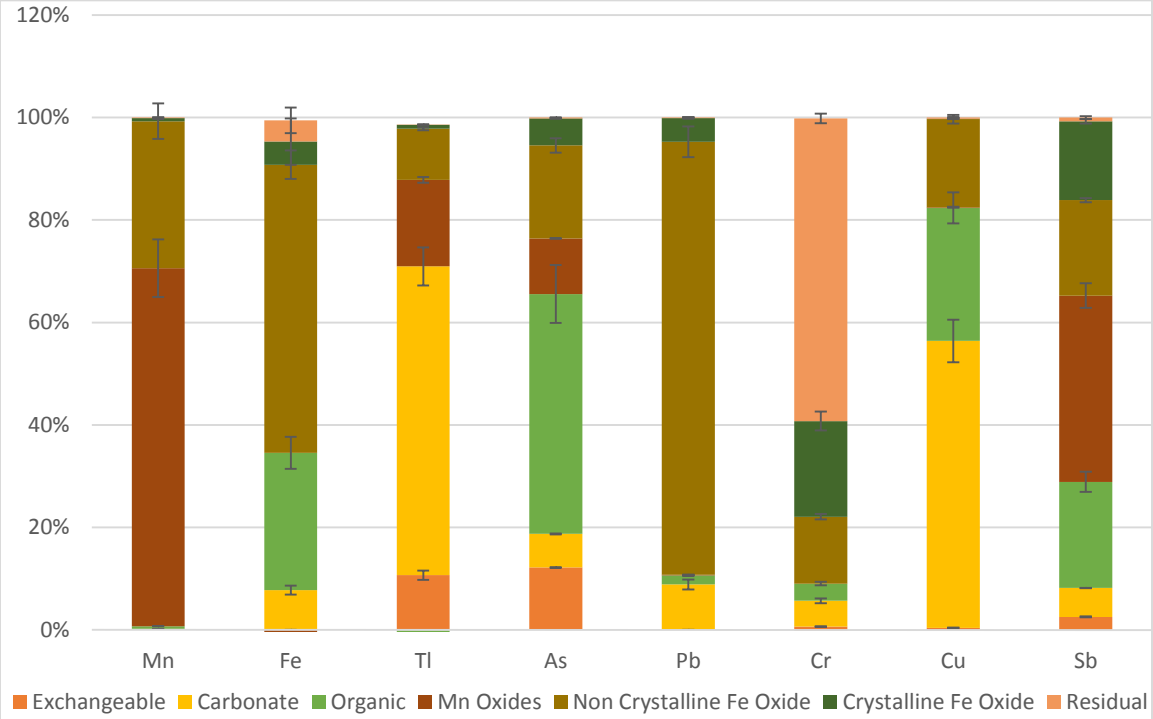

Fig. D-2. Distribution of TICs as defined by sequential extractions for UPA Swab Cleaning Trial.